

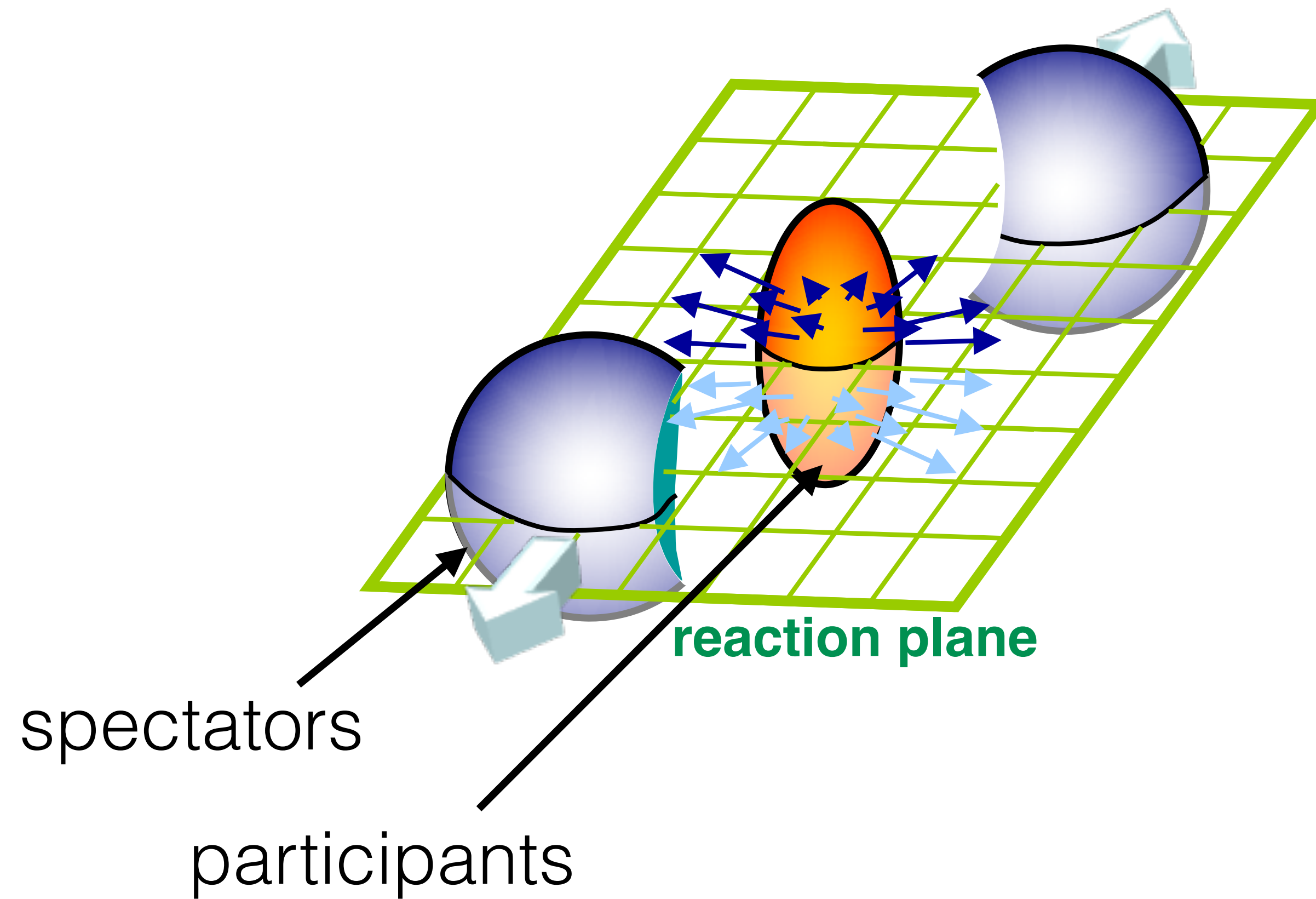
# ***Global and local polarization of $\Lambda$ hyperons in heavy-ion collisions***

**Takafumi Niida**

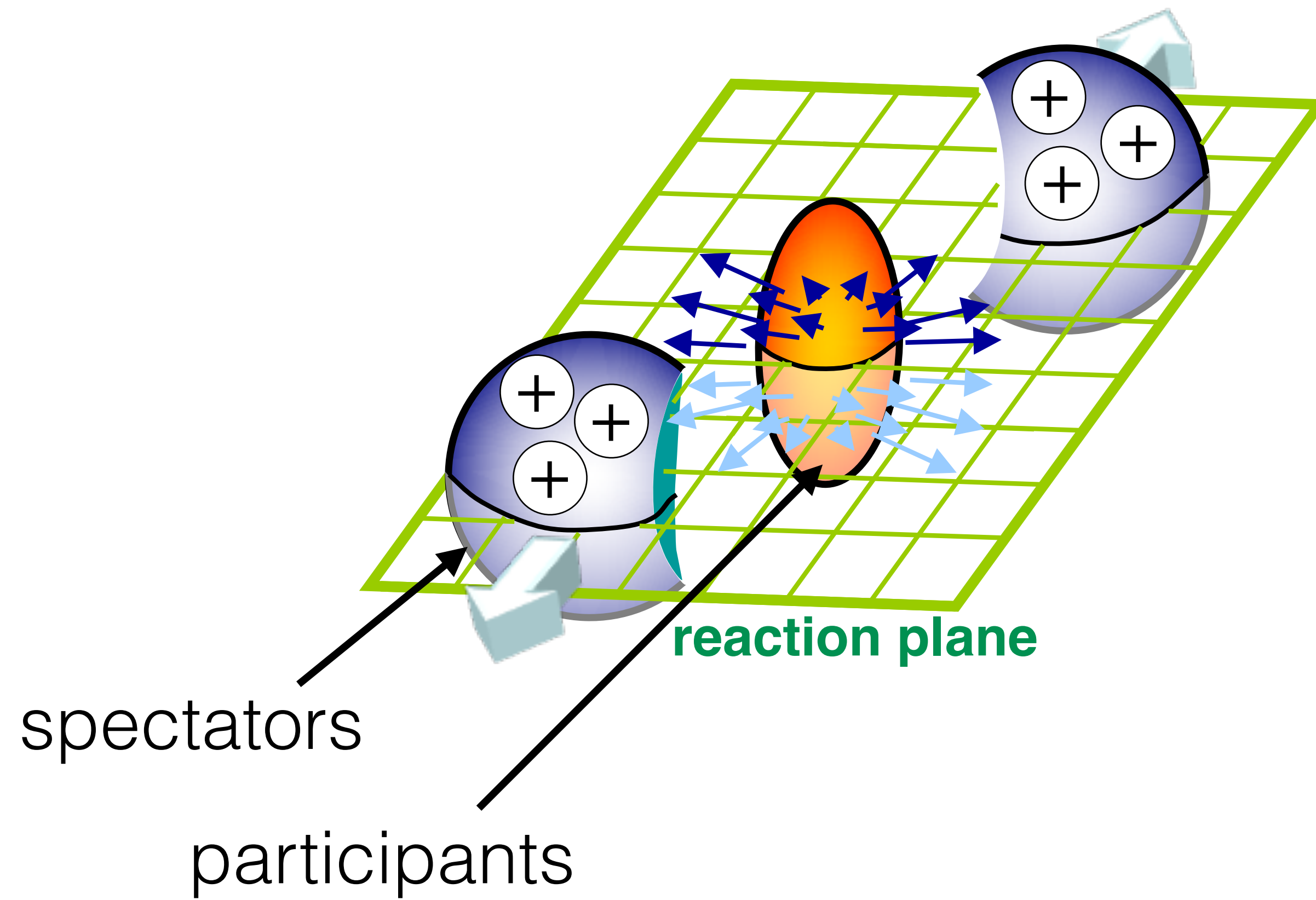


***Nuclear Physics Seminar, BNL***

# Important features in non-central heavy-ion collisions



# Important features in non-central heavy-ion collisions



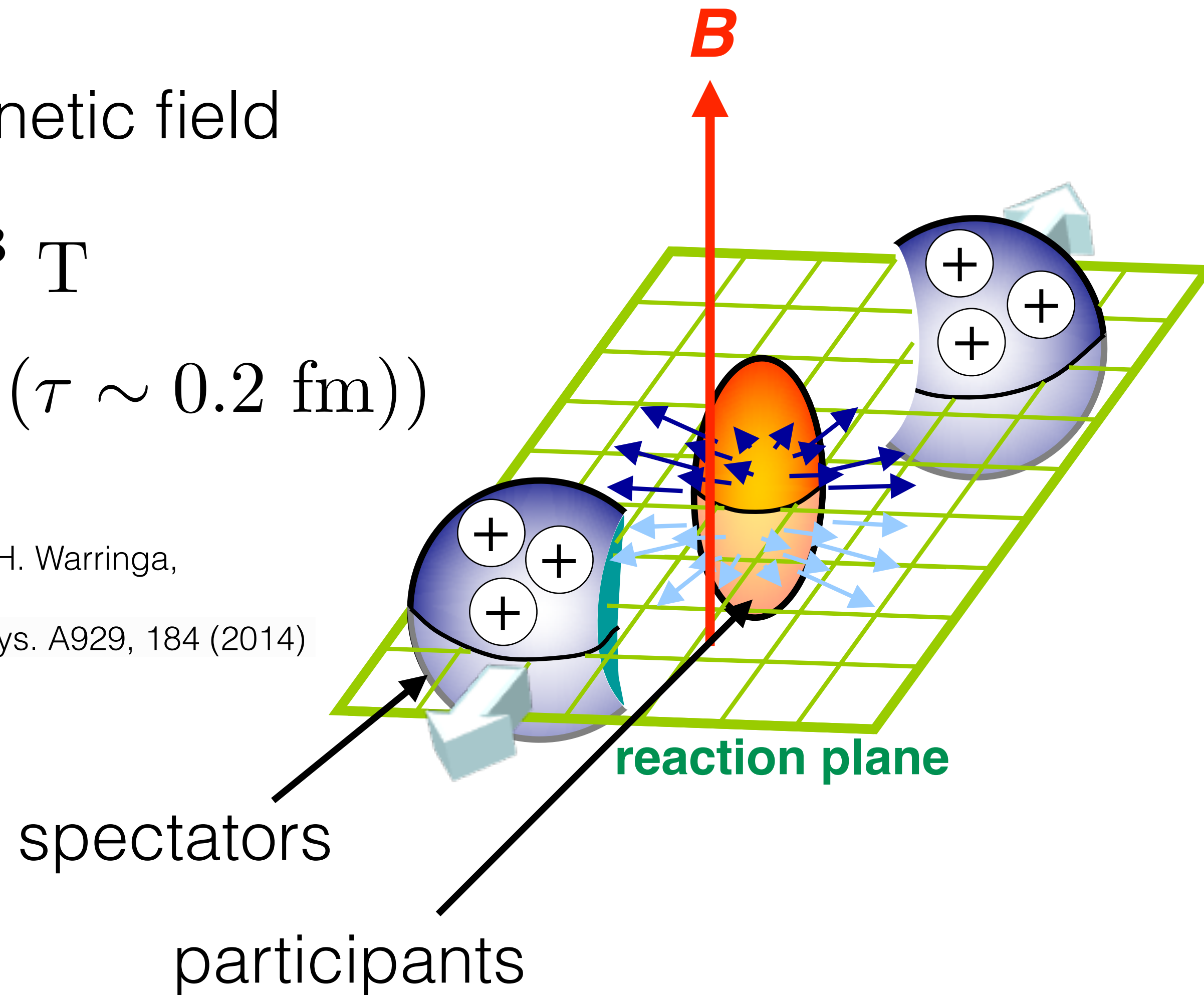
# Important features in non-central heavy-ion collisions

Strong magnetic field

$$B \sim 10^{13} \text{ T}$$

$$(eB \sim m_{\pi}^2 (\tau \sim 0.2 \text{ fm}))$$

D. Kharzeev, L. McLerran, and H. Warringa,  
Nucl.Phys.A803, 227 (2008)  
McLerran and Skokov, Nucl. Phys. A929, 184 (2014)



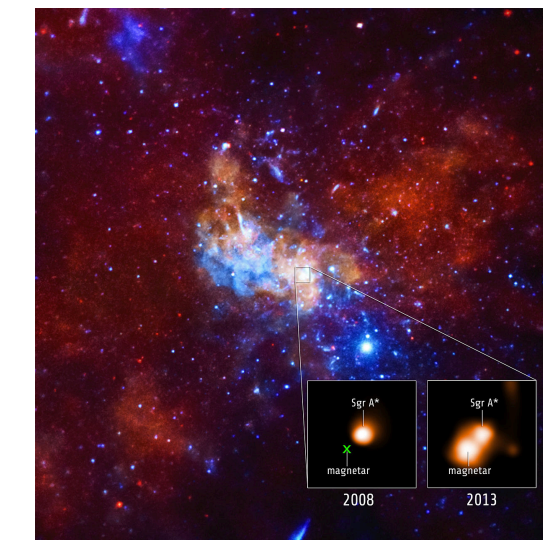
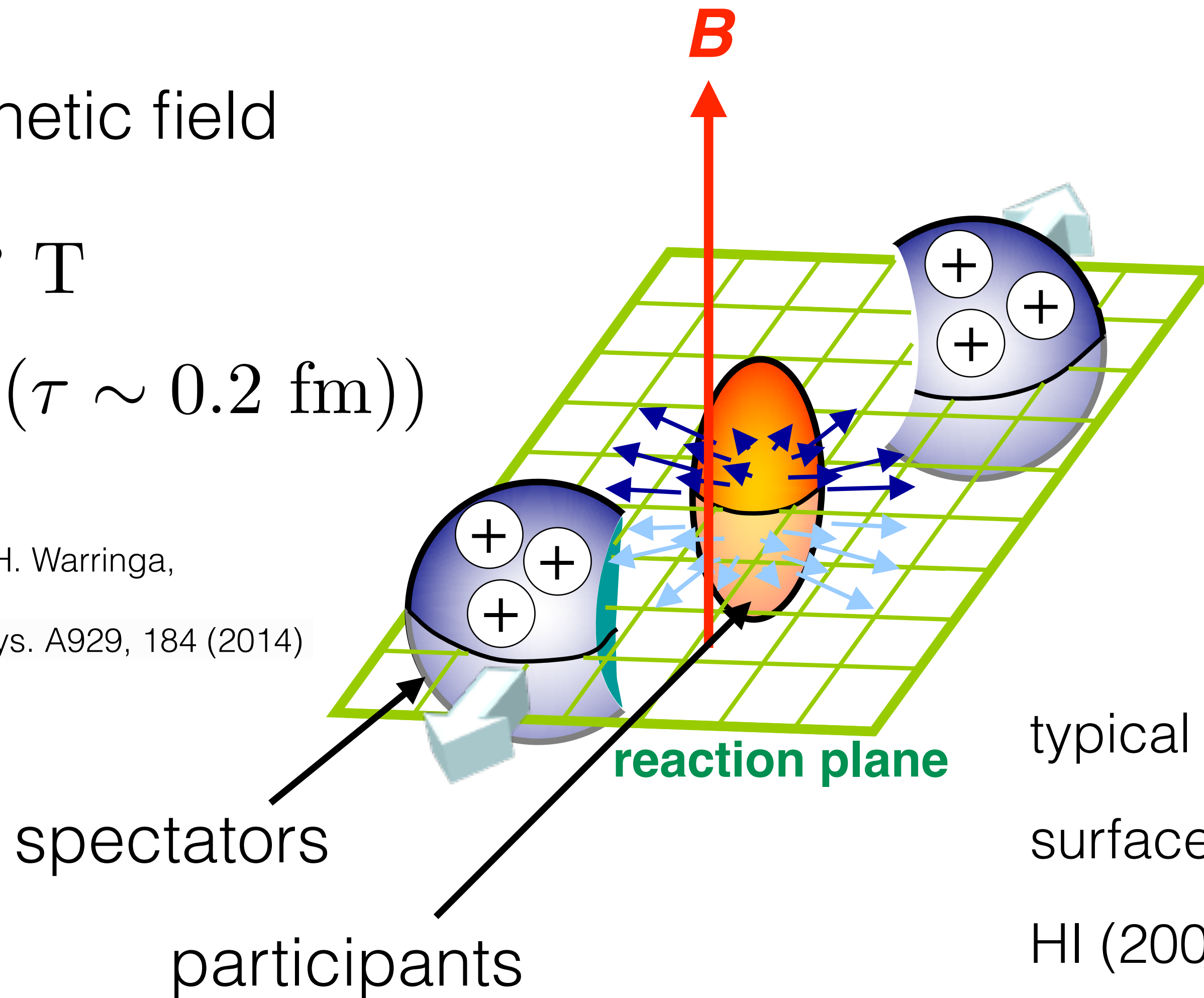
# Important features in non-central heavy-ion collisions

Strong magnetic field

$$B \sim 10^{13} \text{ T}$$

$$(eB \sim m_\pi^2 (\tau \sim 0.2 \text{ fm}))$$

D. Kharzeev, L. McLerran, and H. Warringa,  
Nucl.Phys.A803, 227 (2008)  
McLerran and Skokov, Nucl. Phys. A929, 184 (2014)



magnetar, wikipedia



typical magnet

$$B \sim 0.1 - 0.5 \text{ T}$$

surface on magnetar

$$B \sim 10^{11} \text{ T}$$

HI (200 GeV)

$$B \sim 10^{13} \text{ T}$$

# Important features in non-central heavy-ion collisions

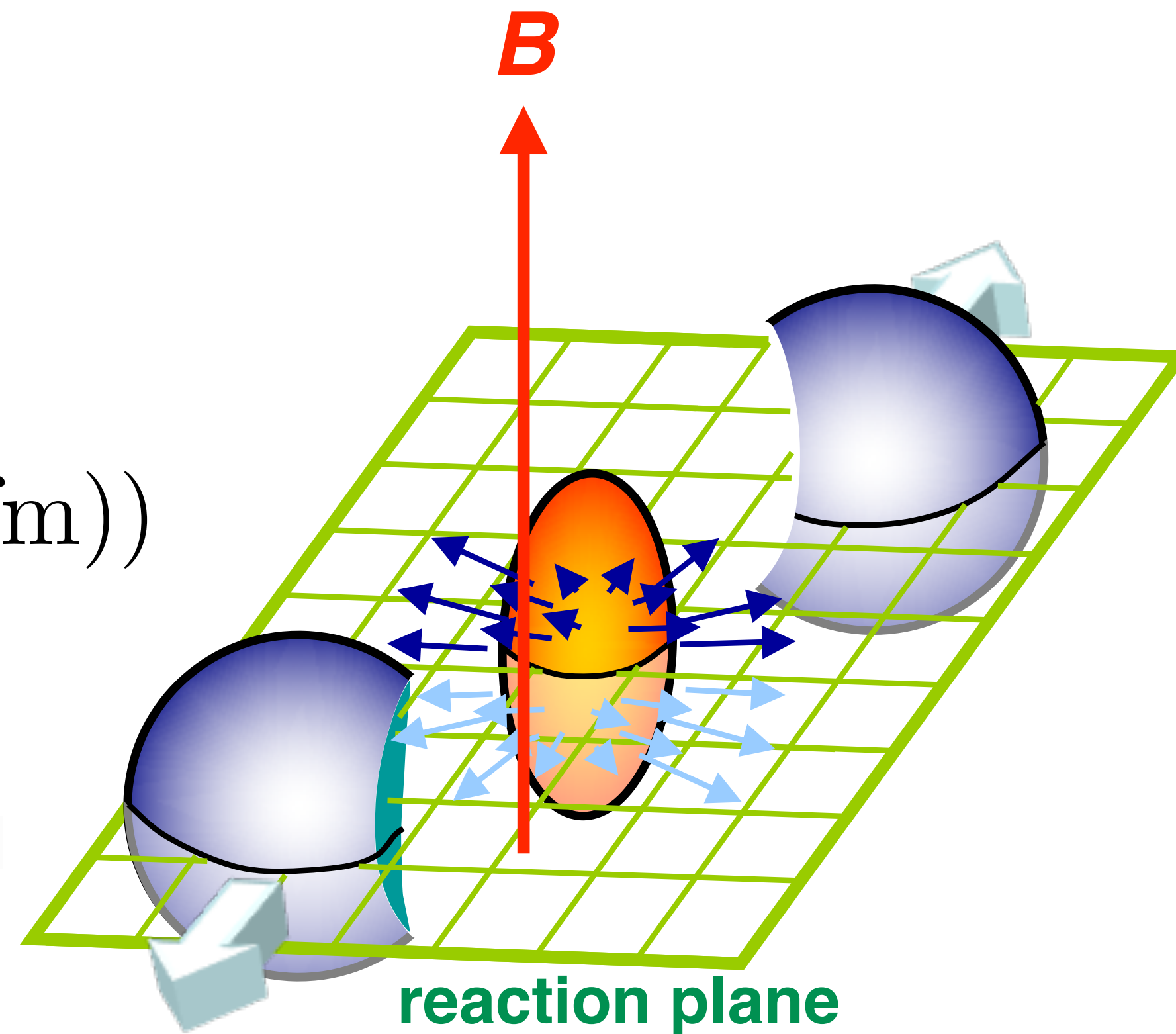
Strong magnetic field

$$B \sim 10^{13} \text{ T}$$

$$(eB \sim m_{\pi}^2 (\tau \sim 0.2 \text{ fm}))$$

D. Kharzeev, L. McLerran, and H. Warringa,  
Nucl.Phys.A803, 227 (2008)

McLerran and Skokov, Nucl. Phys. A929, 184 (2014)



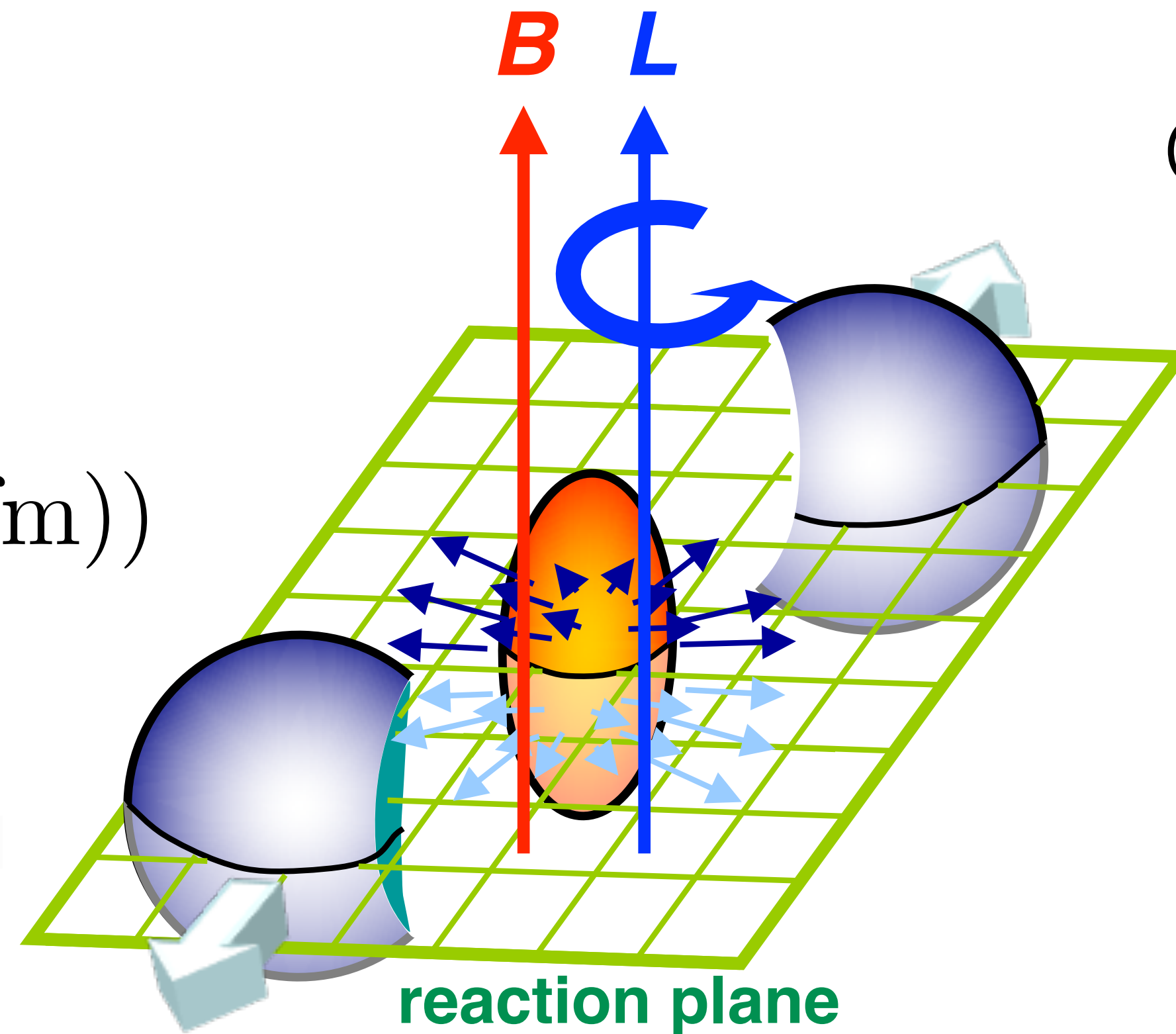
# Important features in non-central heavy-ion collisions

Strong magnetic field

$$B \sim 10^{13} \text{ T}$$

$$(eB \sim m_{\pi}^2 (\tau \sim 0.2 \text{ fm}))$$

D. Kharzeev, L. McLerran, and H. Warringa,  
Nucl.Phys.A803, 227 (2008)  
McLerran and Skokov, Nucl. Phys. A929, 184 (2014)



Orbital angular momentum

$$\mathbf{L} = \mathbf{r} \times \mathbf{p}$$

$$\sim bA\sqrt{s_{NN}} \sim 10^6 \hbar$$

Z.-T. Liang and X.-N. Wang, PRL94, 102301 (2005)

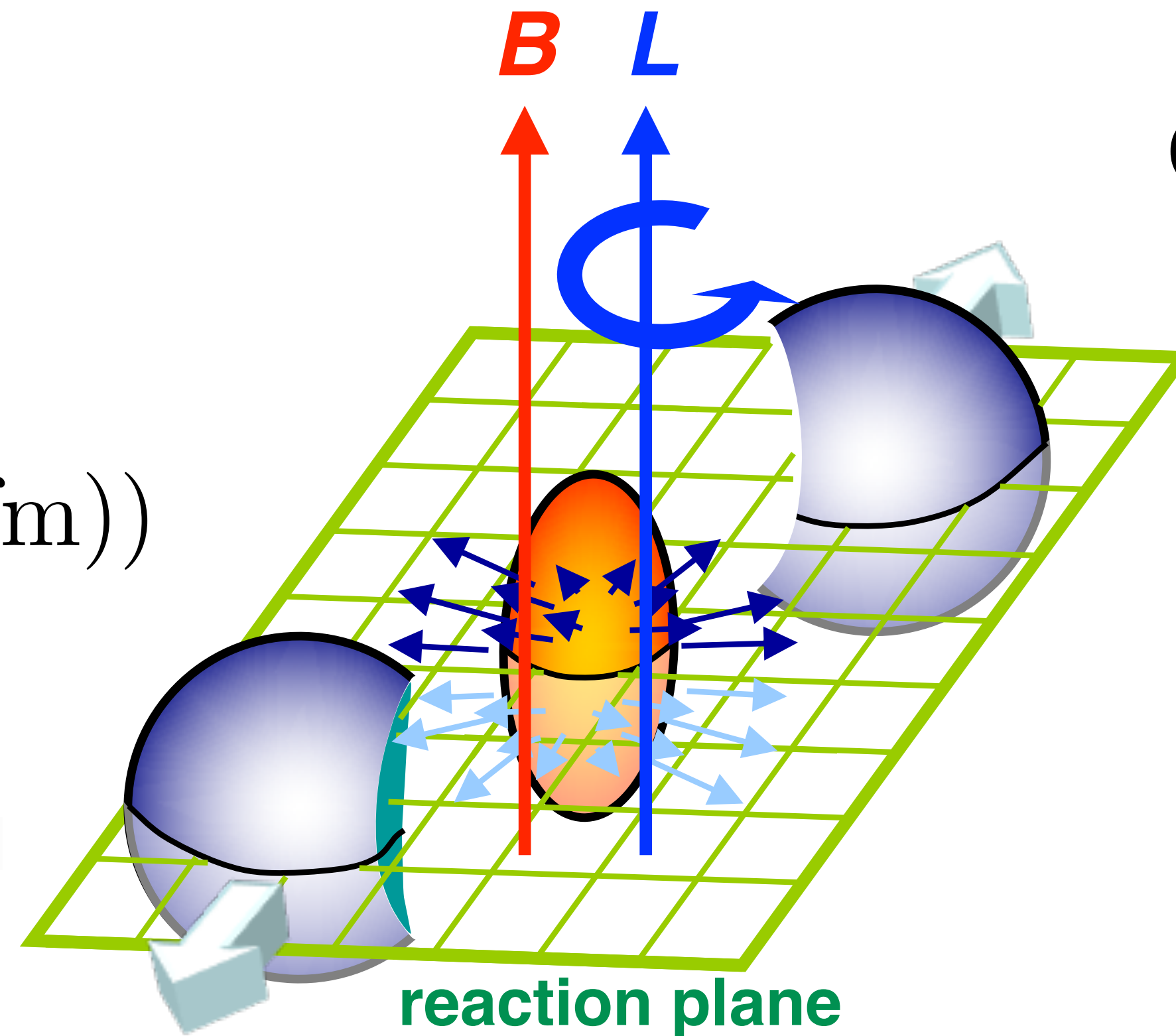
# Important features in non-central heavy-ion collisions

Strong magnetic field

$$B \sim 10^{13} \text{ T}$$

$$(eB \sim m_\pi^2 (\tau \sim 0.2 \text{ fm}))$$

D. Kharzeev, L. McLerran, and H. Warringa,  
Nucl.Phys.A803, 227 (2008)  
McLerran and Skokov, Nucl. Phys. A929, 184 (2014)



Orbital angular momentum

$$\mathbf{L} = \mathbf{r} \times \mathbf{p}$$

$$\sim bA\sqrt{s_{NN}} \sim 10^6 \hbar$$

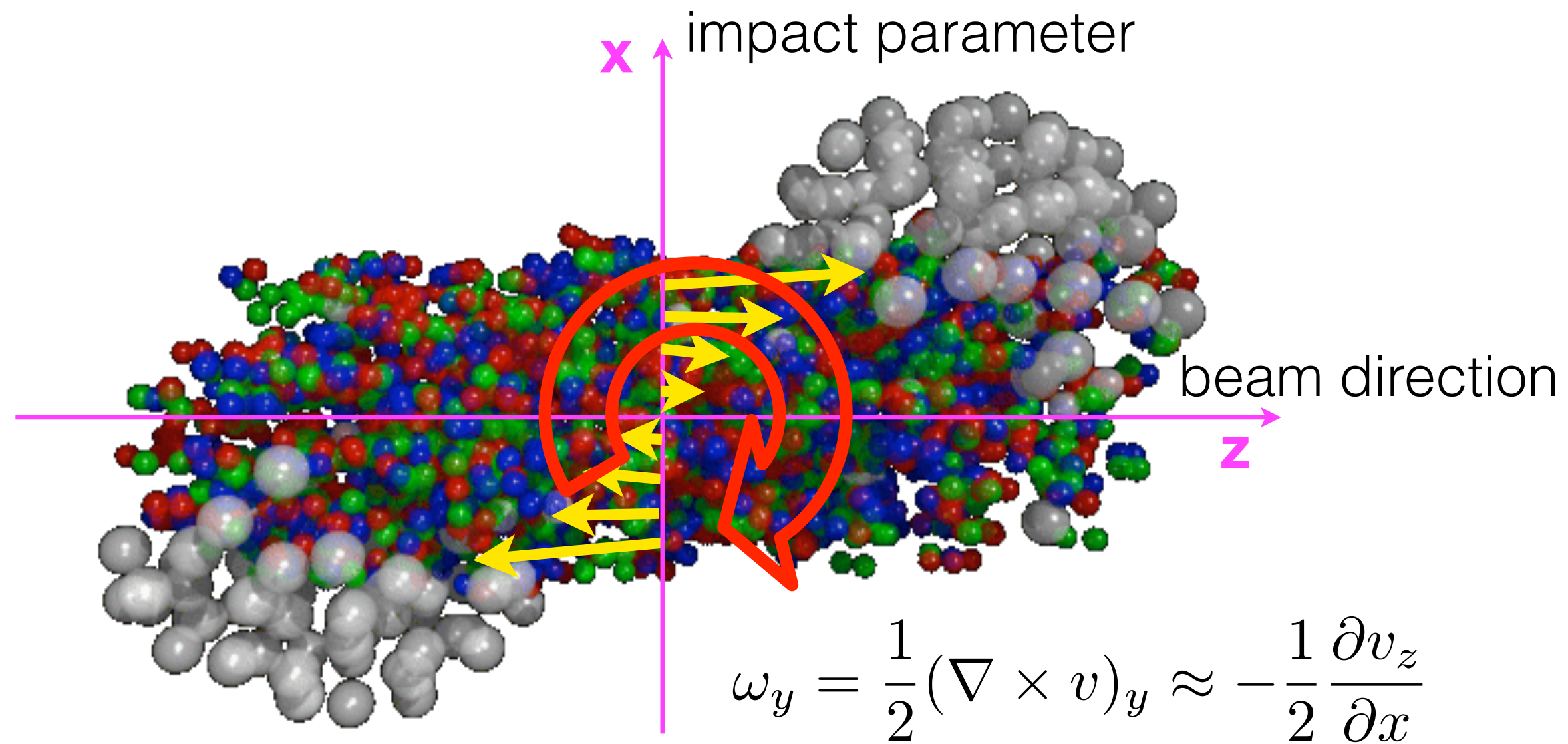
Z.-T. Liang and X.-N. Wang, PRL94, 102301 (2005)

→ Chiral magnetic effect  
Chiral magnetic wave  
**Particle polarization**

→ Chiral vortical effect  
**Particle polarization**



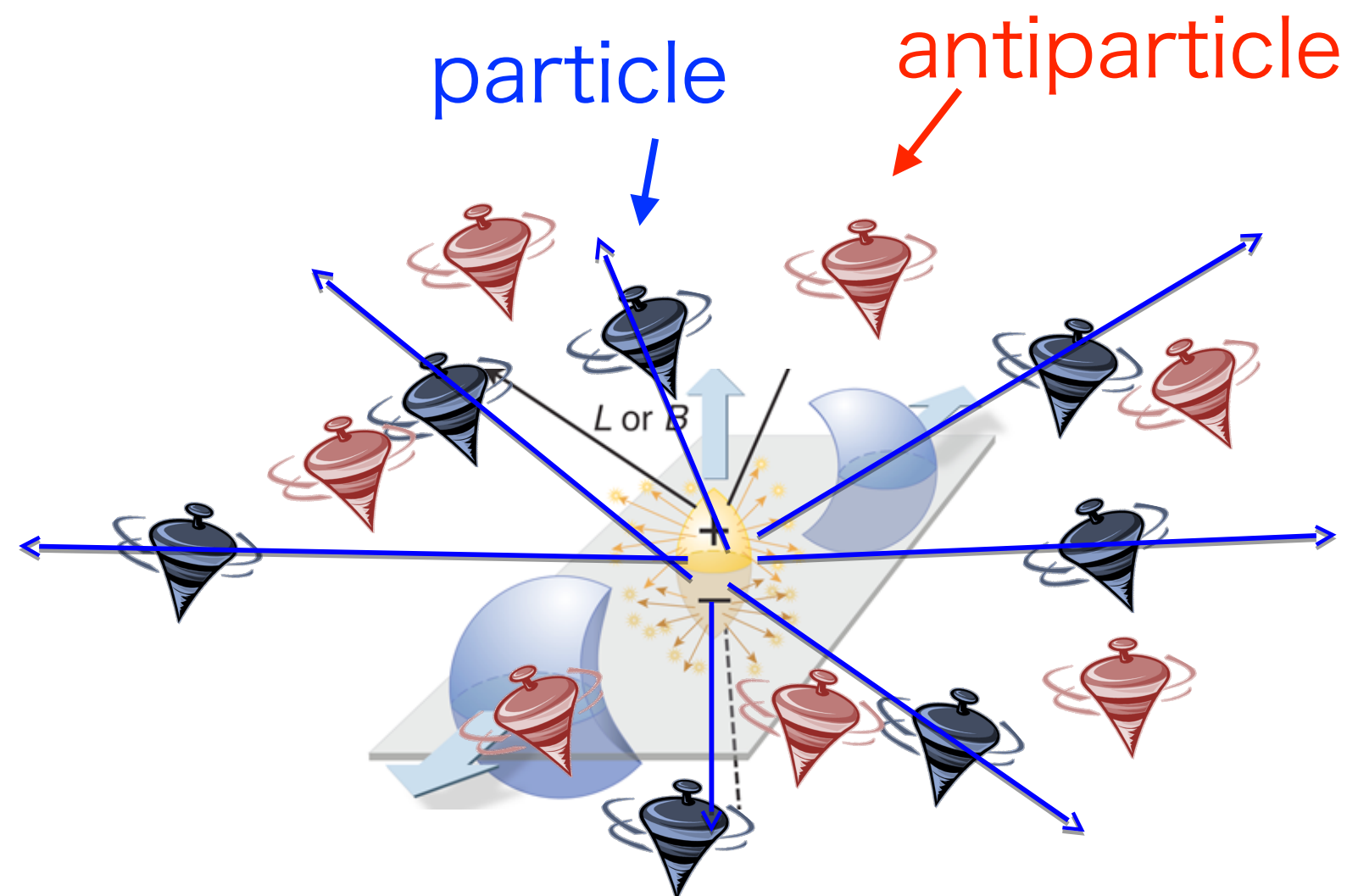
# Global polarization



- Z.-T. Liang and X.-N. Wang, PRL94, 102301 (2005)
- S. Voloshin, nucl-th/0410089 (2004)

- Non-zero angular momentum transfers to the spin degrees of freedom
  - Particles' and anti-particles' spins are aligned with angular momentum,  $\mathbf{L}$

- Magnetic field align particle's spin
  - Particles' and antiparticles' spins are aligned oppositely along  $\mathbf{B}$  due to the opposite sign of magnetic moment



# How to measure the polarization?

## Parity-violating weak decay of hyperons (“self-analyzing”)

Daughter baryon is preferentially emitted in the direction of hyperon’s spin (opposite for anti-particle)

$$\frac{dN}{d\cos\theta^*} \propto 1 + \alpha_H P_H \cos\theta^*$$

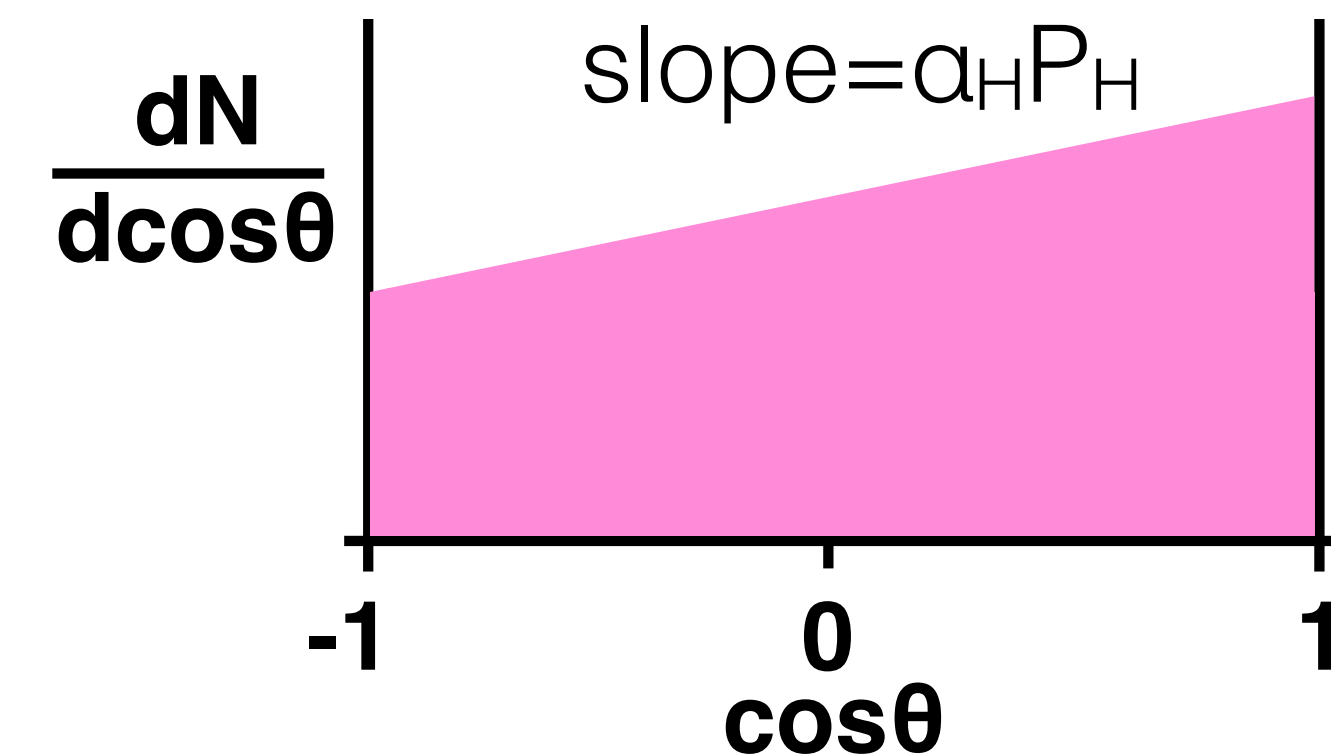
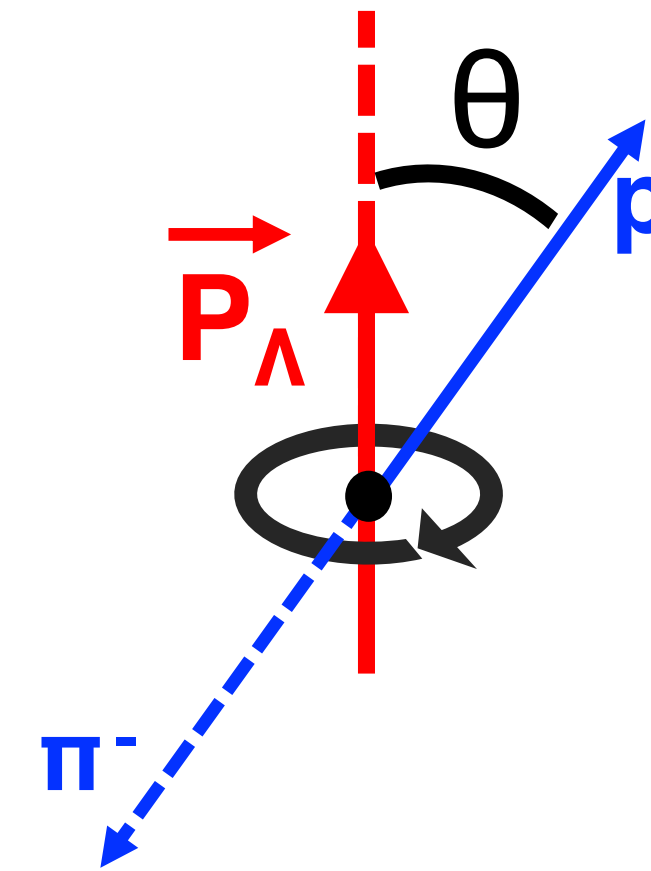
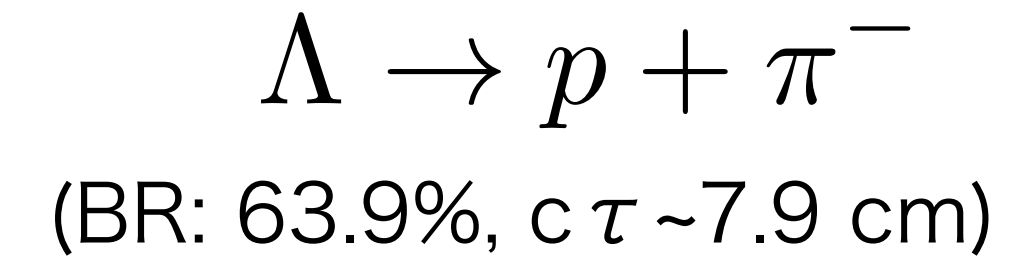
$P_H$ :  $\Lambda$  polarization

$\theta^*$ : polar angle of proton relative to the polarization direction in the  $\Lambda$  rest frame

$\alpha_H$ :  $\Lambda$  decay parameter

$$(\alpha_\Lambda = -\alpha_{\bar{\Lambda}} = 0.642 \pm 0.013)$$

C. Patrignani et al. (PDG), Chin. Phys. C 40, 100001 (2016)



# How to measure the polarization?

## Parity-violating weak decay of hyperons (“self-analyzing”)

Daughter baryon is preferentially emitted in the direction of hyperon’s spin (opposite for anti-particle)

$$\frac{dN}{d\cos\theta^*} \propto 1 + \alpha_H P_H \cos\theta^*$$

$P_H$ :  $\Lambda$  polarization

$\theta^*$ : polar angle of proton relative to the polarization direction in the  $\Lambda$  rest frame

$\alpha_H$ :  $\Lambda$  decay parameter

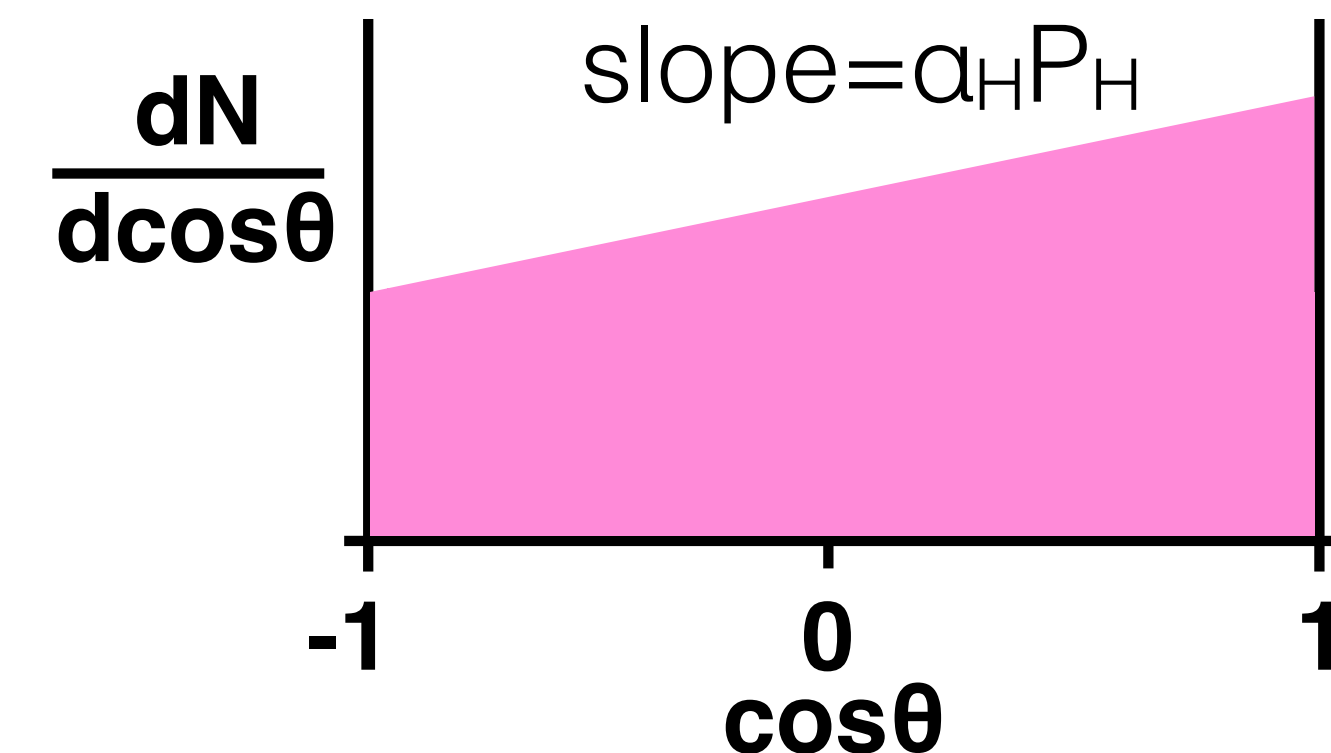
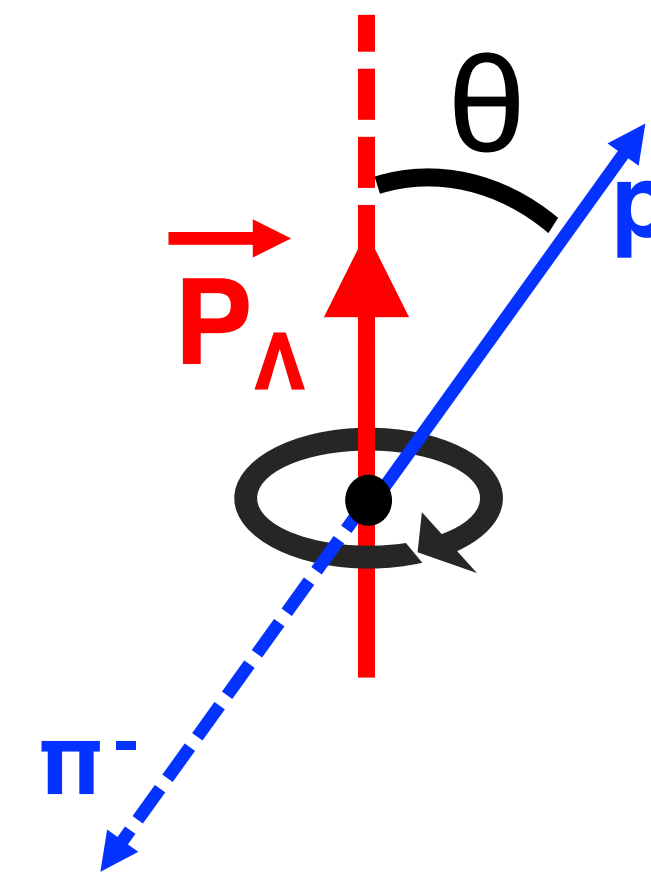
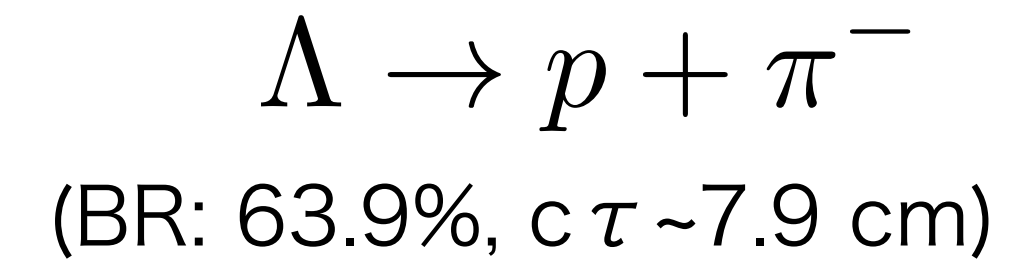
$$(\alpha_\Lambda = -\alpha_{\bar{\Lambda}} = 0.642 \pm 0.013)$$

C. Patrignani et al. (PDG), Chin. Phys. C 40, 100001 (2016)

Note:  $\alpha_H$  recently updated by BESIII Collaboration

$$\alpha_\Lambda = 0.750 \pm 0.009, \alpha_{\bar{\Lambda}} = -0.758 \pm 0.010$$

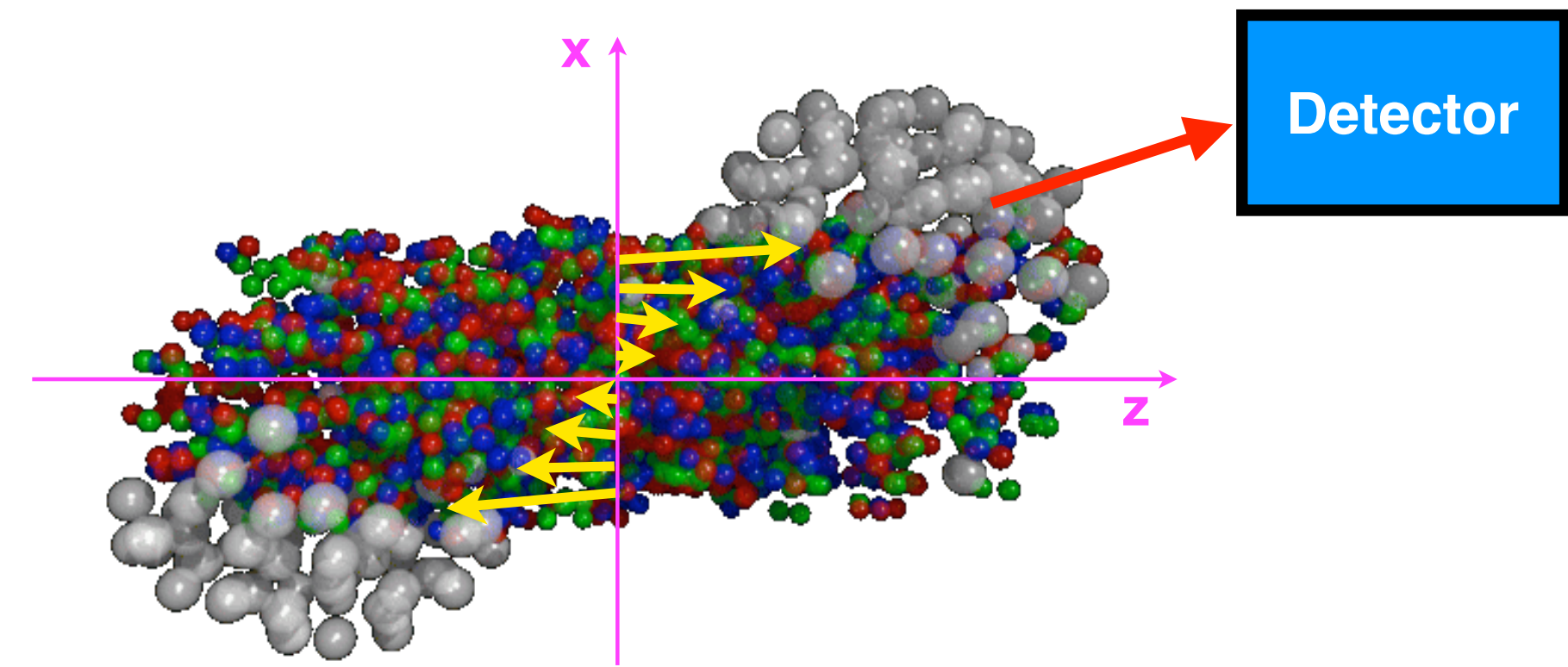
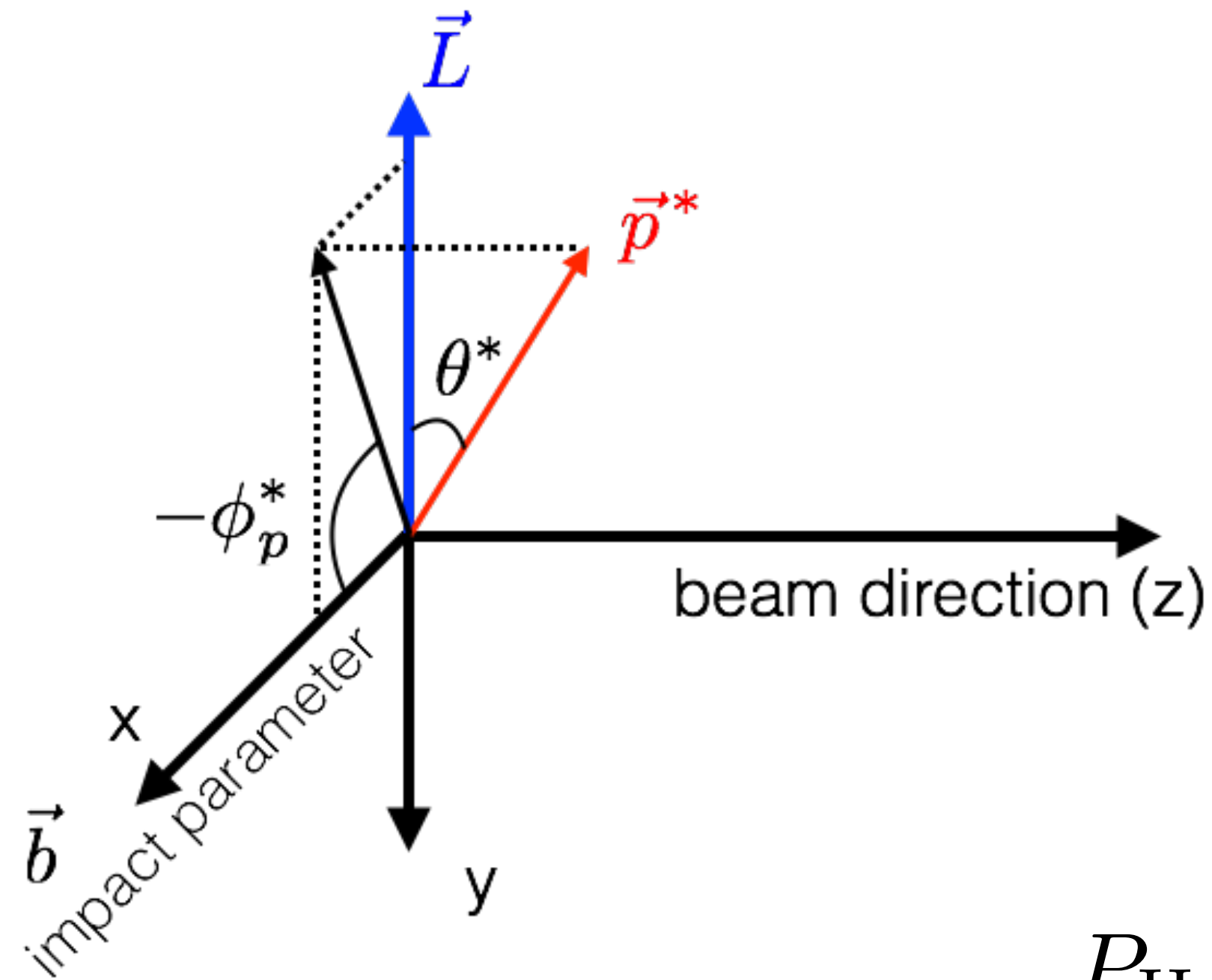
M. Tanabashi et al., (PDG), Phys. Rev. D98, 030001 (2018) and 2019 update



# How to measure the “global” polarization?

“global” polarization : a net spin alignment along a specific direction

Projection onto the transverse plane



Angular momentum direction can be determined by spectator deflection (spectators deflect outwards)

S. Voloshin and TN, PRC94.021901(R)(2016)

$$P_H = \frac{8}{\pi\alpha_H} \frac{\langle \sin(\Psi_1 - \phi_p^*) \rangle}{\text{Res}(\Psi_1)}$$

$\Psi_1$ : azimuthal angle of b

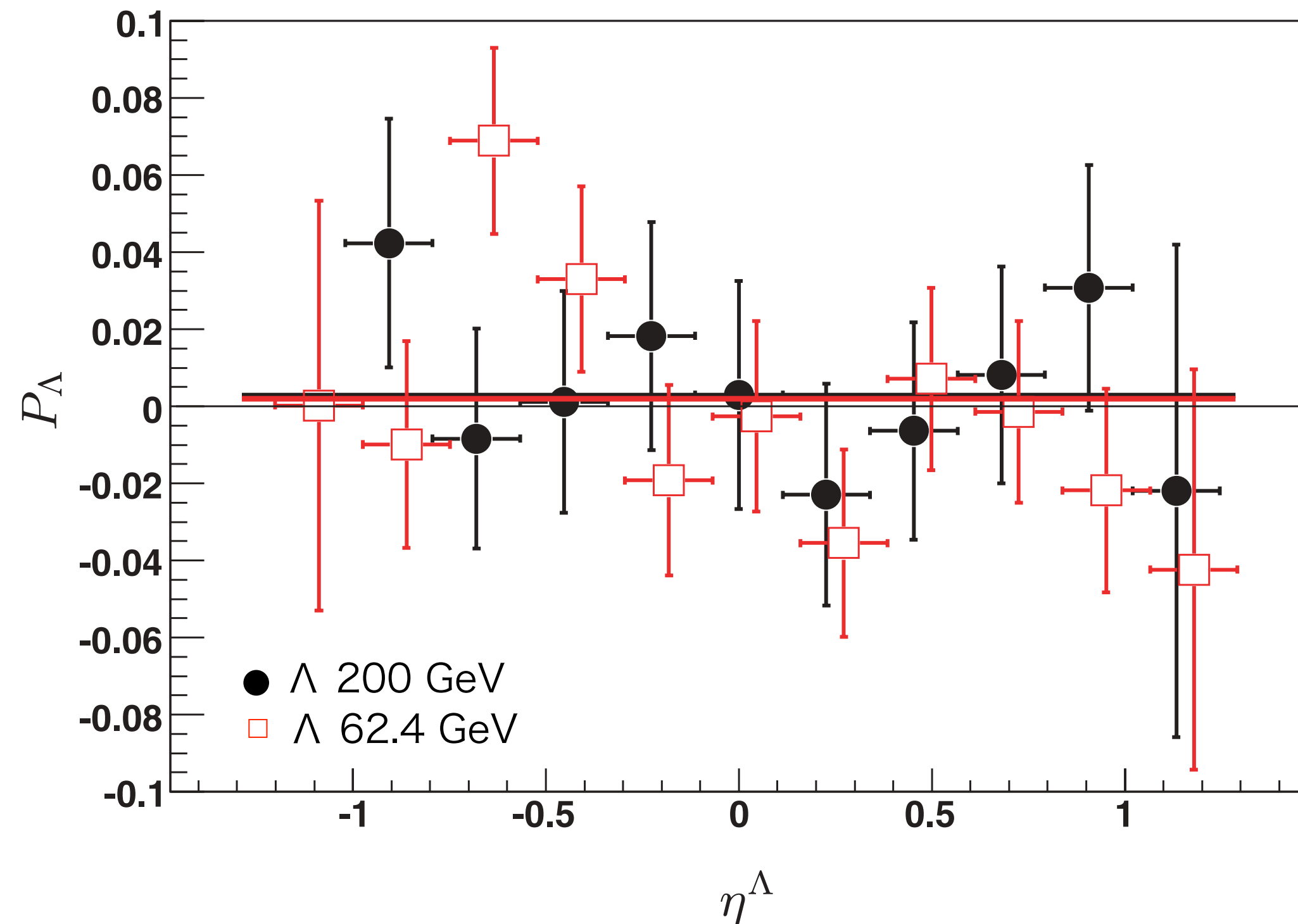
$\phi_p^*$ :  $\phi$  of daughter proton in  $\Lambda$  rest frame

STAR, PRC76, 024915 (2007)

# First paper from STAR in 2007

PHYSICAL REVIEW C **76**, 024915 (2007)

## Global polarization measurement in Au+Au collisions



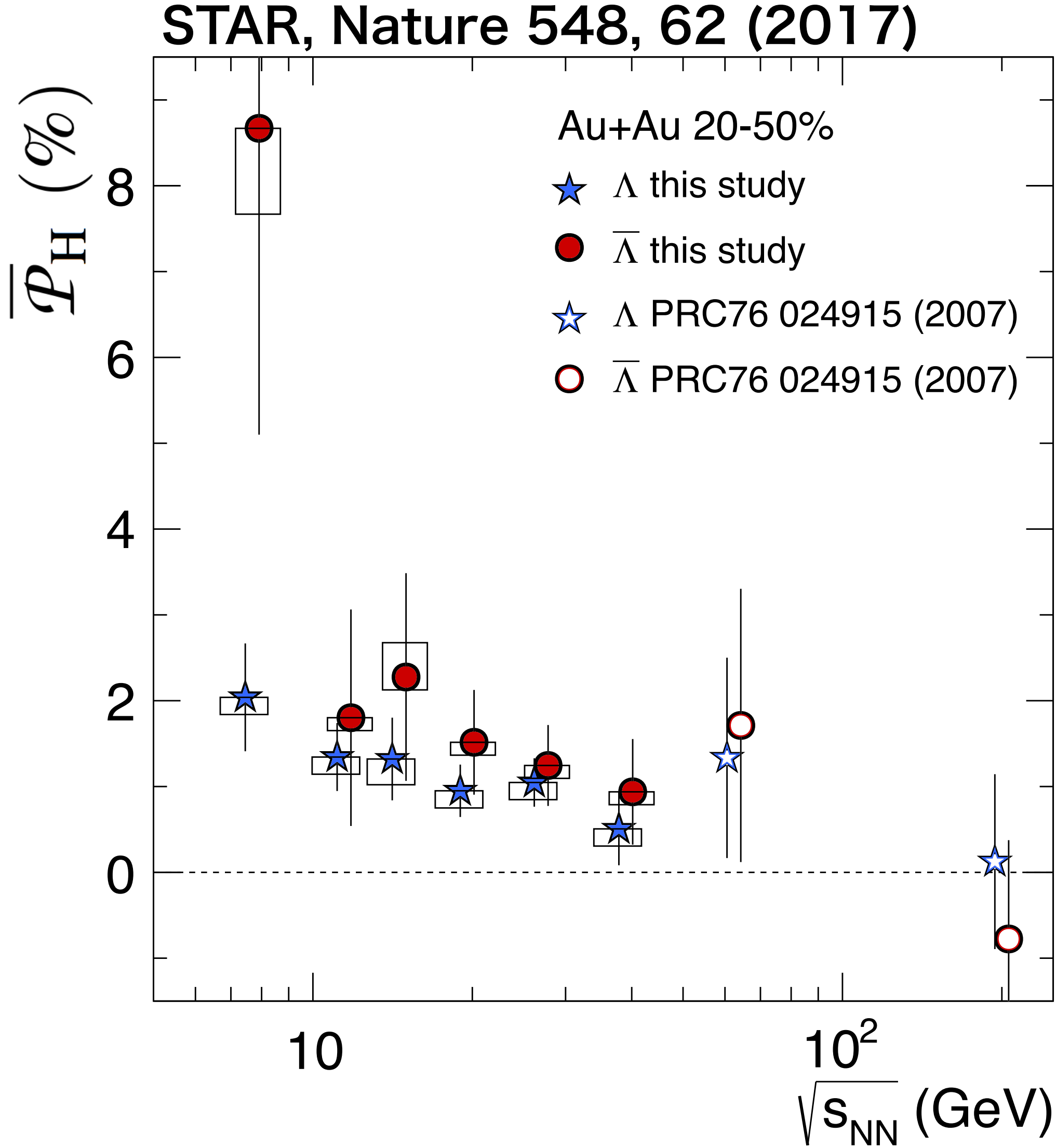
Au+Au collisions at  $\sqrt{s_{NN}} = 62.4$  and 200 GeV in 2004 with very limited statistics ( $\sim 9$ M events)

### III. CONCLUSION

The  $\Lambda$  and  $\bar{\Lambda}$  hyperon global polarization has been measured in Au+Au collisions at center-of-mass energies  $\sqrt{s_{NN}} = 62.4$  and 200 GeV with the STAR detector at RHIC. An upper limit of  $|P_{\Lambda, \bar{\Lambda}}| \leq 0.02$  for the global polarization of  $\Lambda$  and  $\bar{\Lambda}$  hyperons within the STAR detector acceptance is

Results were consistent with zero..., giving an upper limit of  $P_H < 2\%$

# First observation in BES-I



Positive polarization signal at lower energies!

-- The most vortical fluid!

$$\omega = (P_\Lambda + P_{\bar{\Lambda}})k_B T / \hbar$$

$$\sim 0.02-0.09 \text{ fm}^{-1}$$

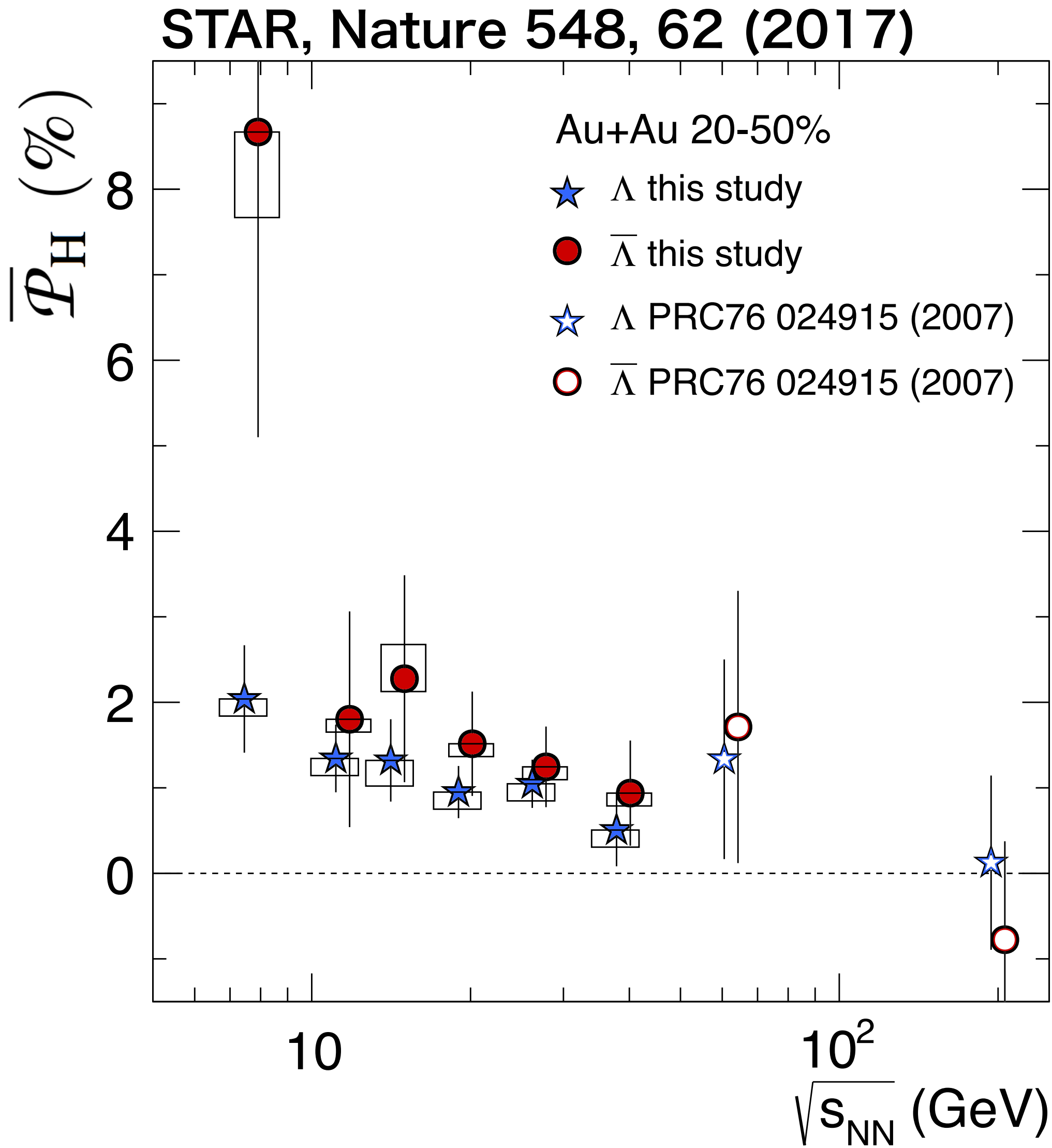
$\mu_\Lambda$ :  $\Lambda$  magnetic moment  
T: temperature at thermal equilibrium

$$\sim 0.6-2.7 \times 10^{22} \text{ s}^{-1} \quad (T=160 \text{ MeV})$$

-  $P_H$  looks to increase in lower energies

Becattini, Karpenko, Lisa, Upsal, and Voloshin, PRC95.054902 (2017)

# First observation in BES-I



Positive polarization signal at lower energies!

-- The most vortical fluid!

$$\omega = (P_{\Lambda} + P_{\bar{\Lambda}})k_B T / \hbar$$

$$\sim 0.02-0.09 \text{ fm}^{-1}$$

$\mu_{\Lambda}$ :  $\Lambda$  magnetic moment  
T: temperature at thermal equilibrium

$$\sim 0.6-2.7 \times 10^{22} \text{ s}^{-1} \quad (T=160 \text{ MeV})$$

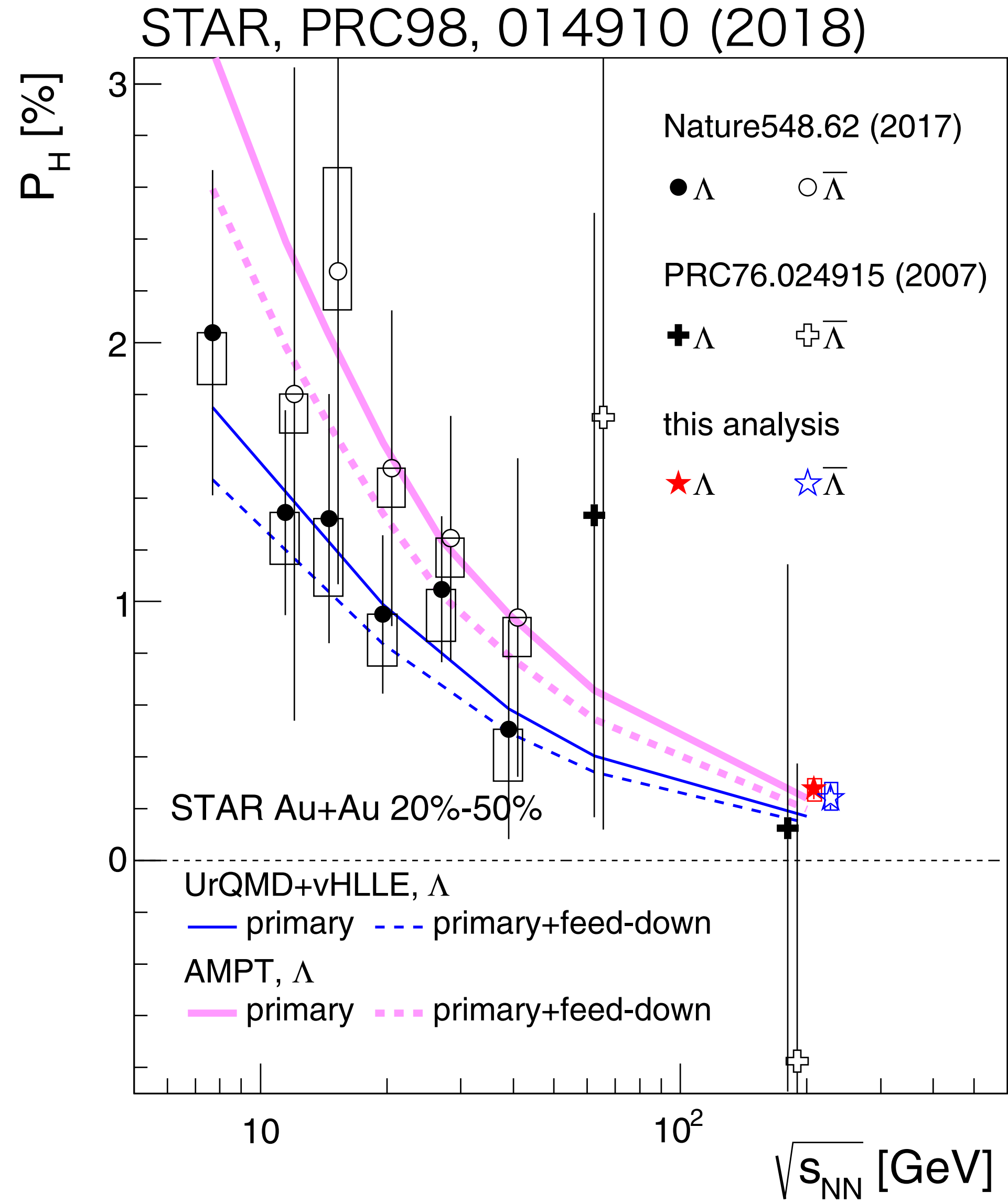
- $P_H$  looks to increase in lower energies
- Hint of the difference in  $P_H$  between  $\Lambda$  and anti- $\Lambda$   
-- Effect of the initial magnetic field?  $\rightarrow$  BESII

$$P_{\Lambda} \simeq \frac{1}{2} \frac{\omega}{T} + \frac{\mu_{\Lambda} B}{T}$$

$$P_{\bar{\Lambda}} \simeq \frac{1}{2} \frac{\omega}{T} - \frac{\mu_{\Lambda} B}{T}$$

Becattini, Karpenko, Lisa, Upsal, and Voloshin, PRC95.054902 (2017)

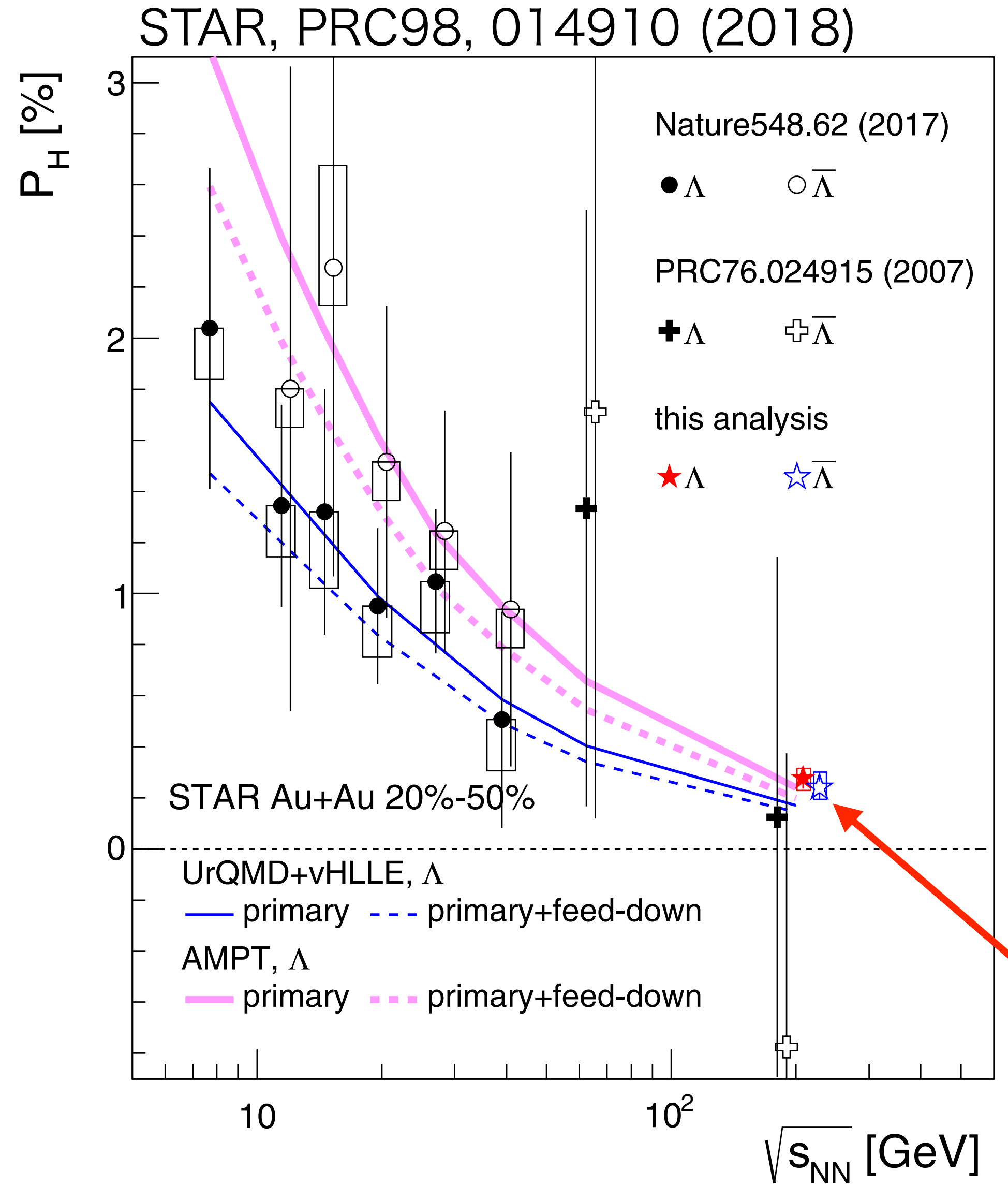
# Precise measurements at $\sqrt{s_{NN}} = 200$ GeV



- Confirmed energy dependence of  $P_H$  with new results for 200 GeV
  - $>5\sigma$  significance utilizing 1.5B events (2010+2011+2014)
  - partly due to stronger shear flow structure in lower  $\sqrt{s_{NN}}$  because of baryon stopping



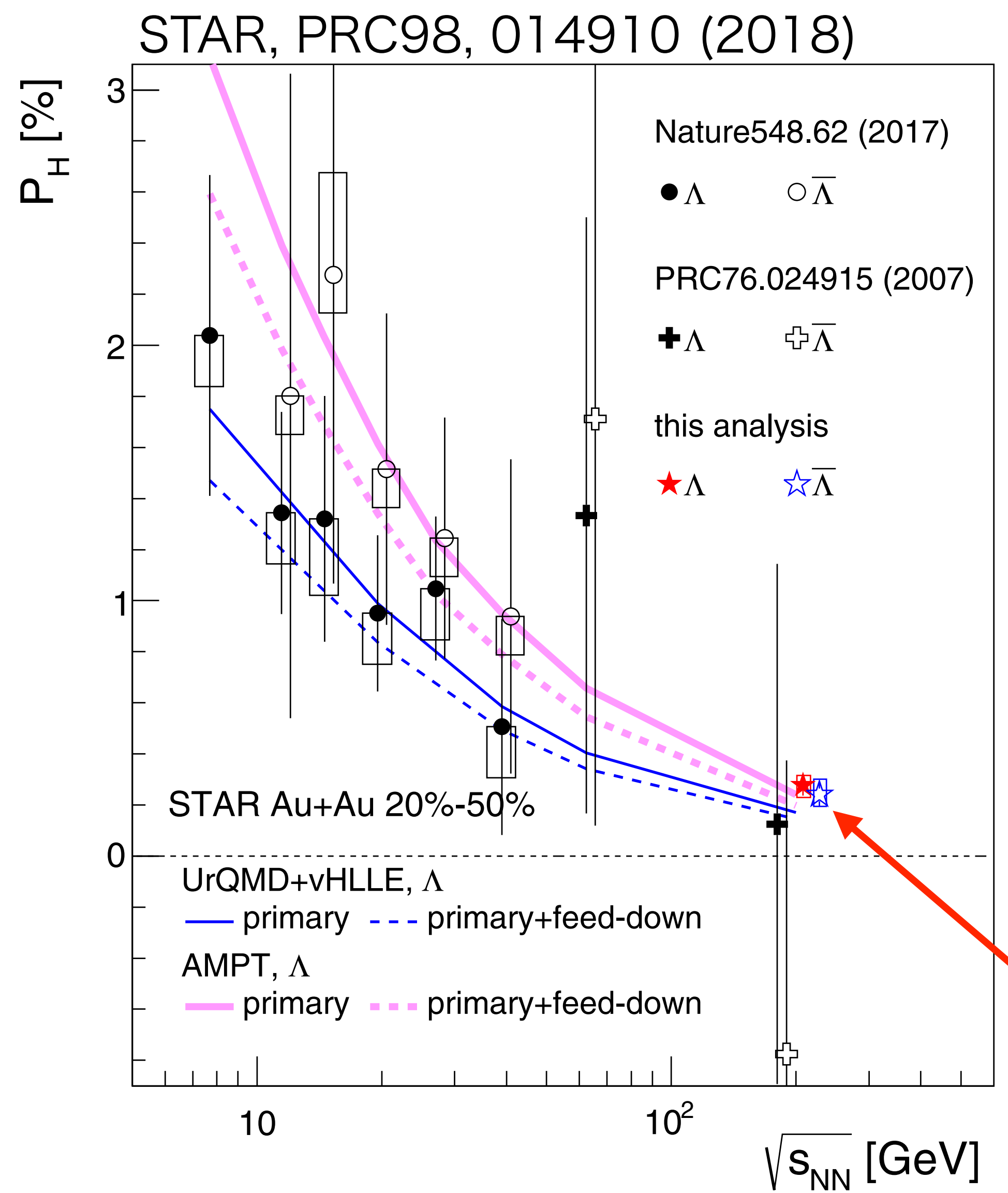
# Precise measurements at $\sqrt{s_{NN}} = 200$ GeV



- Confirmed energy dependence of  $P_H$  with new results for 200 GeV
  - $>5\sigma$  significance utilizing 1.5B events (2010+2011+2014)
  - partly due to stronger shear flow structure in lower  $\sqrt{s_{NN}}$  because of baryon stopping

$P_H(\Lambda)$  [%] =  $0.277 \pm 0.040(\text{stat}) \pm_{0.049}^{0.039}(\text{sys})$   
 $P_H(\bar{\Lambda})$  [%] =  $0.240 \pm 0.045(\text{stat}) \pm_{0.045}^{0.061}(\text{sys})$

# Precise measurements at $\sqrt{s_{NN}} = 200$ GeV

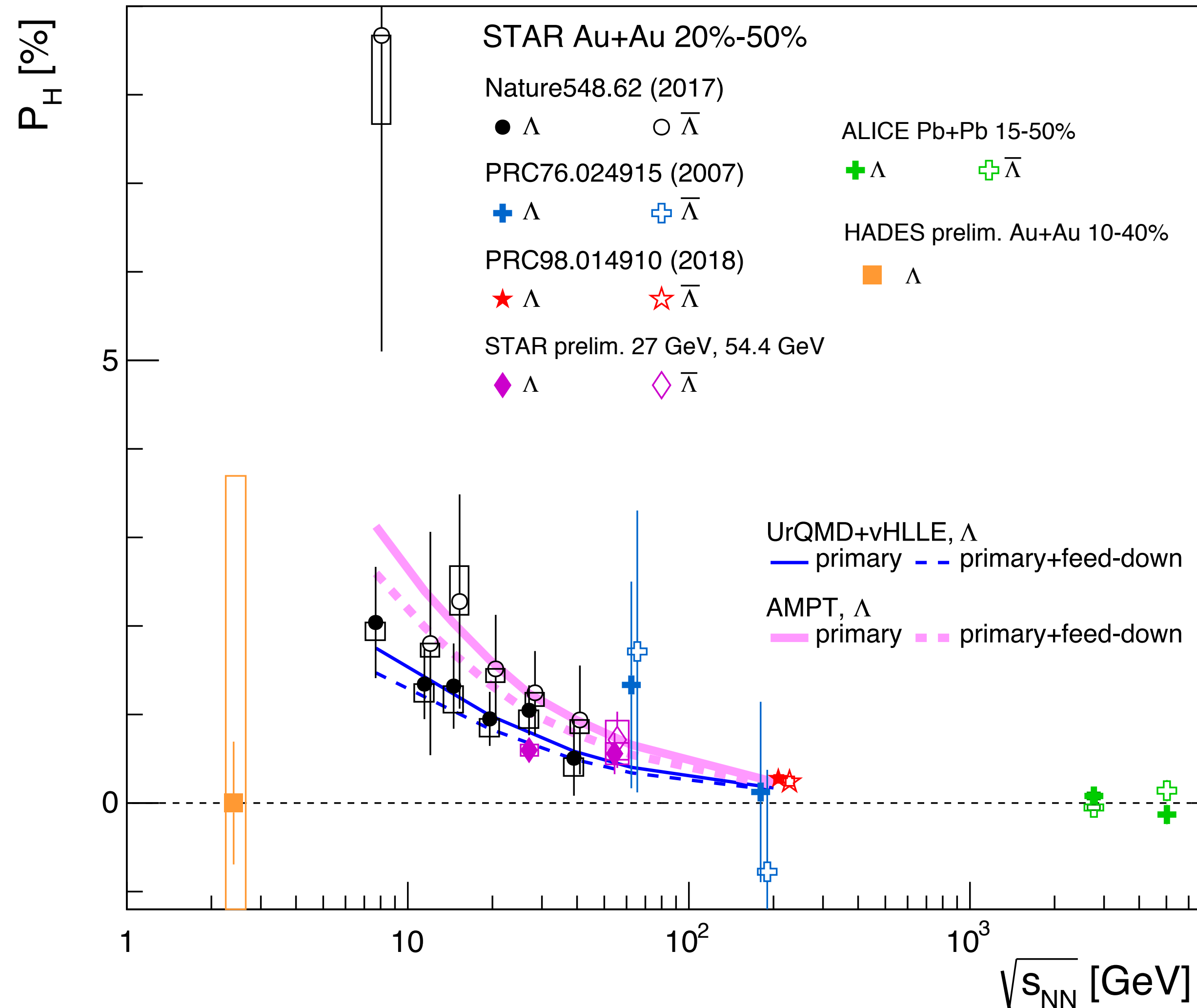


- Confirmed energy dependence of  $P_H$  with new results for 200 GeV
  - $>5\sigma$  significance utilizing 1.5B events (2010+2011+2014)
  - partly due to stronger shear flow structure in lower  $\sqrt{s_{NN}}$  because of baryon stopping
- Theoretical models can describe the data well
  - I. Karpenko and F. Becattini, EPJC(2017)77:213, UrQMD+vHLLE
  - H. Li et al., PRC96, 054908 (2017), AMPT
  - Y. Sun and C.-M. Ko, PRC96, 024906 (2017), CKE
  - Y. Xie et al., PRC95, 031901(R) (2017), PICR
  - D.-X. Wei et al., PRC99, 014905 (2019), AMPT

$$P_H(\Lambda) [\%] = 0.277 \pm 0.040(\text{stat}) \pm_{0.049}^{0.039}(\text{sys})$$

$$P_H(\bar{\Lambda}) [\%] = 0.240 \pm 0.045(\text{stat}) \pm_{0.045}^{0.061}(\text{sys})$$

# Collection of recent results



- **STAR** Au+Au at  $\sqrt{s_{NN}} = 27$  and 54.4 GeV (preliminary)

- **ALICE** Pb+Pb at  $\sqrt{s_{NN}} = 2.76$  and 5.02 TeV

$$\sqrt{s_{NN}} = 2.76 \text{ TeV}$$

$$P_H(\Lambda) [\%] = 0.08 \pm 0.10(\text{stat.}) \pm 0.04(\text{syst.})$$

$$P_H(\bar{\Lambda}) [\%] = -0.05 \pm 0.10(\text{stat.}) \pm 0.03(\text{syst.})$$

$$\sqrt{s_{NN}} = 5.02 \text{ TeV}$$

$$P_H(\Lambda) [\%] = -0.13 \pm 0.11(\text{stat.}) \pm 0.04(\text{syst.})$$

$$P_H(\bar{\Lambda}) [\%] = 0.14 \pm 0.12(\text{stat.}) \pm 0.03(\text{syst.})$$

- **HADES** Au+Au at  $\sqrt{s_{NN}} = 2.4$  GeV (preliminary)

$$P_H(\Lambda) [\%] = 3.672 \pm 0.699 \text{ (stat.)}$$

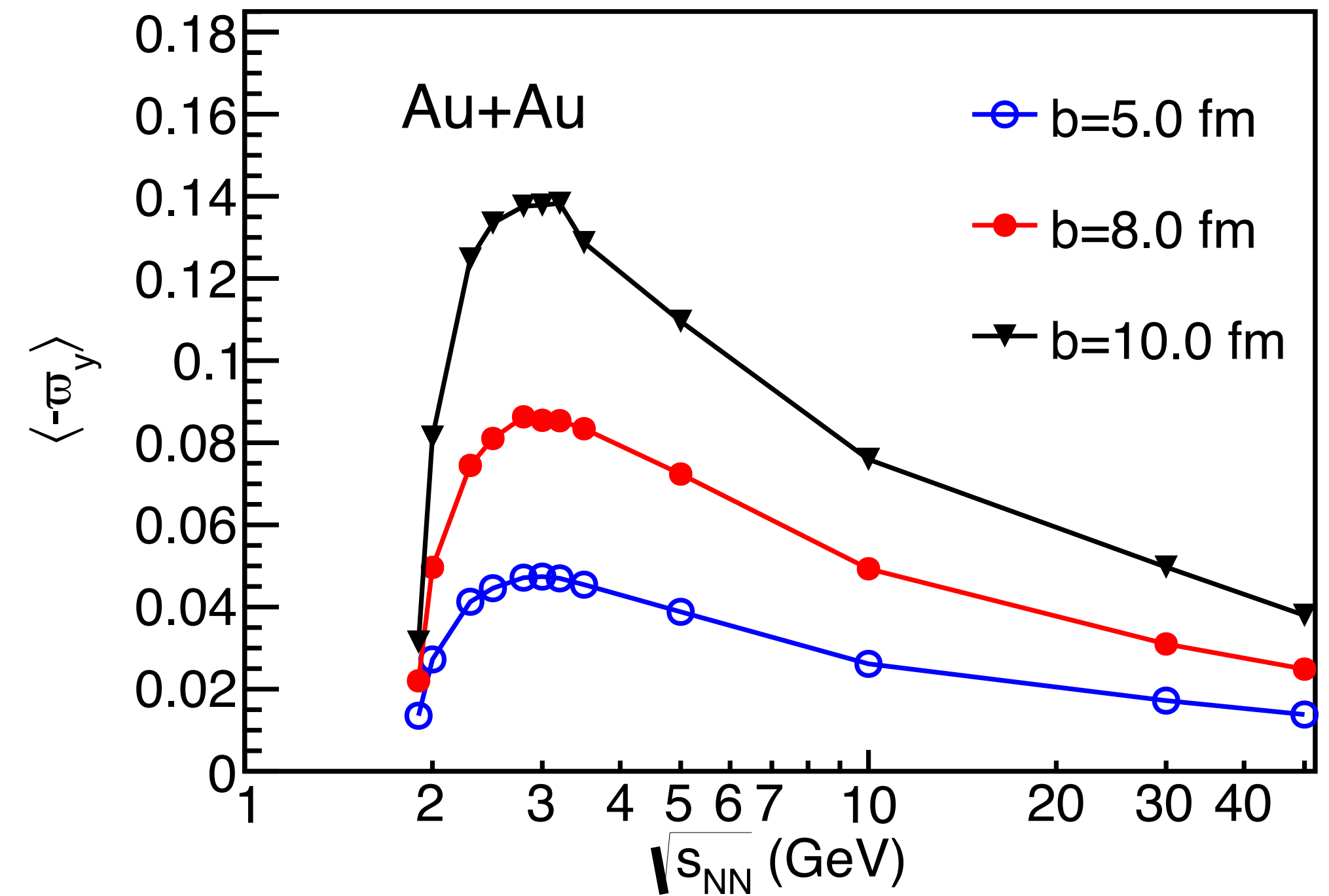
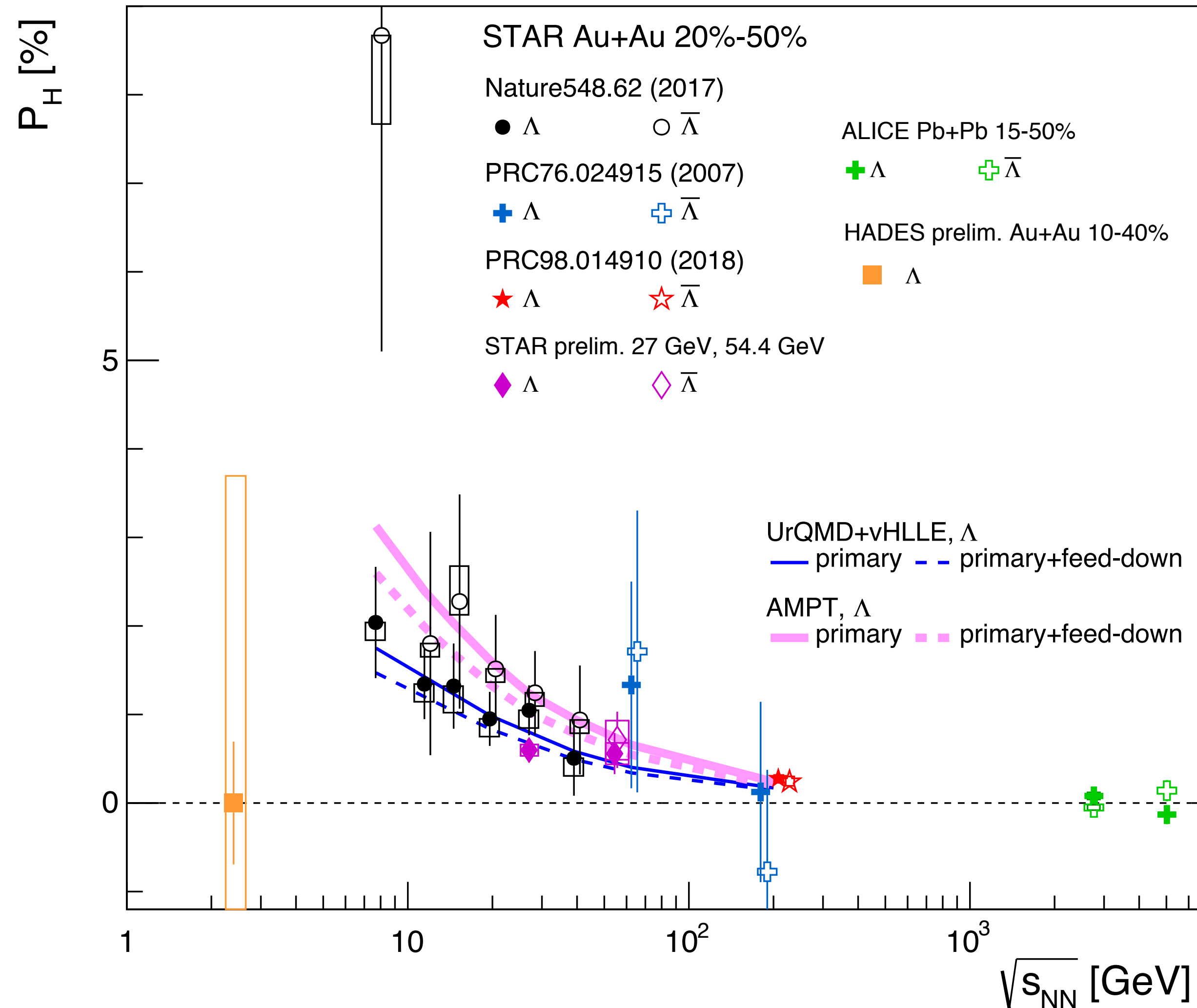
$$P_H^{\text{BG}} [\%] = 3.689 \pm 1.133 \text{ (stat.)}$$

# Collection of recent results

ALICE, arXiv1909.01281

F. Kornas (HADES), SQM2019

J. Adams, K. Okubo (STAR), QM2019



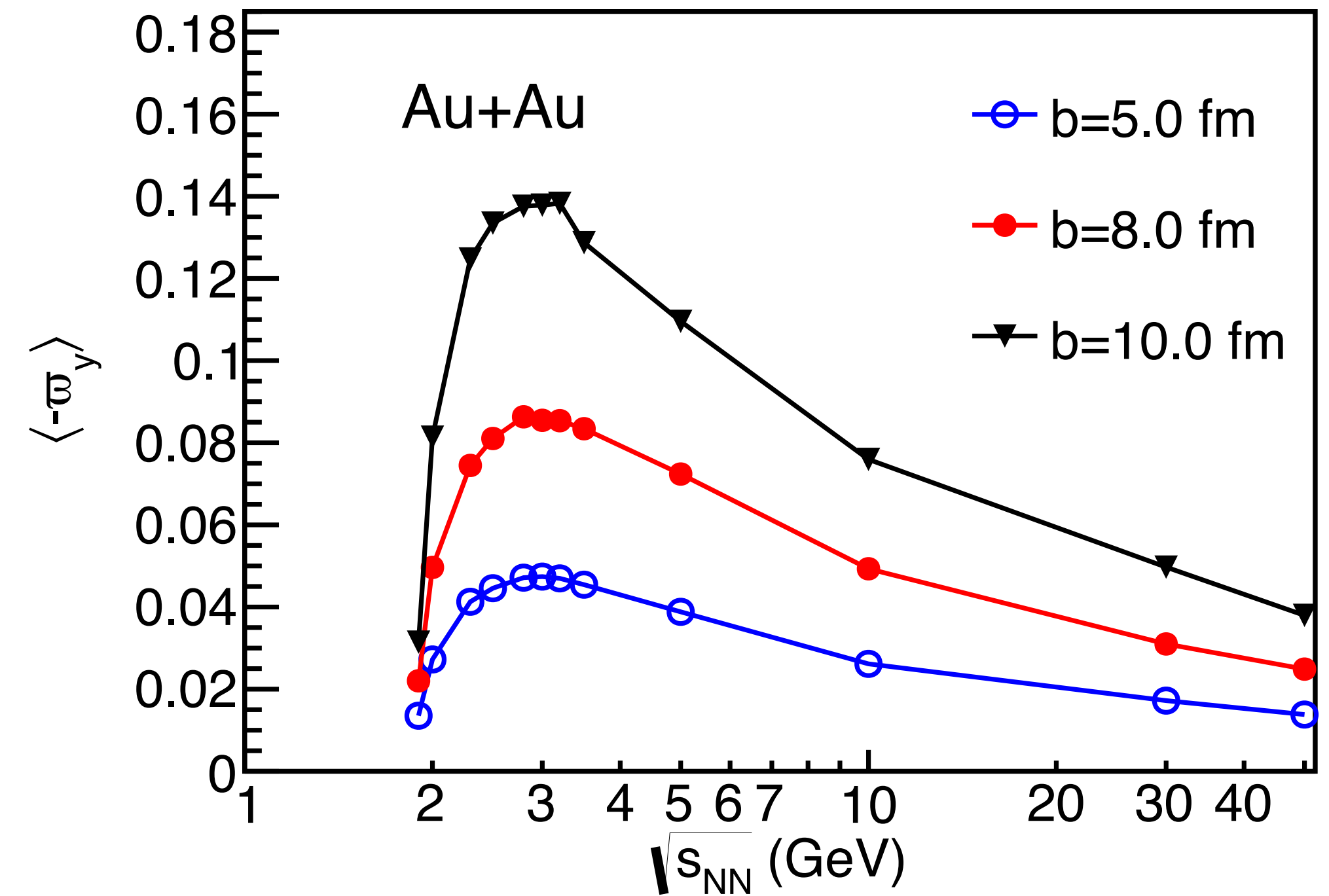
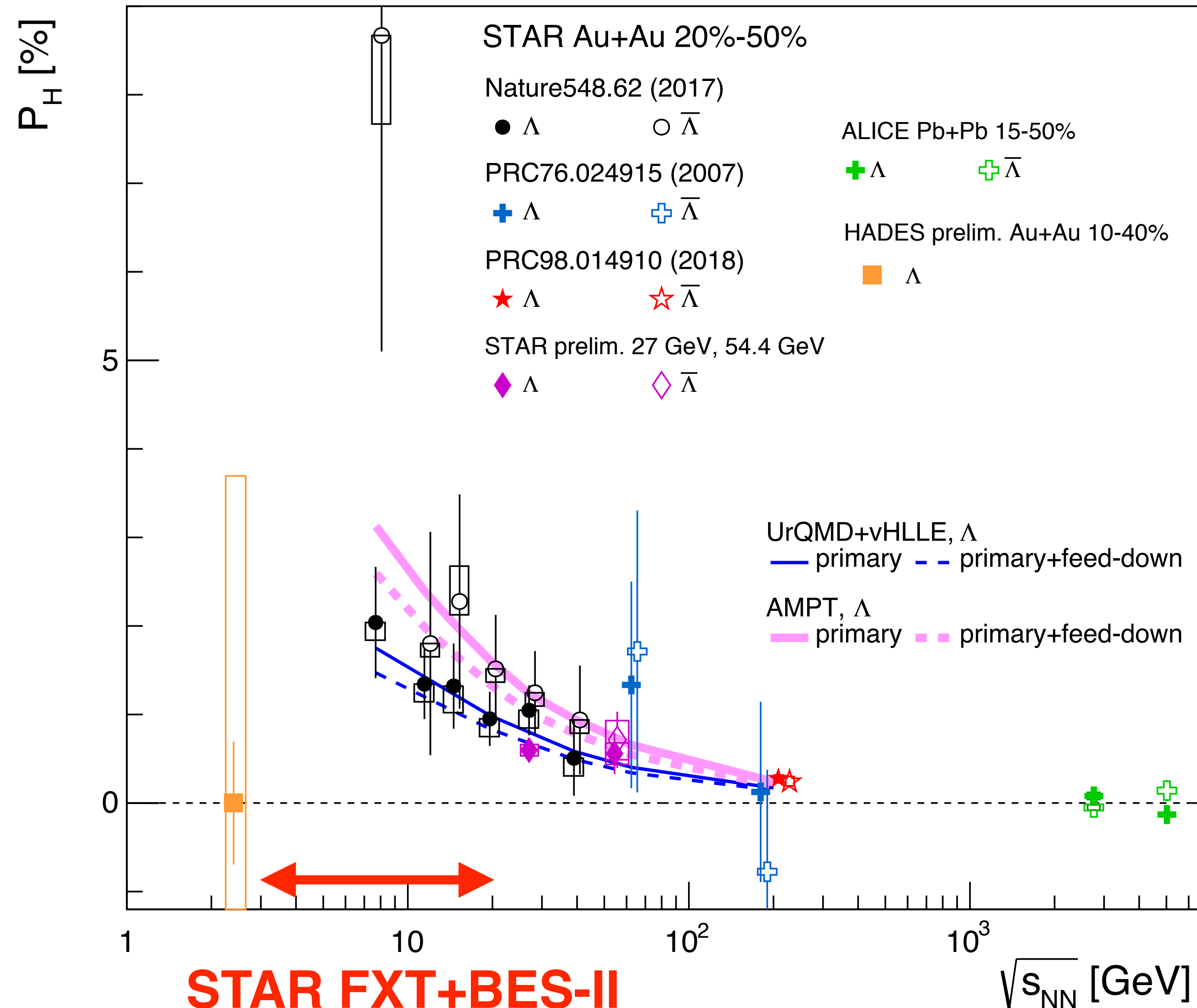
Interesting energy dependence of thermal vorticity (UrQMD)  
 X.-G. Deng et al., arXiv:2001.01371

# Collection of recent results

ALICE, arXiv1909.01281

F. Kornas (HADES), SQM2019

J. Adams, K. Okubo (STAR), QM2019

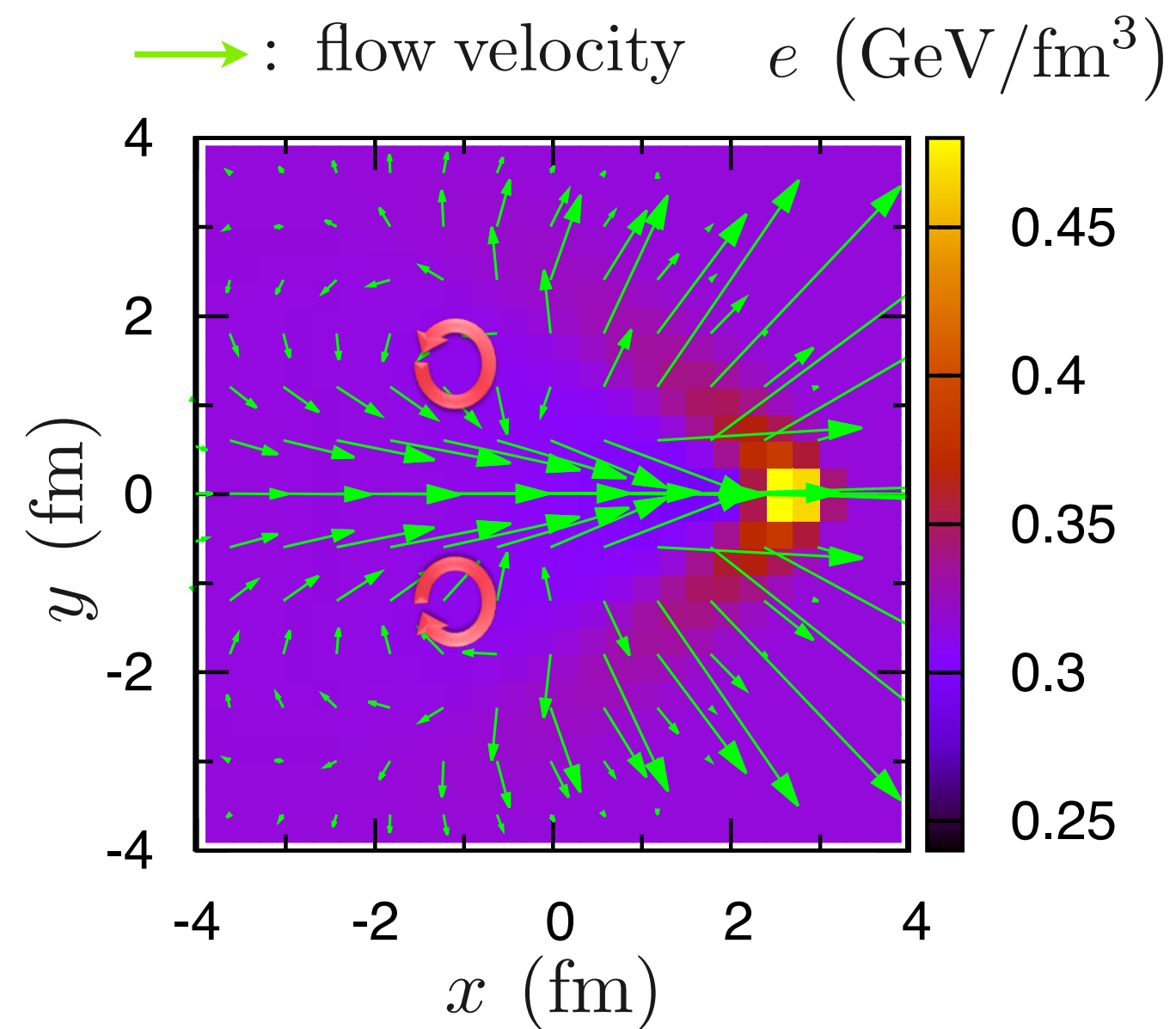


Interesting energy dependence  
of thermal vorticity (UrQMD)  
X.-G. Deng et al., arXiv:2001.01371

More interesting results will come!

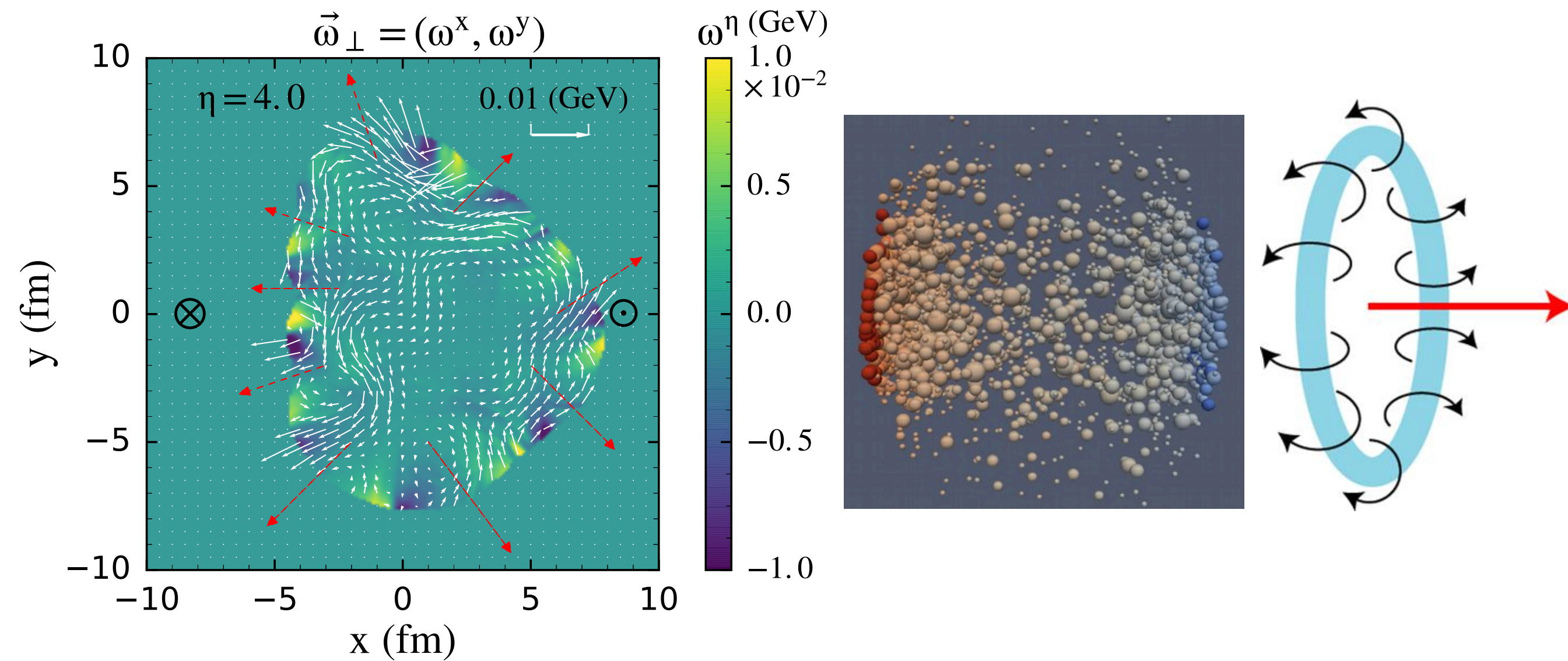
# Local vorticity

Vortex induced by jet



Y. Tachibana and T. Hirano, NPA904-905 (2013) 1023  
 B. Betz, M. Gyulassy, and G. Torrieri, PRC76.044901 (2007)

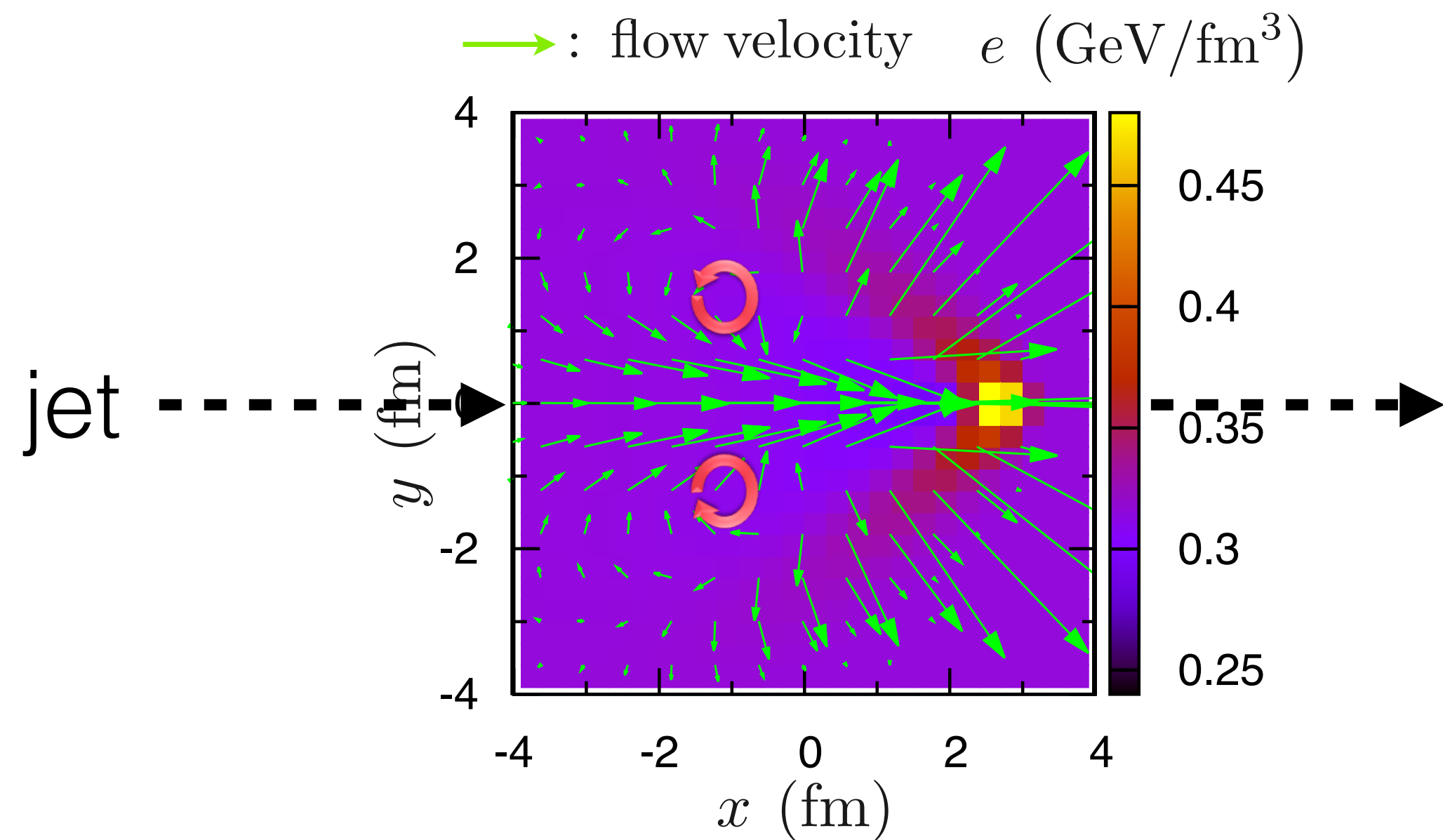
Local vorticity induced by collective flow



L.-G. Pang, H. Peterson, Q. Wang, and X.-N. Wang, PRL117, 192301 (2016)  
 F. Becattini and I. Karpenko, PRL120.012302 (2018)  
 S. Voloshin, EPJ Web Conf.171, 07002 (2018)  
 X.-L. Xia et al., PRC98.024905 (2018)

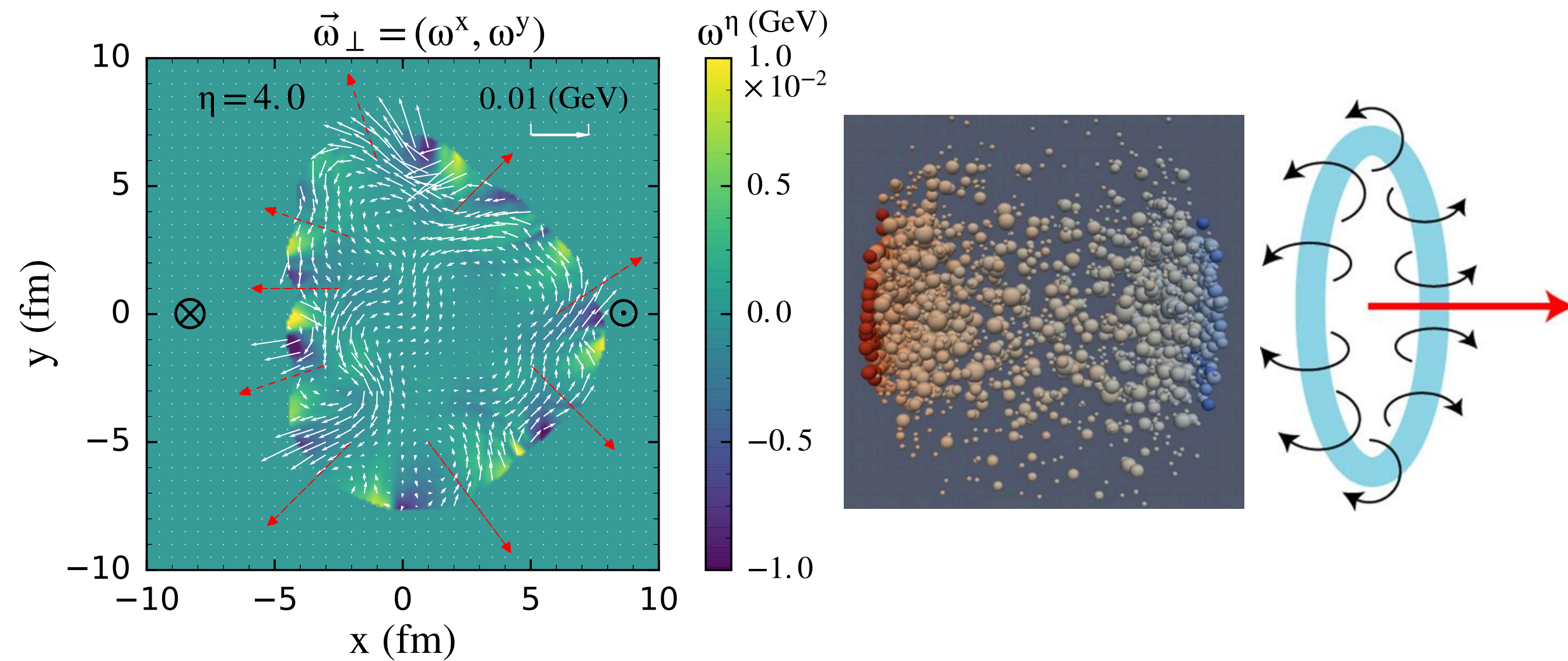
# Local vorticity

Vortex induced by jet



Y. Tachibana and T. Hirano, NPA904-905 (2013) 1023  
 B. Betz, M. Gyulassy, and G. Torrieri, PRC76.044901 (2007)

Local vorticity induced by collective flow

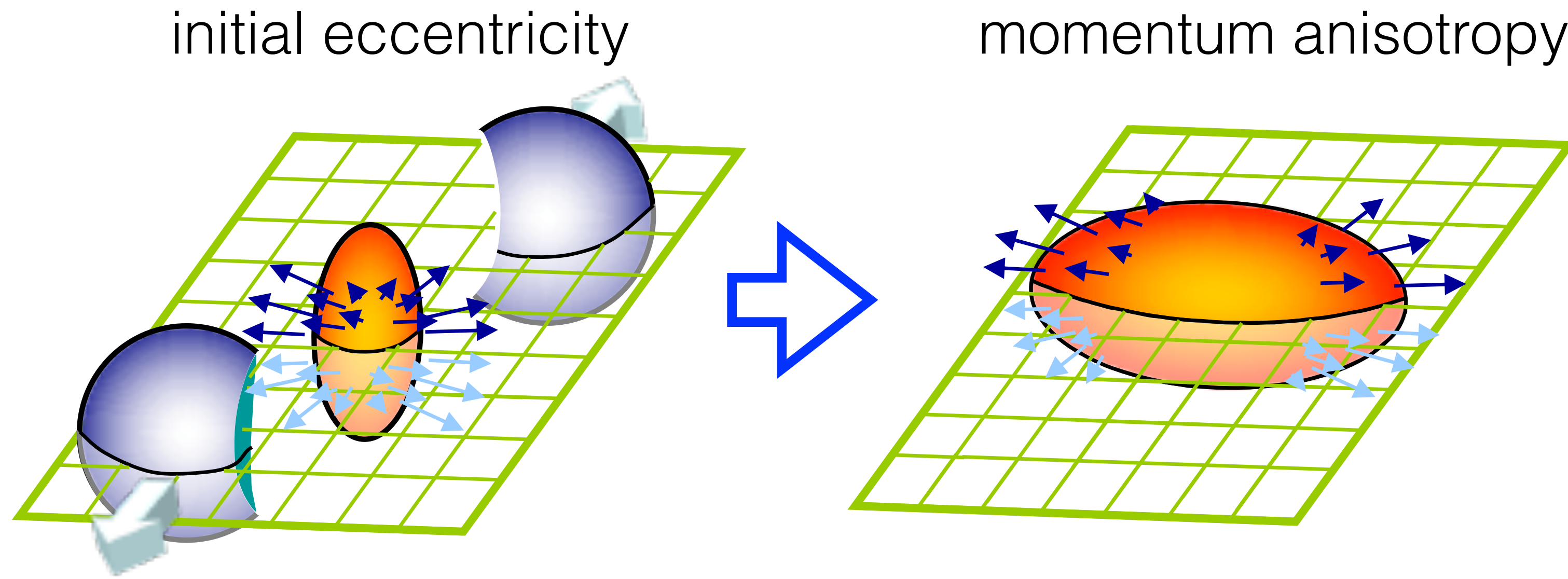


L.-G. Pang, H. Peterson, Q. Wang, and X.-N. Wang, PRL117, 192301 (2016)  
 F. Becattini and I. Karpenko, PRL120.012302 (2018)  
 S. Voloshin, EPJ Web Conf.171, 07002 (2018)  
 X.-L. Xia et al., PRC98.024905 (2018)

# Local vorticity due to the elliptic flow?

S. Voloshin, SQM2017

F. Becattini and I. Karpenko, PRL120.012302 (2018)



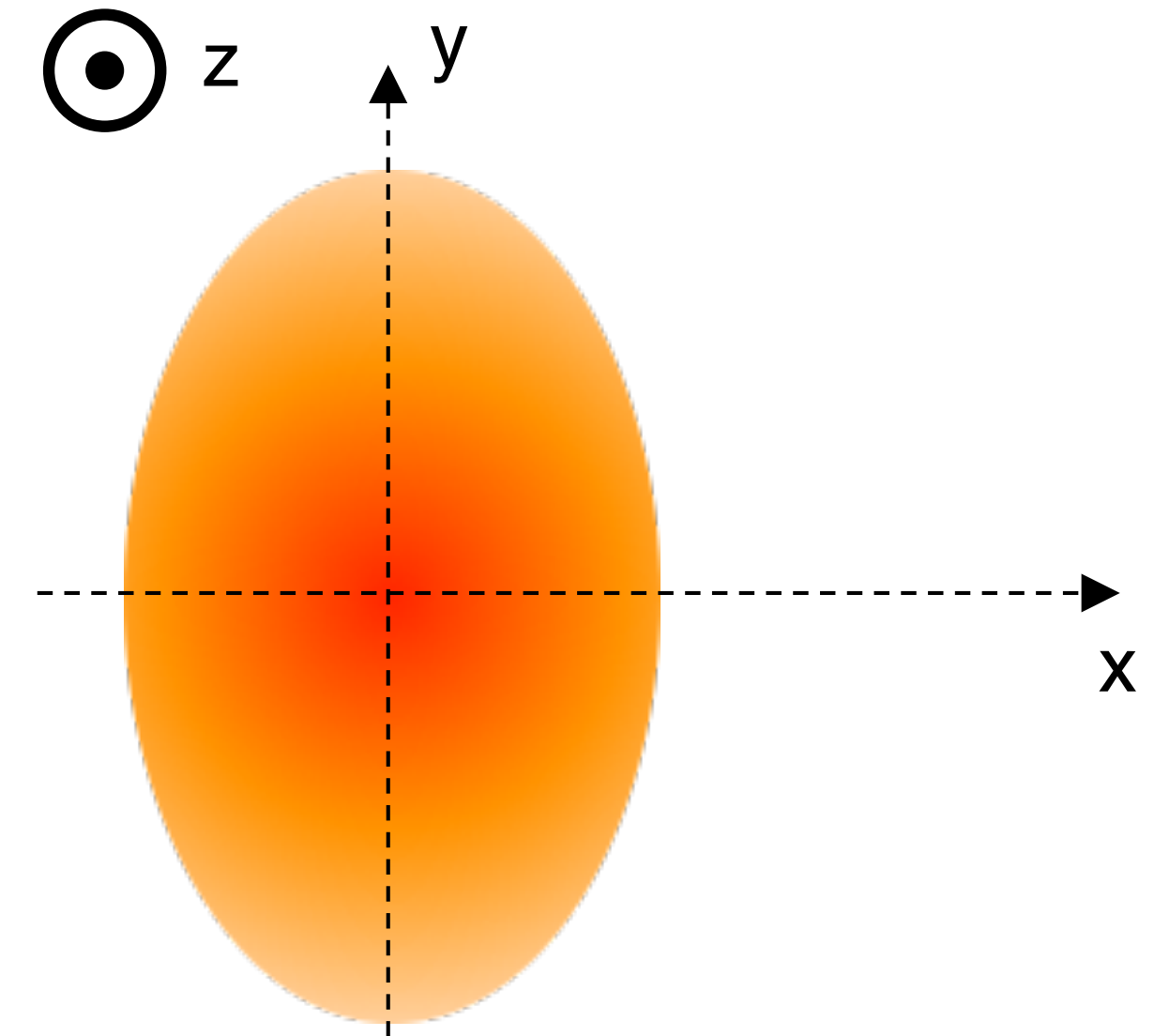
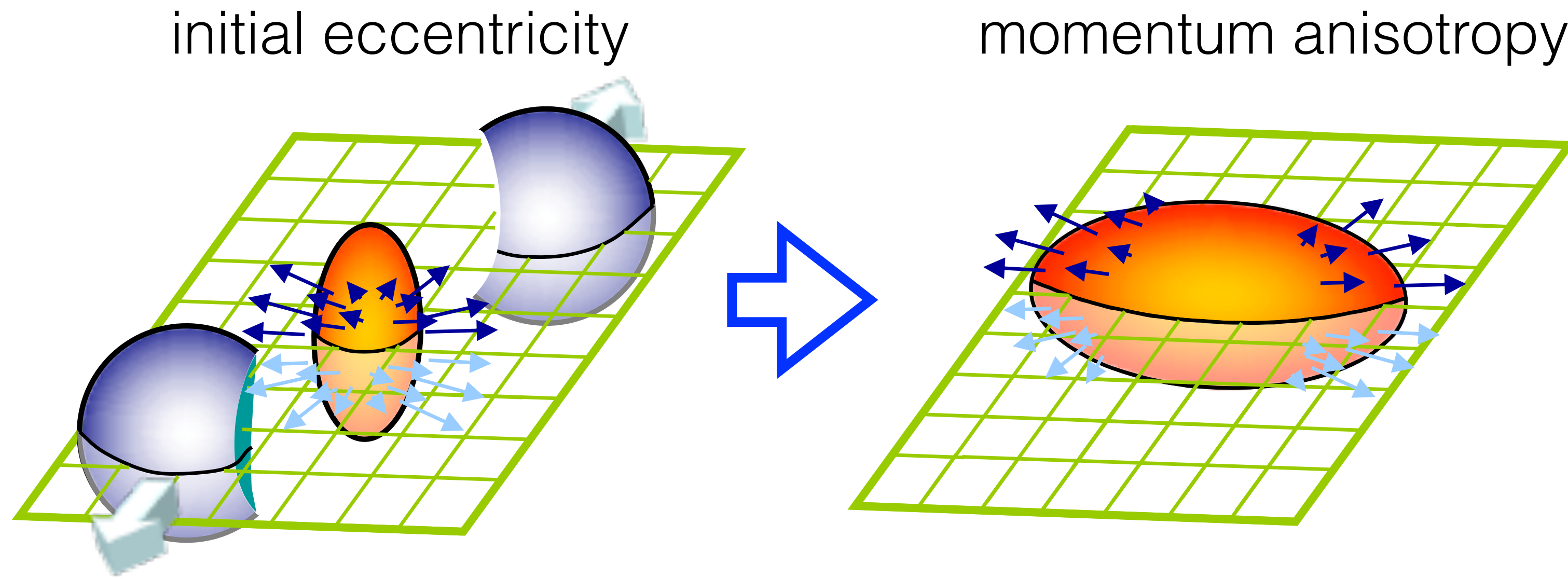
Stronger flow in in-plane (short-axis) than in out-of-plane (long axis) due to different pressure gradient, called the elliptic flow



# Local vorticity due to the elliptic flow?

S. Voloshin, SQM2017

F. Becattini and I. Karpenko, PRL120.012302 (2018)

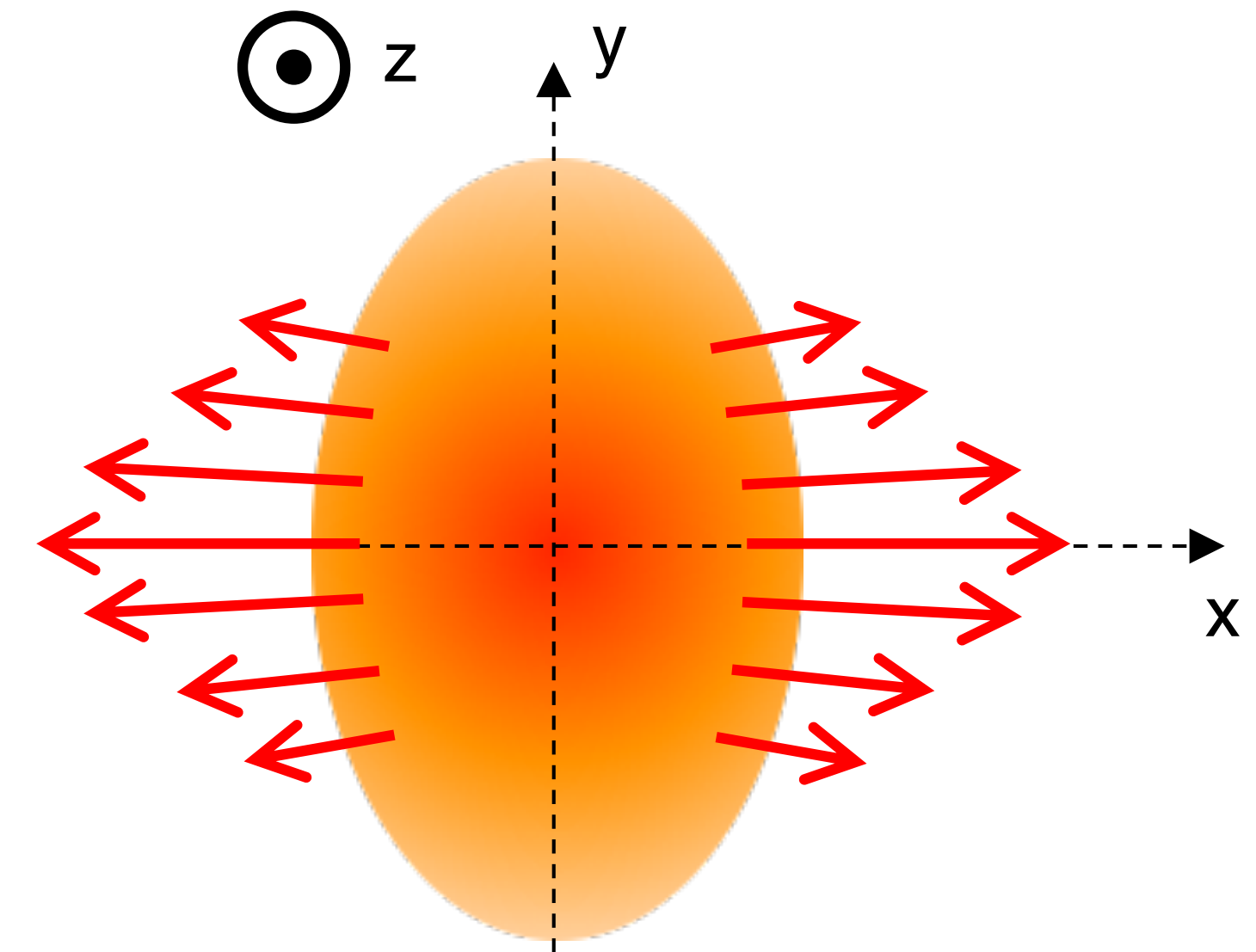
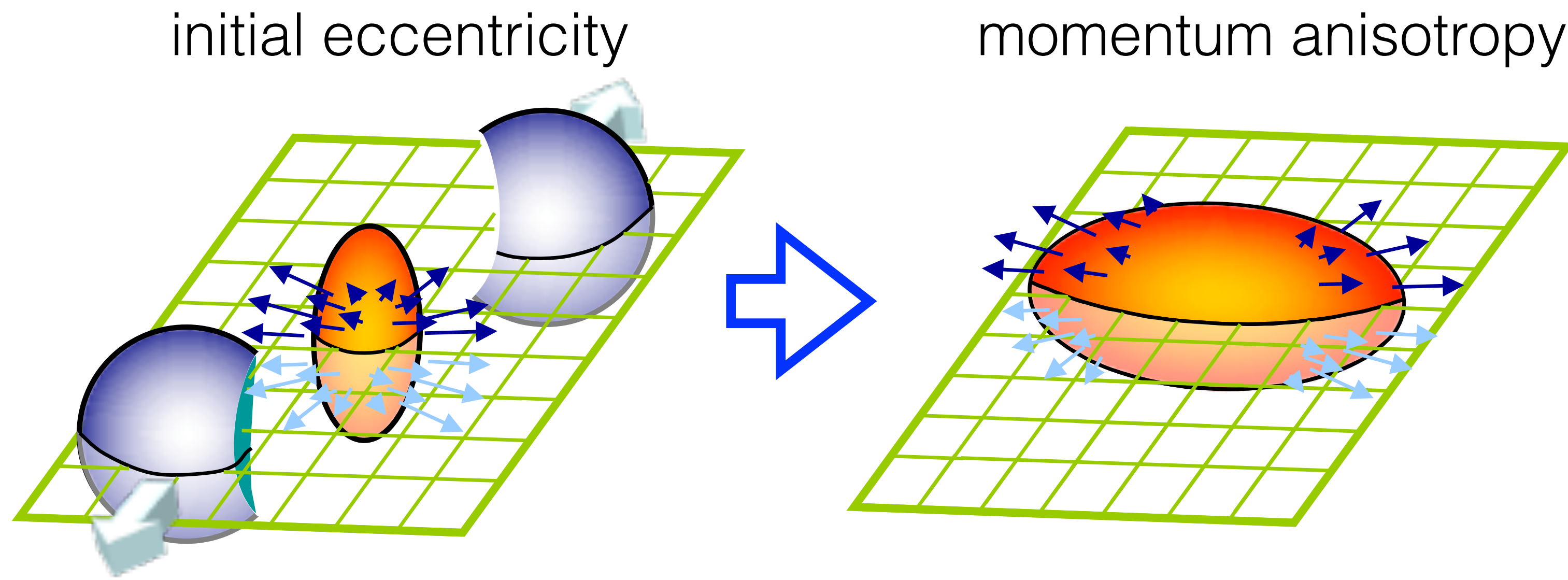


Stronger flow in in-plane (short-axis) than in out-of-plane (long axis) due to different pressure gradient, called the elliptic flow

# Local vorticity due to the elliptic flow?

S. Voloshin, SQM2017

F. Becattini and I. Karpenko, PRL120.012302 (2018)

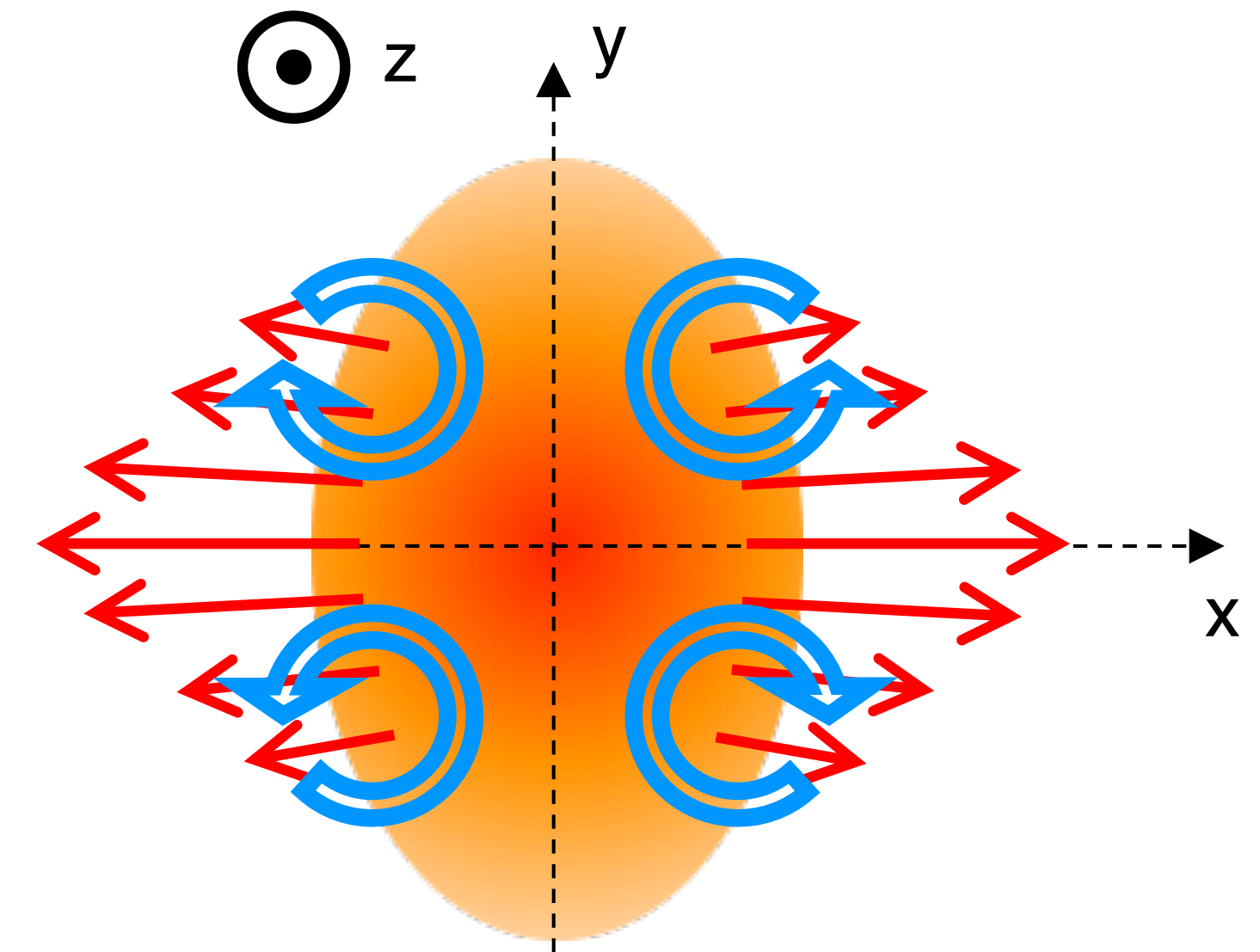
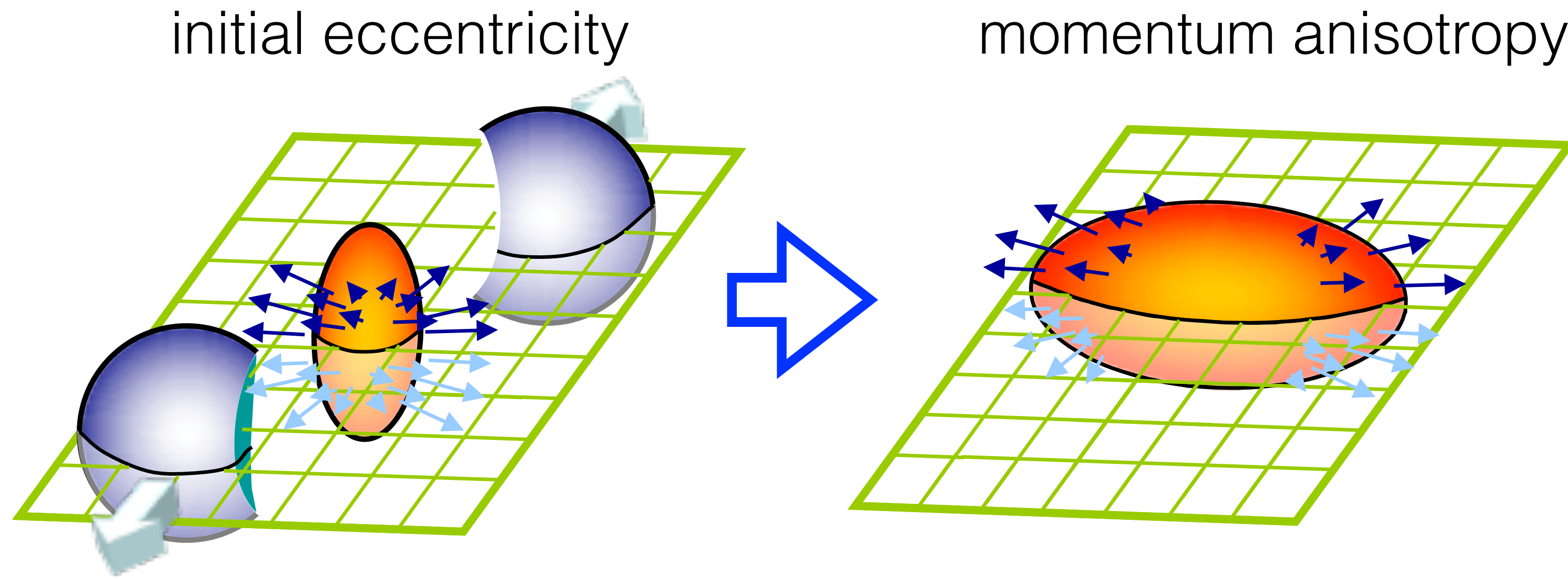


Stronger flow in in-plane (short-axis) than in out-of-plane (long axis) due to different pressure gradient, called the elliptic flow

# Local vorticity due to the elliptic flow?

S. Voloshin, SQM2017

F. Becattini and I. Karpenko, PRL120.012302 (2018)



Stronger flow in in-plane (short-axis) than in out-of-plane (long axis)  
due to different pressure gradient, called the elliptic flow

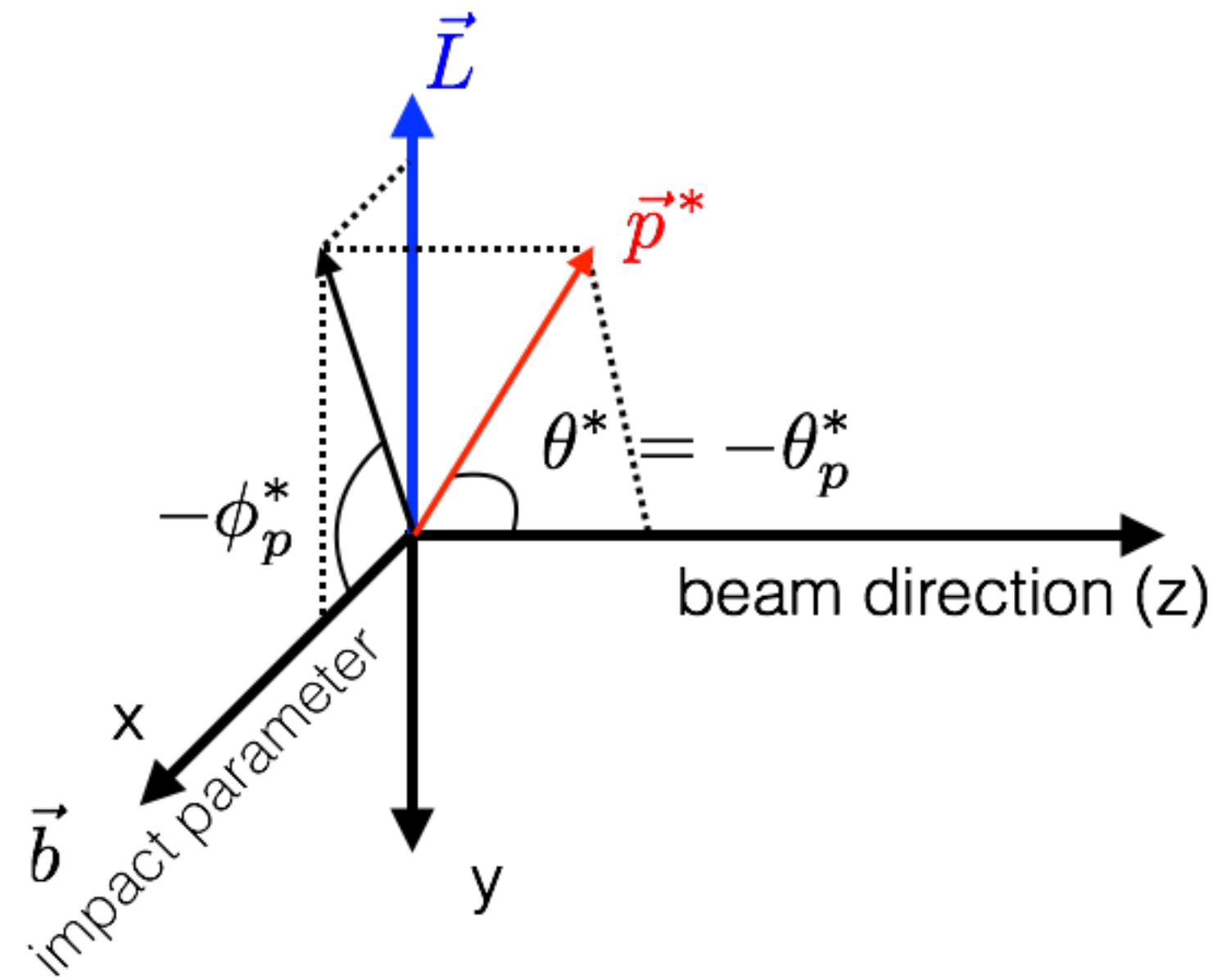
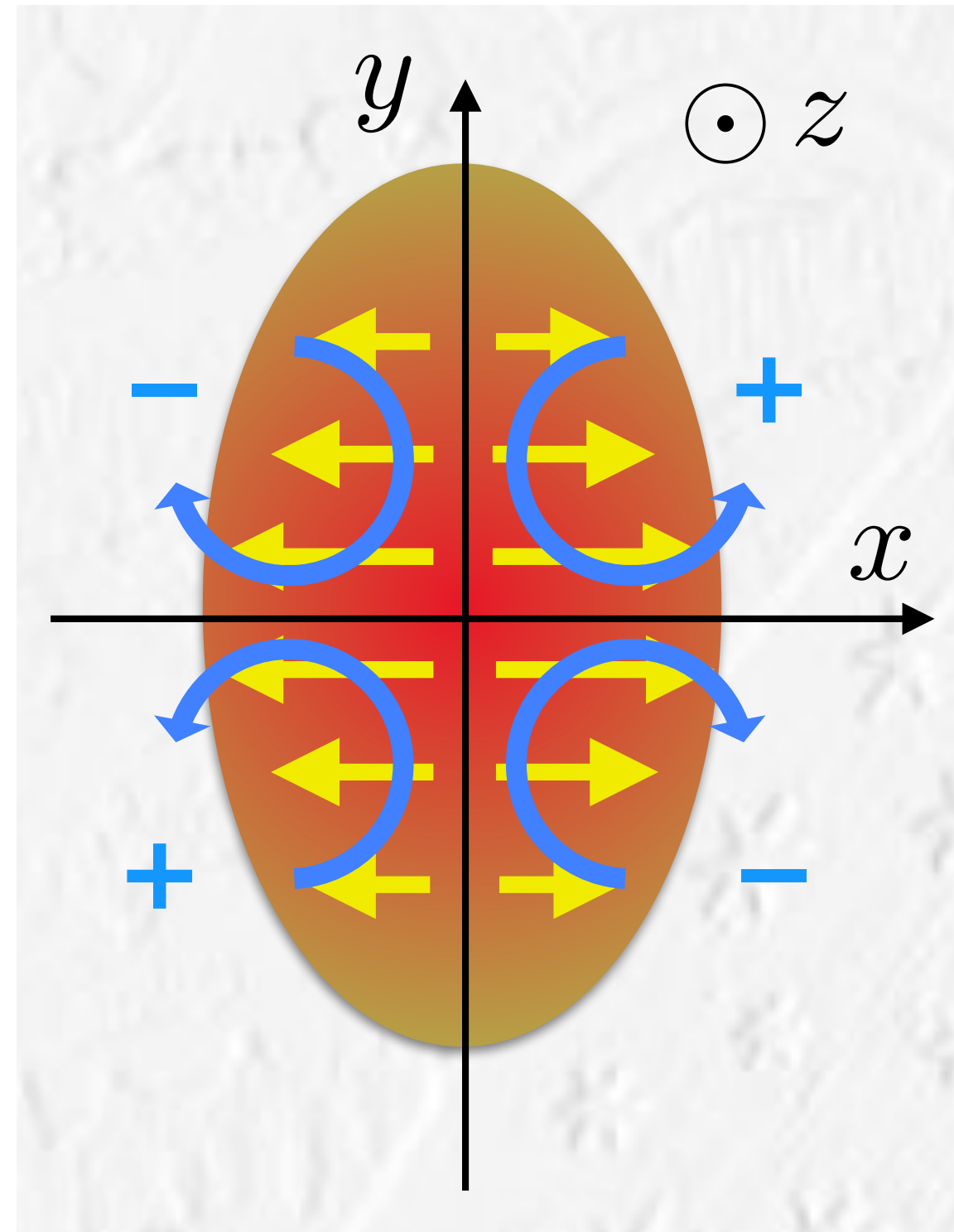
Vorticity along the beam axis!?

The rotational axis would depend on azimuthal angle

# Polarization along the beam direction

S. Voloshin, SQM2017

F. Becattini and I. Karpenko, PRL120.012302 (2018)



$$\begin{aligned} \frac{dN}{d\Omega^*} &= \frac{1}{4\pi} (1 + \alpha_H \mathbf{P}_H \cdot \mathbf{p}_p^*) \\ \langle \cos \theta_p^* \rangle &= \int \frac{dN}{d\Omega^*} \cos \theta_p^* d\Omega^* \\ &= \alpha_H P_z \langle (\cos \theta_p^*)^2 \rangle \\ \therefore P_z &= \frac{\langle \cos \theta_p^* \rangle}{\alpha_H \langle (\cos \theta_p^*)^2 \rangle} \\ &= \frac{3 \langle \cos \theta_p^* \rangle}{\alpha_H} \quad (\text{if perfect detector}) \end{aligned}$$

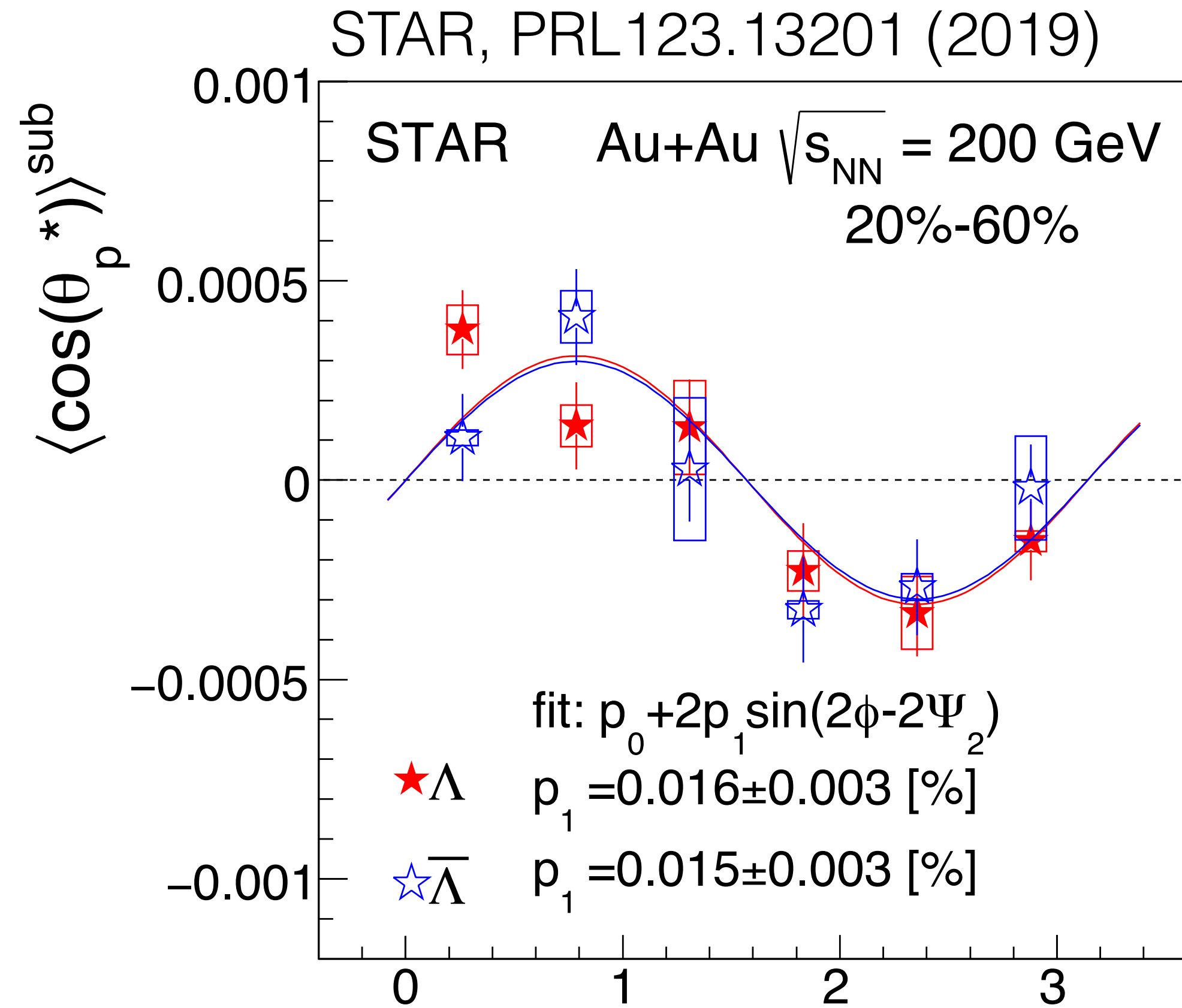
$\alpha_H$ : hyperon decay parameter

$\theta_p^*$ :  $\theta$  of daughter proton in  $\Lambda$  rest frame

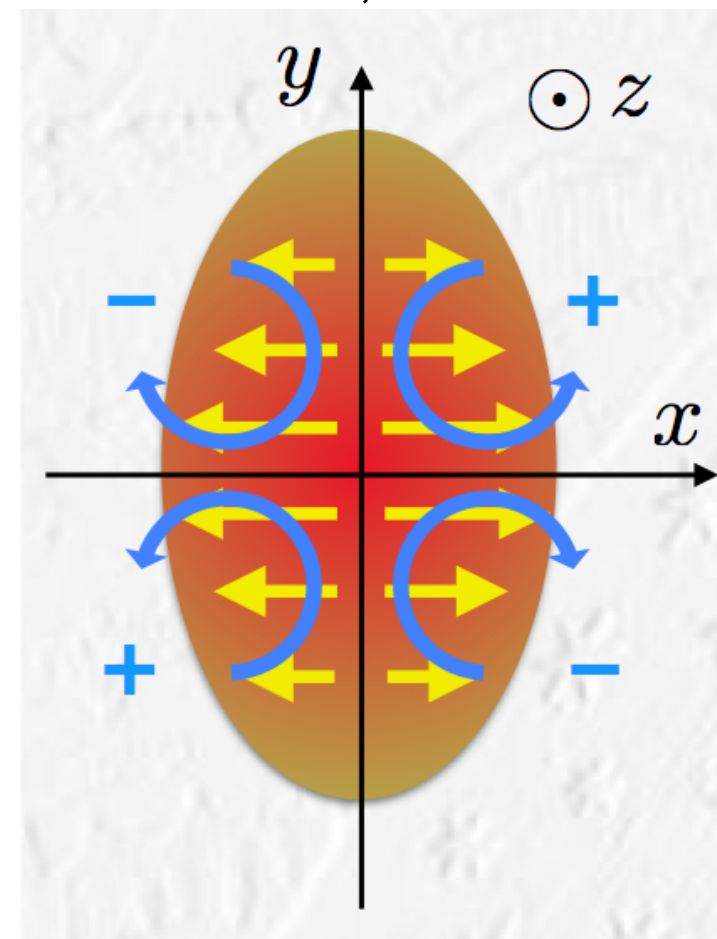
Stronger flow in in-plane than in out-of-plane could make local polarization along beam axis!

Longitudinal component,  $P_z$ , can be expressed with  $\langle \cos \theta_p^* \rangle$ .  $\langle (\cos \theta_p^*)^2 \rangle$  accounts for an acceptance effect

# Polarization along the beam direction



S. Voloshin, SQM2017

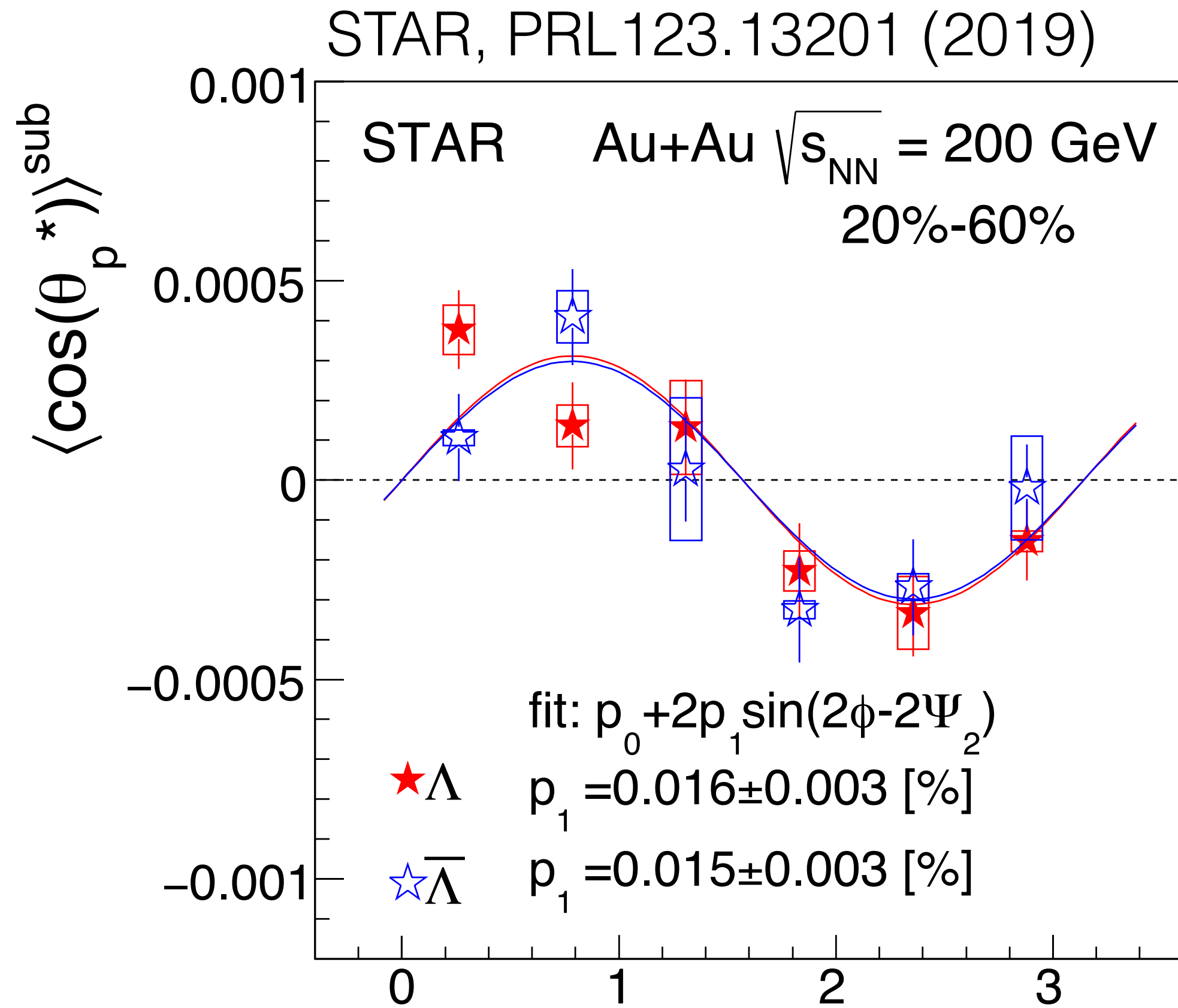


□ Sine structure as expected from the elliptic flow!

$$P_z \propto \langle \cos \theta_p^* \rangle \quad \phi - \Psi_2 \text{ [rad]}$$

- Effect of  $\Psi_2$  resolution is not corrected here

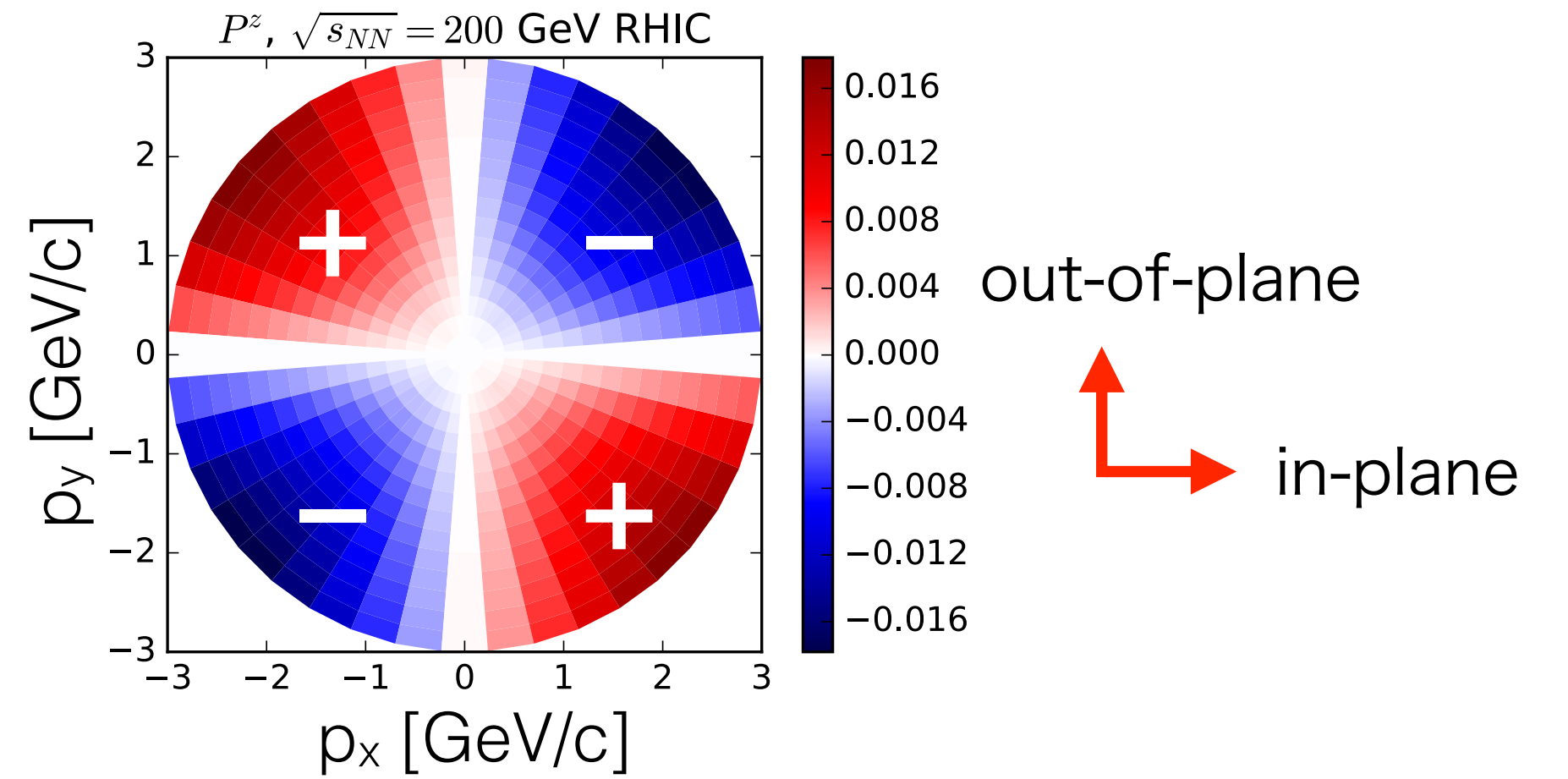
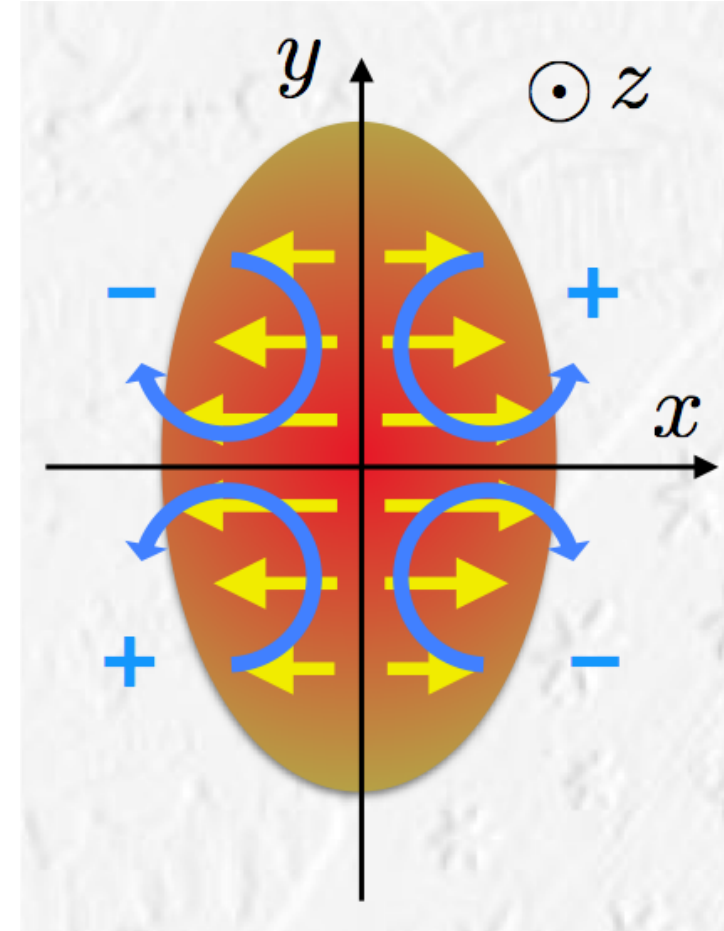
# Polarization along the beam direction



$$P_z \propto \langle \cos \theta_p^* \rangle \quad \phi - \Psi_2 \text{ [rad]}$$

- Effect of  $\Psi_2$  resolution is not corrected here

S. Voloshin, SQM2017

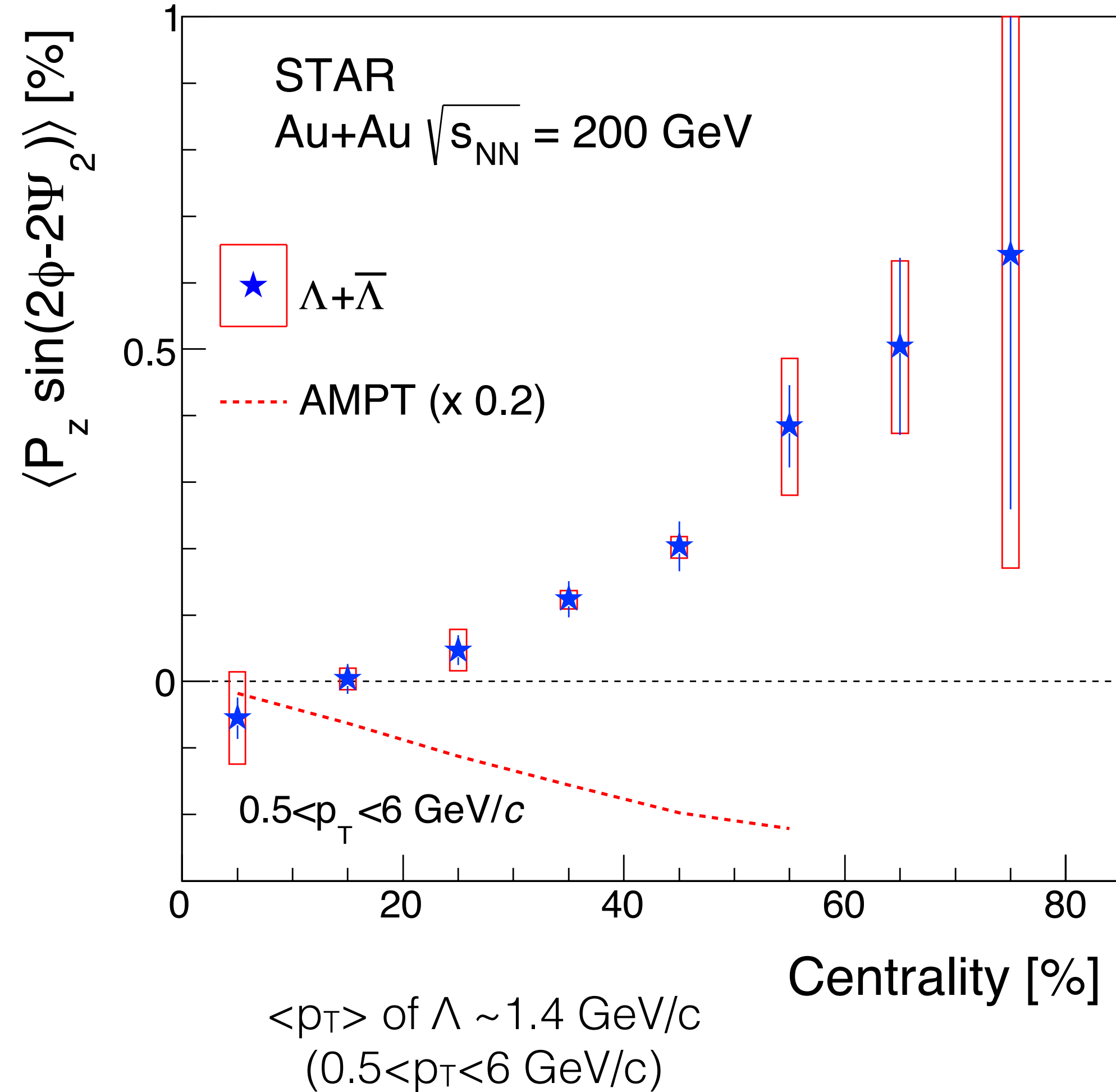


- Sine structure as expected from the elliptic flow!
- Some models (viscous hydro, AMPT) cannot describe the sign but some of them (chiral kinetic, PICR) can do.

- F. Becattini and I. Karpenko, PRL.120.012302 (2018)
- X. Xia, H. Li, Z. Tang, Q. Wang, PRC98.024905 (2018)
- Y. Sun and C.-M. Ko, PRC99, 011903(R) (2019)
- Y. Xie, D. Wang, and L. P. Csernai, arXiv:1907.00773

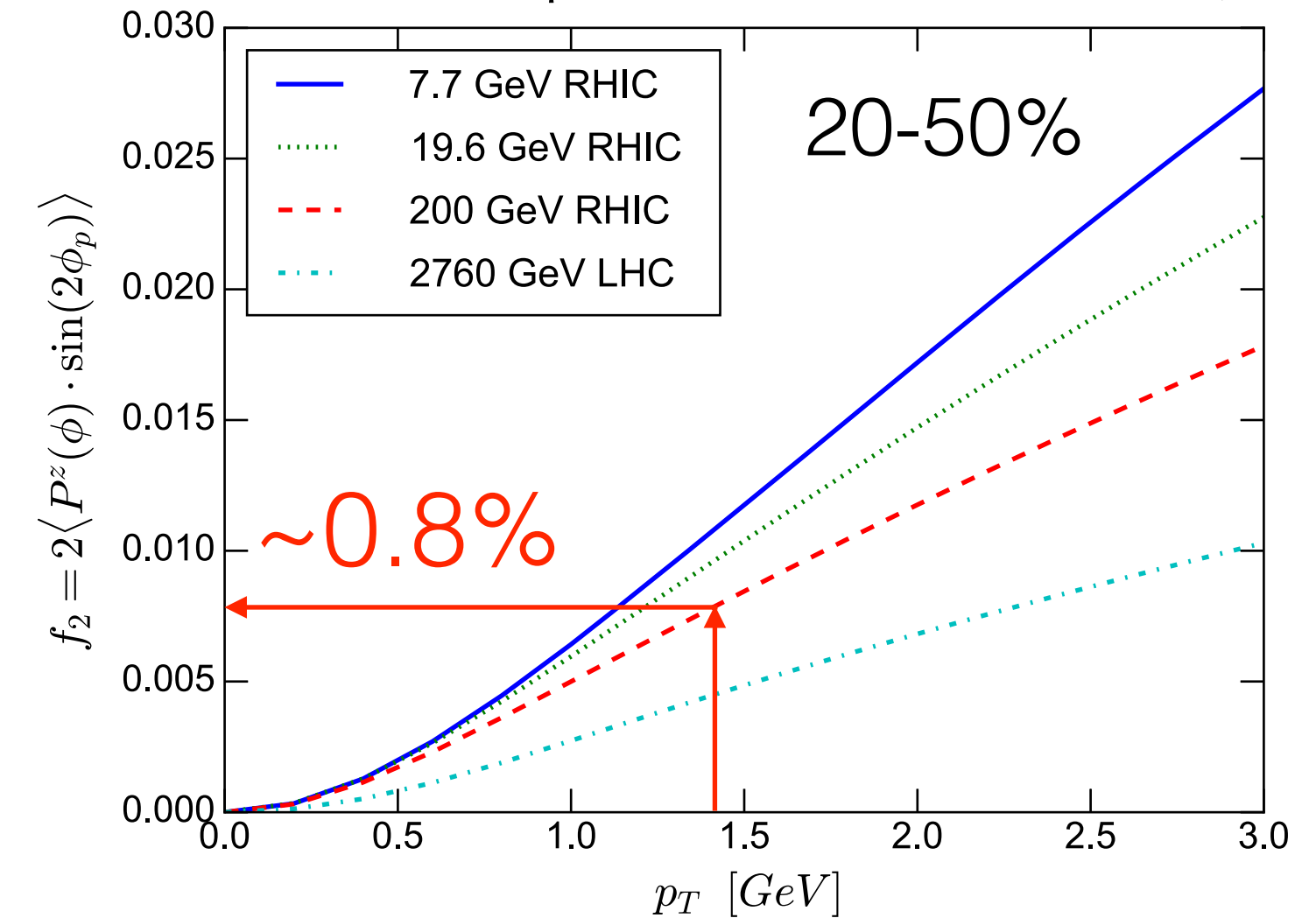
# Centrality dependence of $P_z$ modulation

STAR, PRL123.13201 (2019)



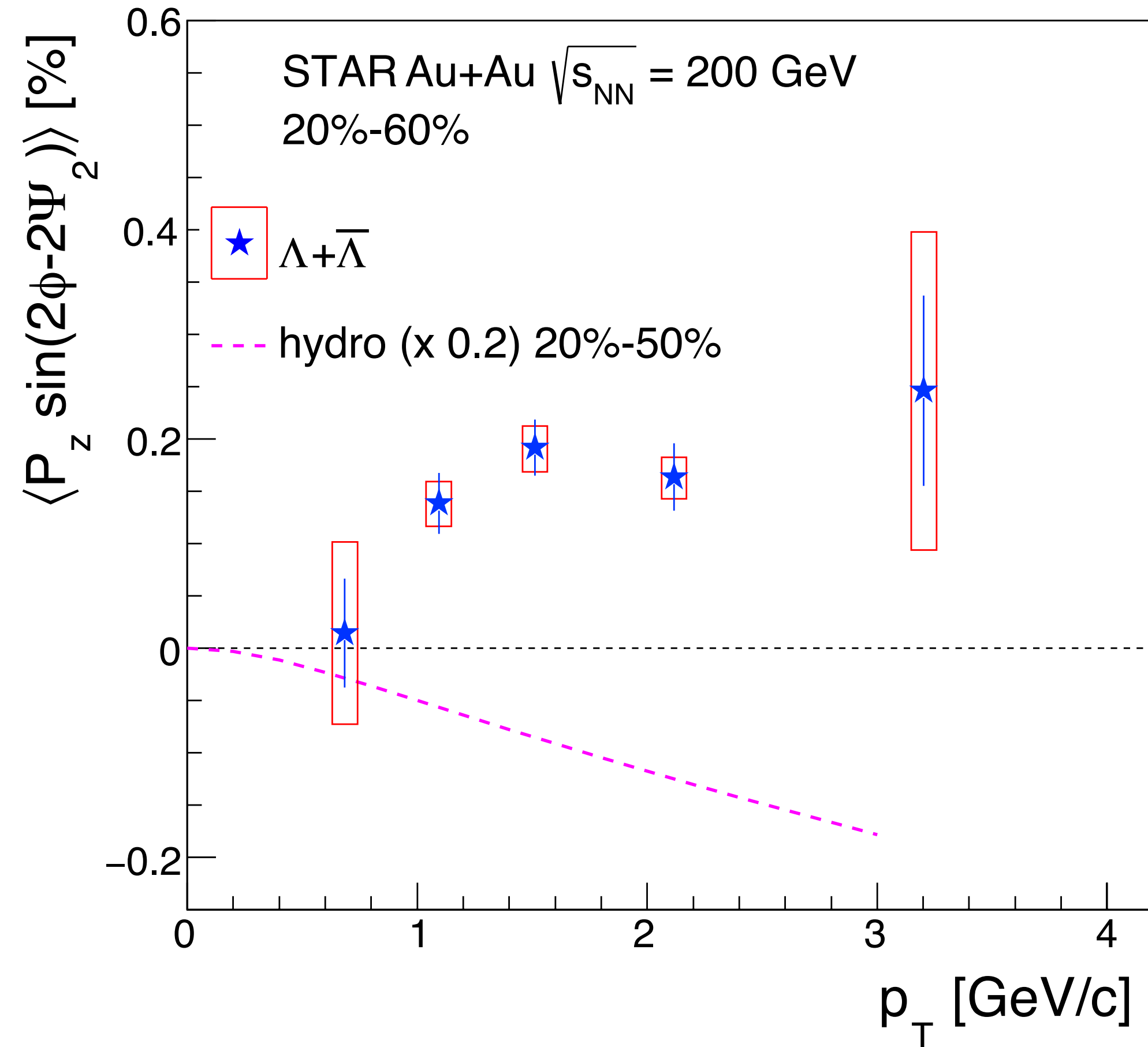
- Strong centrality dependence as in  $v_2$
- Similar magnitude to the global polarization
- ~5 times smaller magnitude than the hydro and AMPT with the opposite sign!

F. Becattini and I. Karpenko, PRL.120.012302 (2018)



# $p_T$ dependence of $P_z$ modulation

STAR, PRL123.13201 (2019)



- No strong  $p_T$  dependence for  $p_T > 1$  GeV/c
- A hint of drop-off at  $p_T < 1$  GeV/c
- Hydrodynamic model also predicts a mild  $p_T$  dependence but with the opposite sign and larger magnitude

Hydrodynamic model

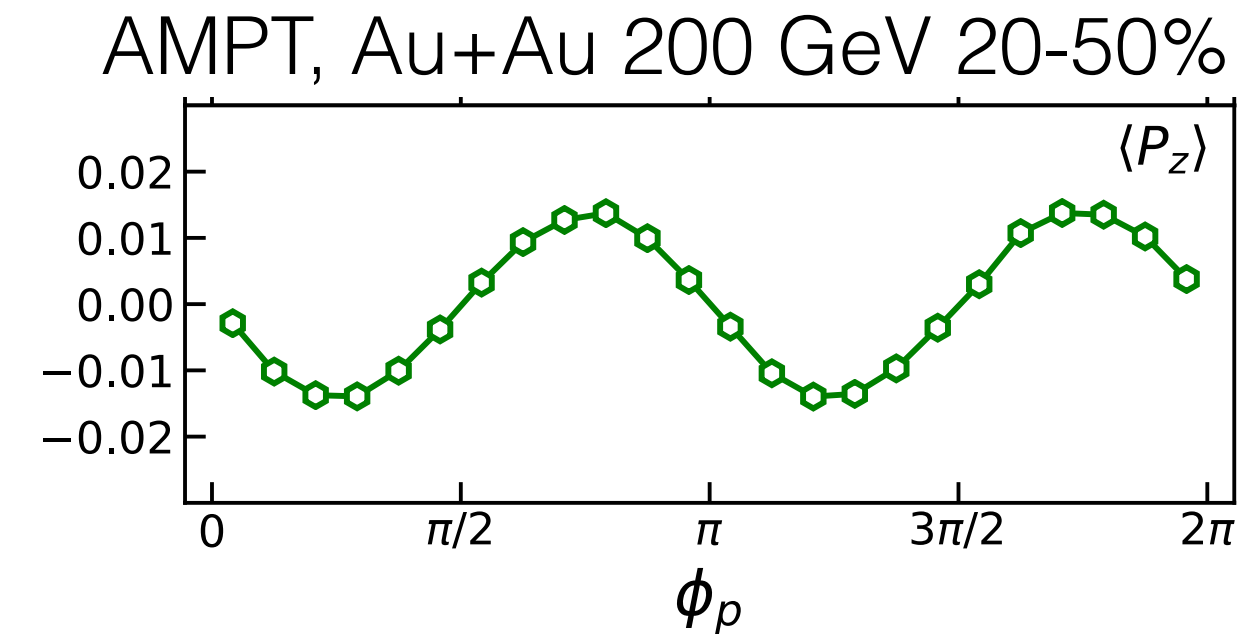
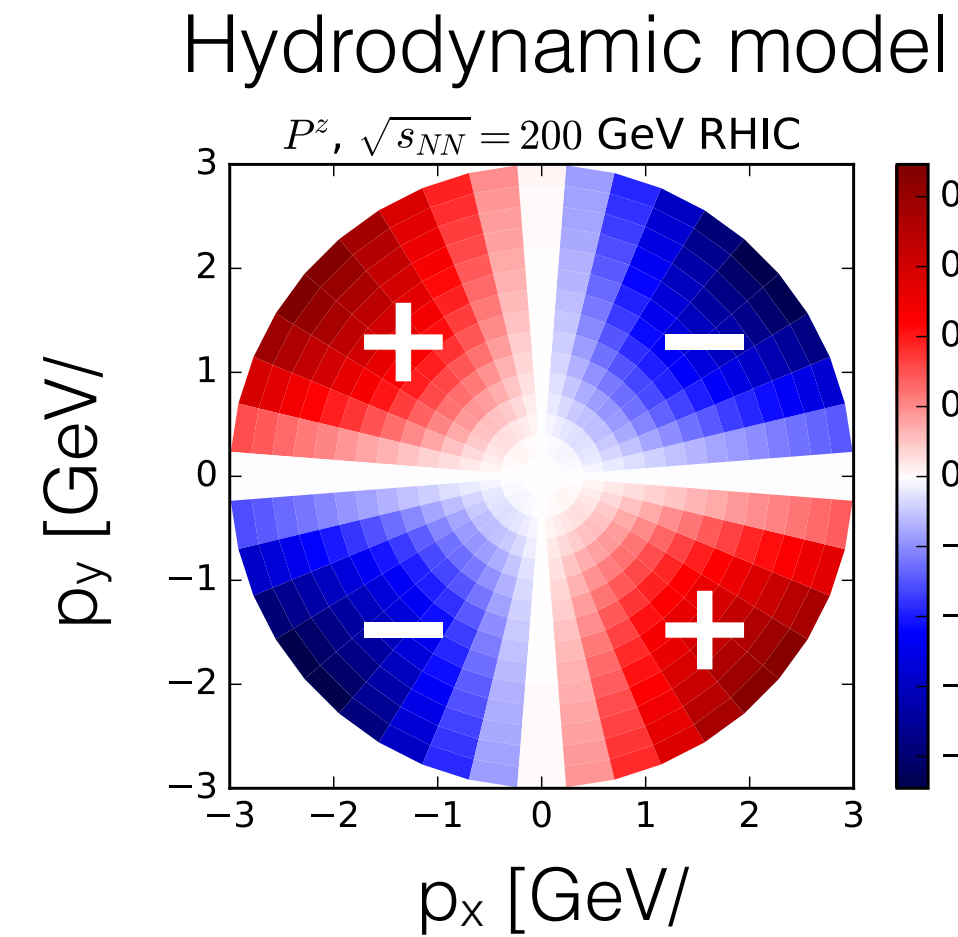
F. Becattini and I. Karpenko, PRL.120.012302 (2018)



# Disagreement in $P_z$ sign

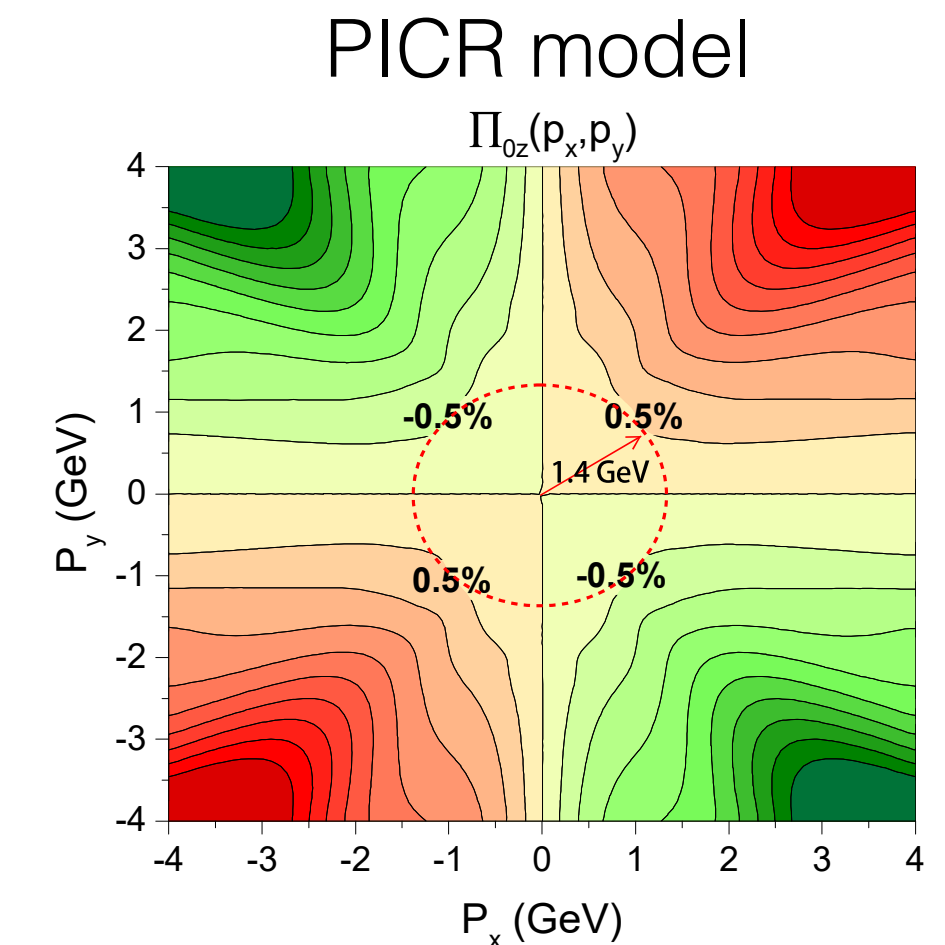
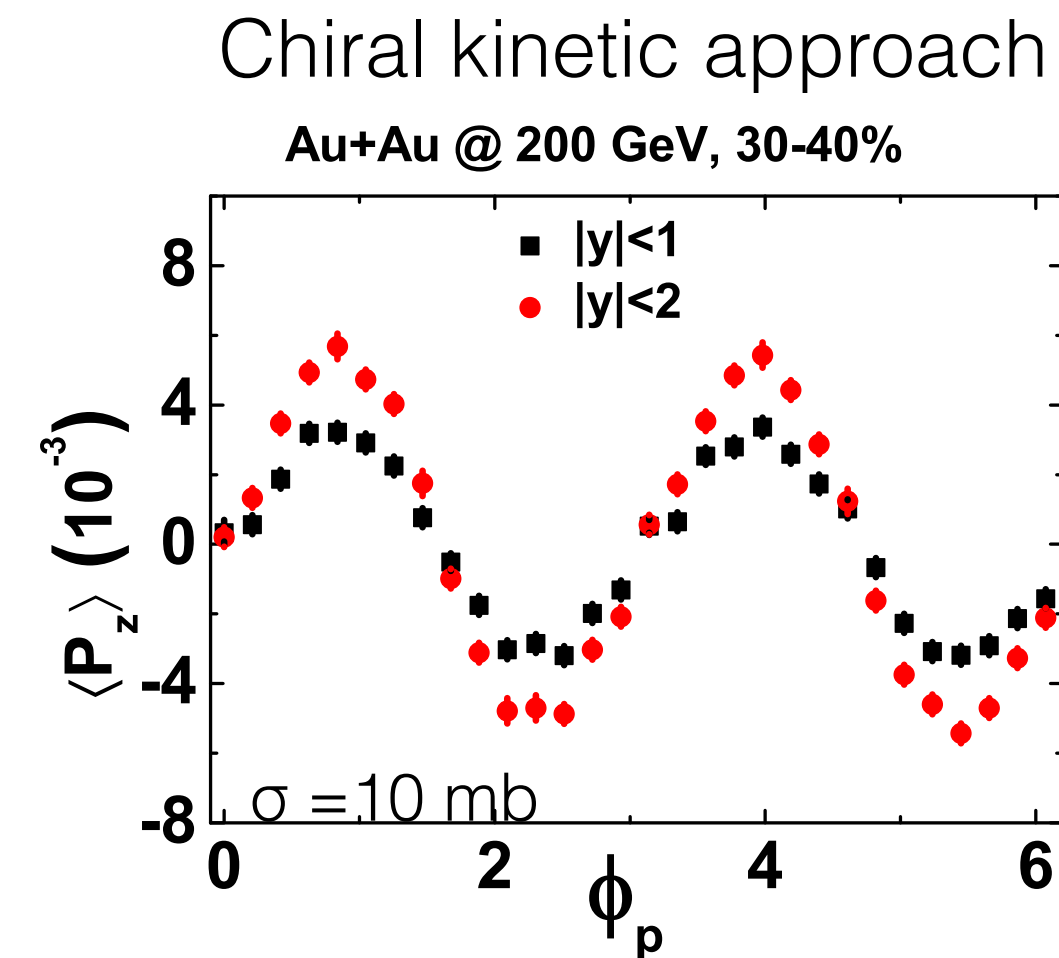
## Opposite sign

- UrQMD IC + hydrodynamic model
  - Assuming a local thermal equilibrium
 F. Becattini and I. Karpenko, PRL.120.012302 (2018)
- AMPT
  - X. Xia, H. Li, Z. Tang, Q. Wang, PRC98.024905 (2018)



## Same sign

- Chiral kinetic approach
  - Assuming non-equilibrium of spin degree of freedom
 Y. Sun and C.-M. Ko, PRC99, 011903(R) (2019)
- High resolution (3+1)D PICR hydrodynamic model
  - Yang-Mills flux tube IC
 Y. Xie, D. Wang, and L. P. Csernai, arXiv:1907.00773

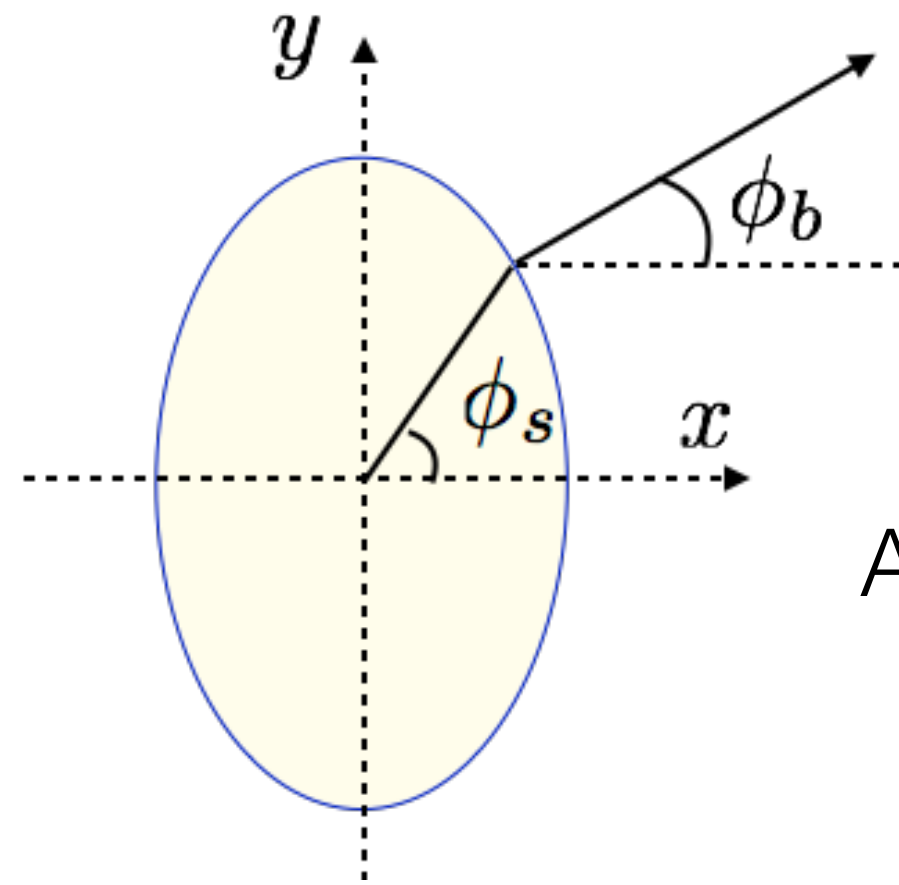
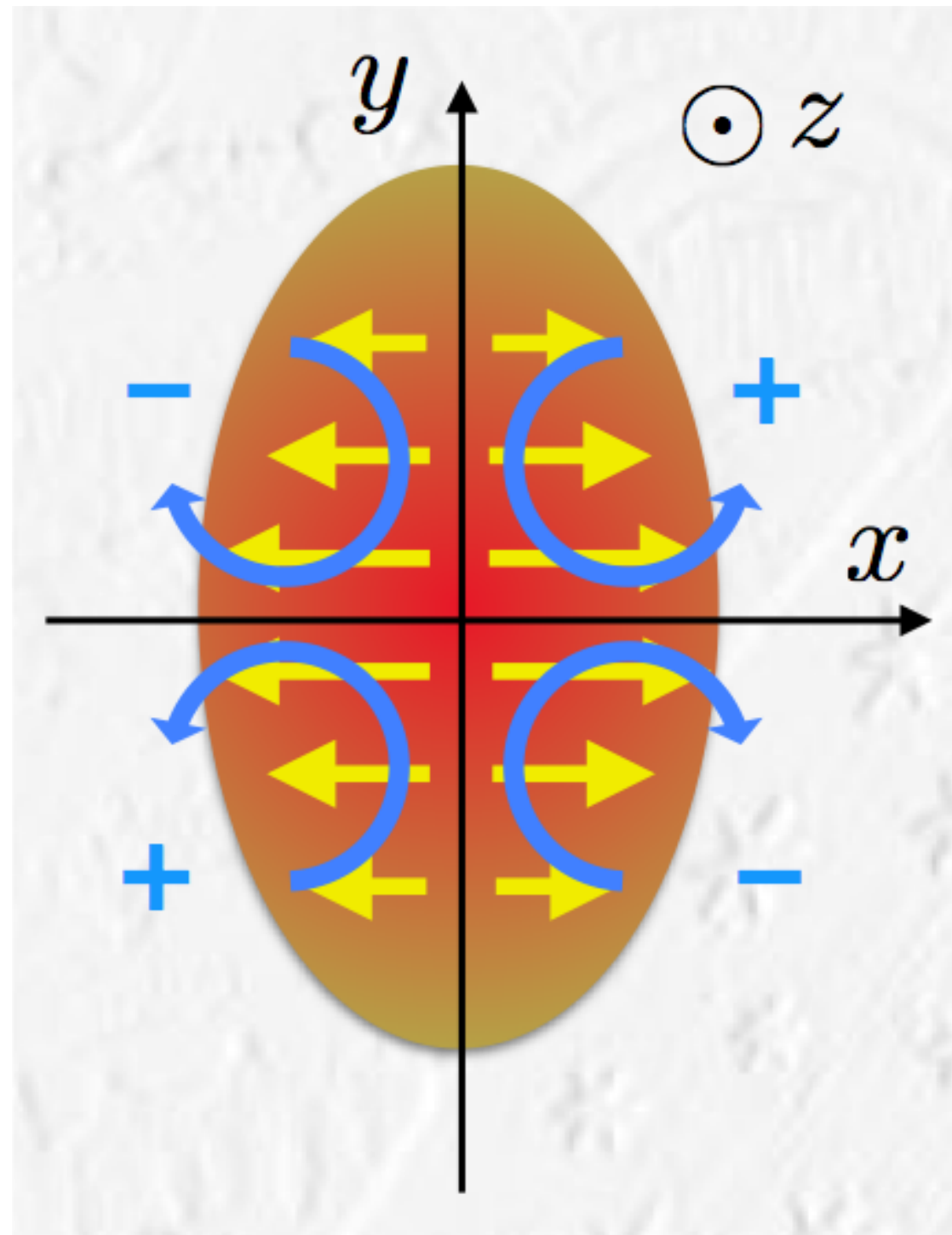


*Incomplete thermal equilibrium of spin degree of freedom?*

*Importance of relativistic contribution as well as kinematic vorticity in hydro.*

# Estimate kinematic vorticity with the blast-wave model

S. Voloshin, SQM2017  
EPJ Web Conf.171, 07002 (2018)



$$r_{max} = R[1 - a \cos(2\phi_s)],$$

$$\rho_t = \rho_{t,max}[r/r_{max}(\phi_s)][1 + b \cos(2\phi_s)] \approx \rho_{t,max}(r/R)[1 + (a + b) \cos(2\phi_s)].$$

R: reference source radius  
 $\rho_t$ : transverse flow velocity

Approximation of the kinetic vorticity in the blast-wave model:

$$\omega_z = 1/2(\nabla \times \mathbf{v})_z \approx (\rho_{t,nmax}/R) \sin(n\phi_s) [b_n - a_n].$$

spatial anisotropy  
flow anisotropy

Sine modulation of  $\omega_z$  is expected with the factor  $(b_n - a_n)$ .

The sign could be negative depending on the relation of flow and spatial anisotropy.

# Blast-wave model parameterization

- Hydro-inspired model parameterized with freeze-out condition assuming the longitudinal boost invariance
  - Freeze-out temperature  $T_f$
  - Radial flow rapidity  $\rho_0$  and its modulation  $\rho_2$
  - Source size  $R_x$  and  $R_y$

$$\rho(r, \phi_s) = \tilde{r}[\rho_0 + \rho_2 \cos(2\phi_b)]$$

$$\tilde{r}(r, \phi_s) = \sqrt{(r \cos \phi_s)^2 / R_x^2 + (r \sin \phi_s)^2 / R_y^2}$$

- Calculate vorticity at the freeze-out using the parameters extracted from spectra,  $v_2$ , and HBT fit

$$\langle \omega_z \sin(2\phi) \rangle = \frac{\int d\phi_s \int r dr I_2(\alpha_t) K_1(\beta_t) \omega_z \sin(2\phi_b)}{\int d\phi_s \int r dr I_0(\alpha_t) K_1(\beta_t)}$$

$$\omega_z = \frac{1}{2} \left( \frac{\partial u_y}{\partial x} - \frac{\partial u_x}{\partial y} \right),$$

$u$ : local flow velocity,  $I_n, K_n$ : modified Bessel functions

F. Retiere and M. Lisa, PRC70.044907 (2004)

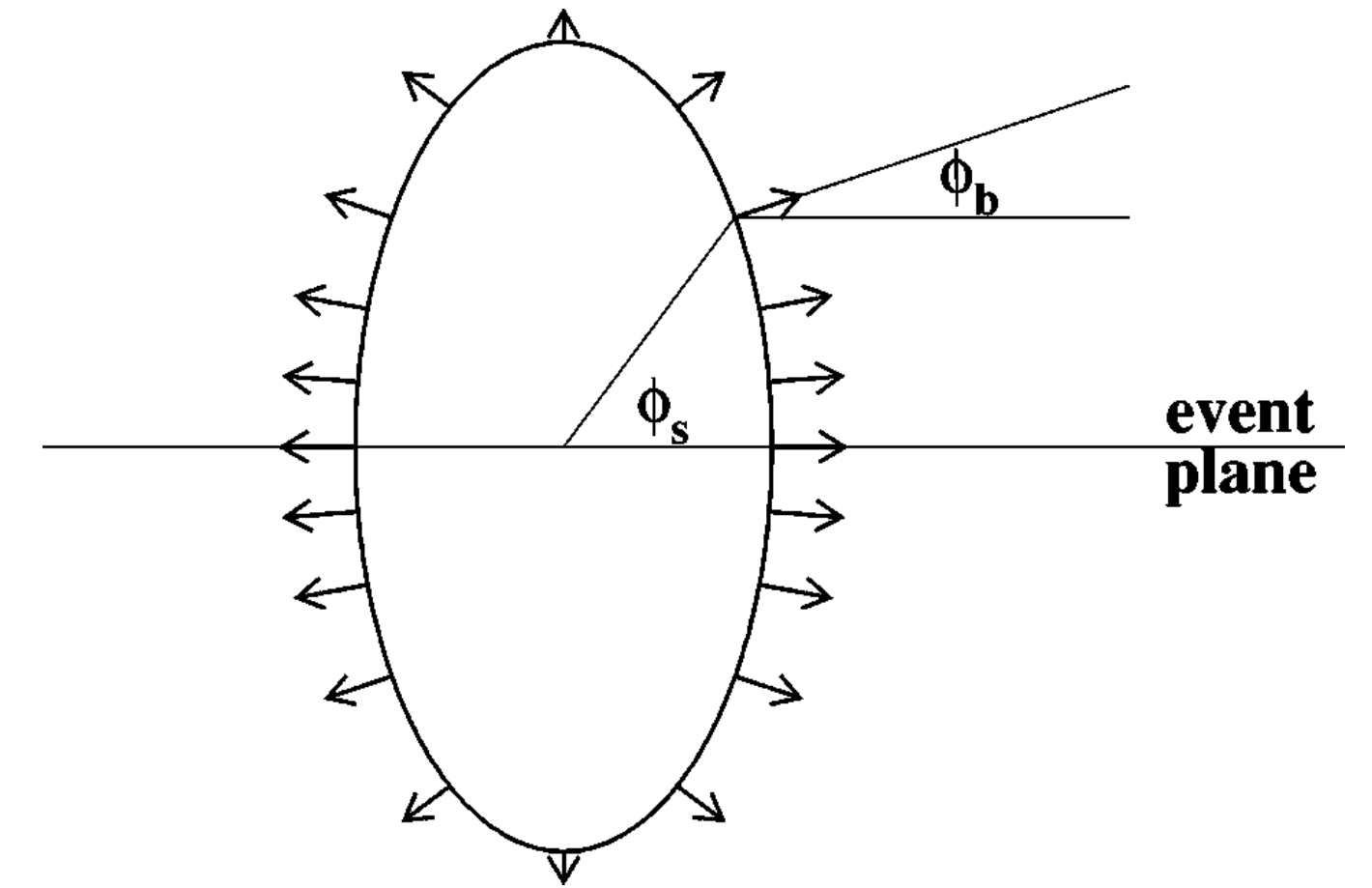
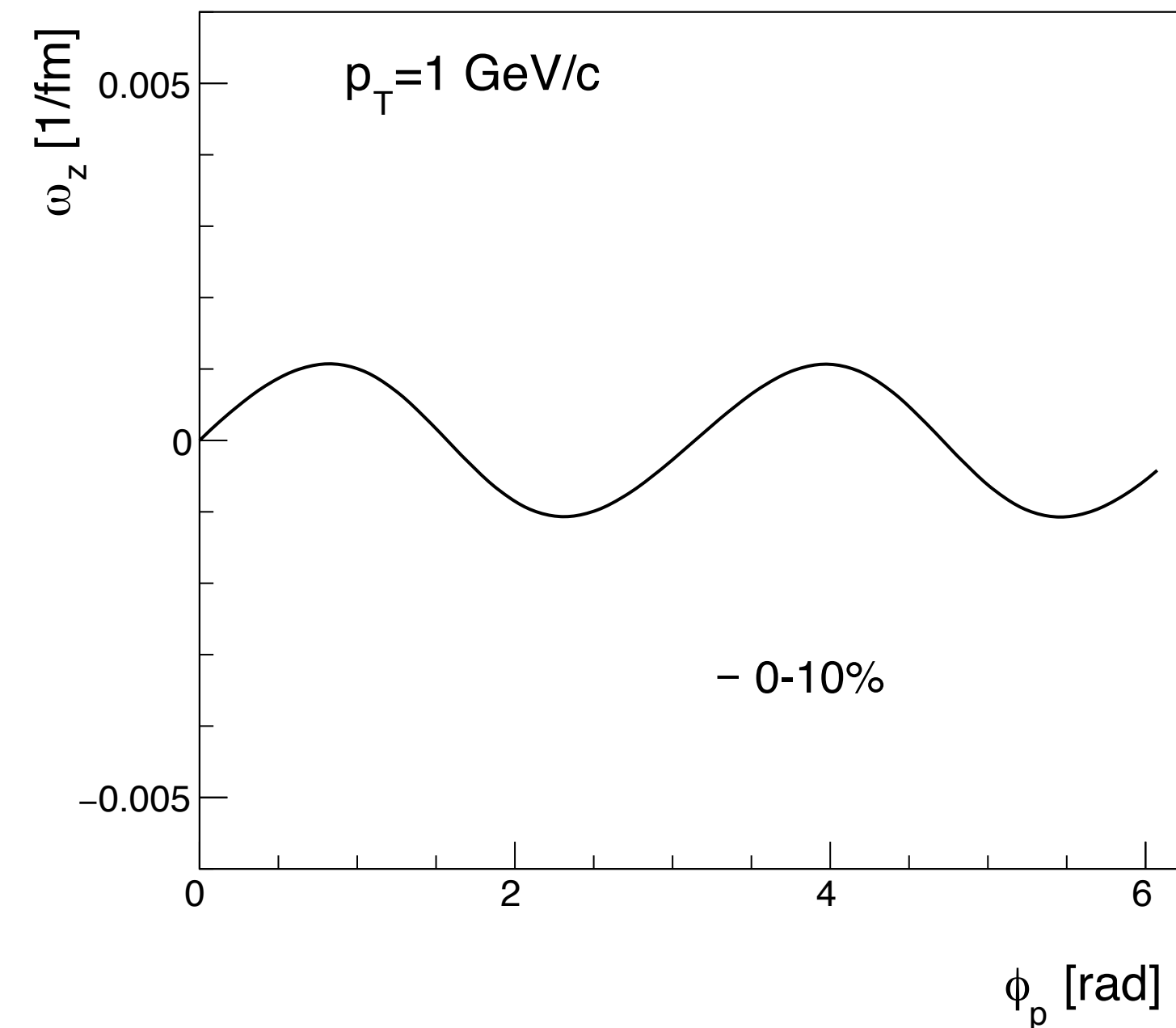
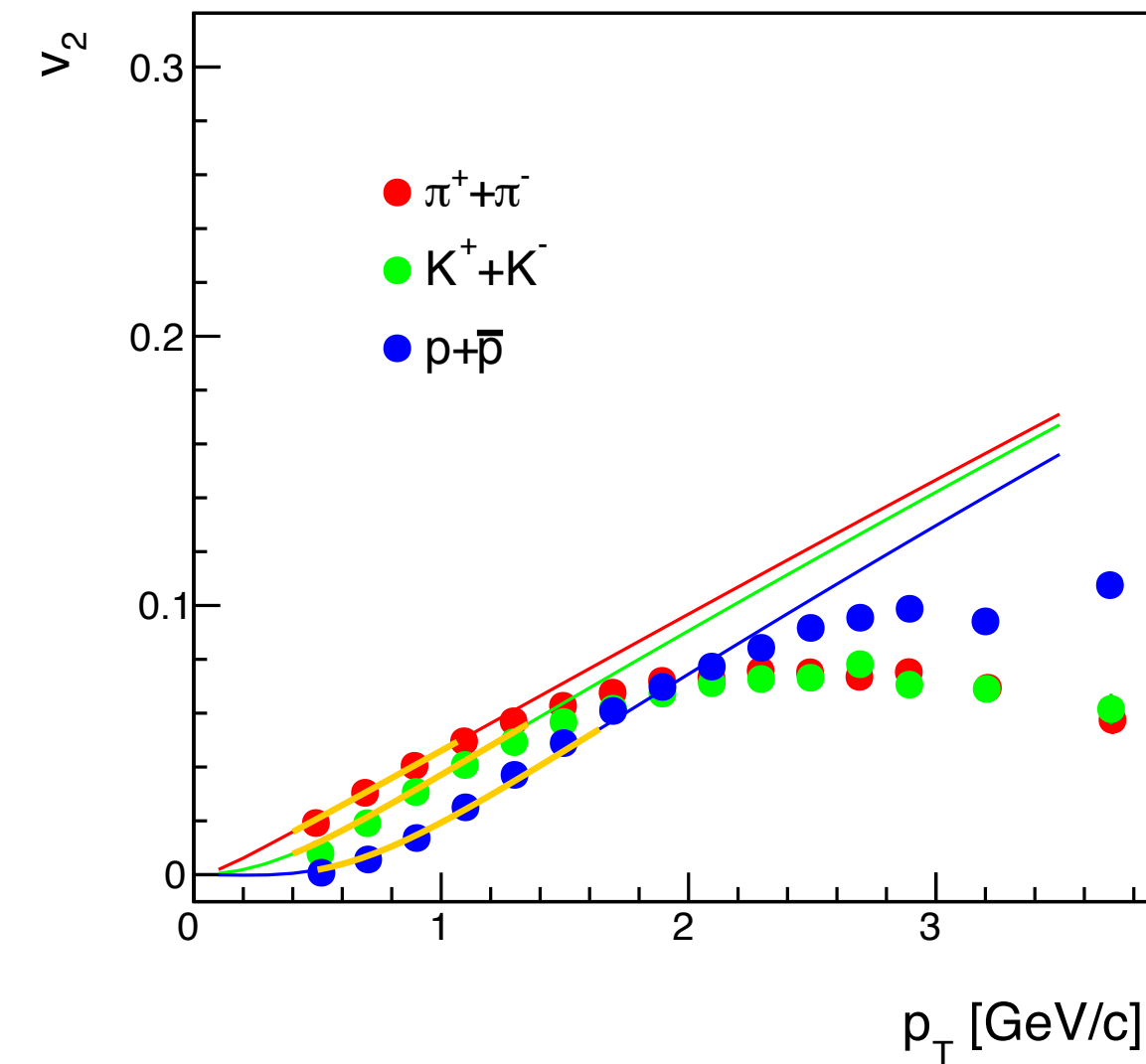
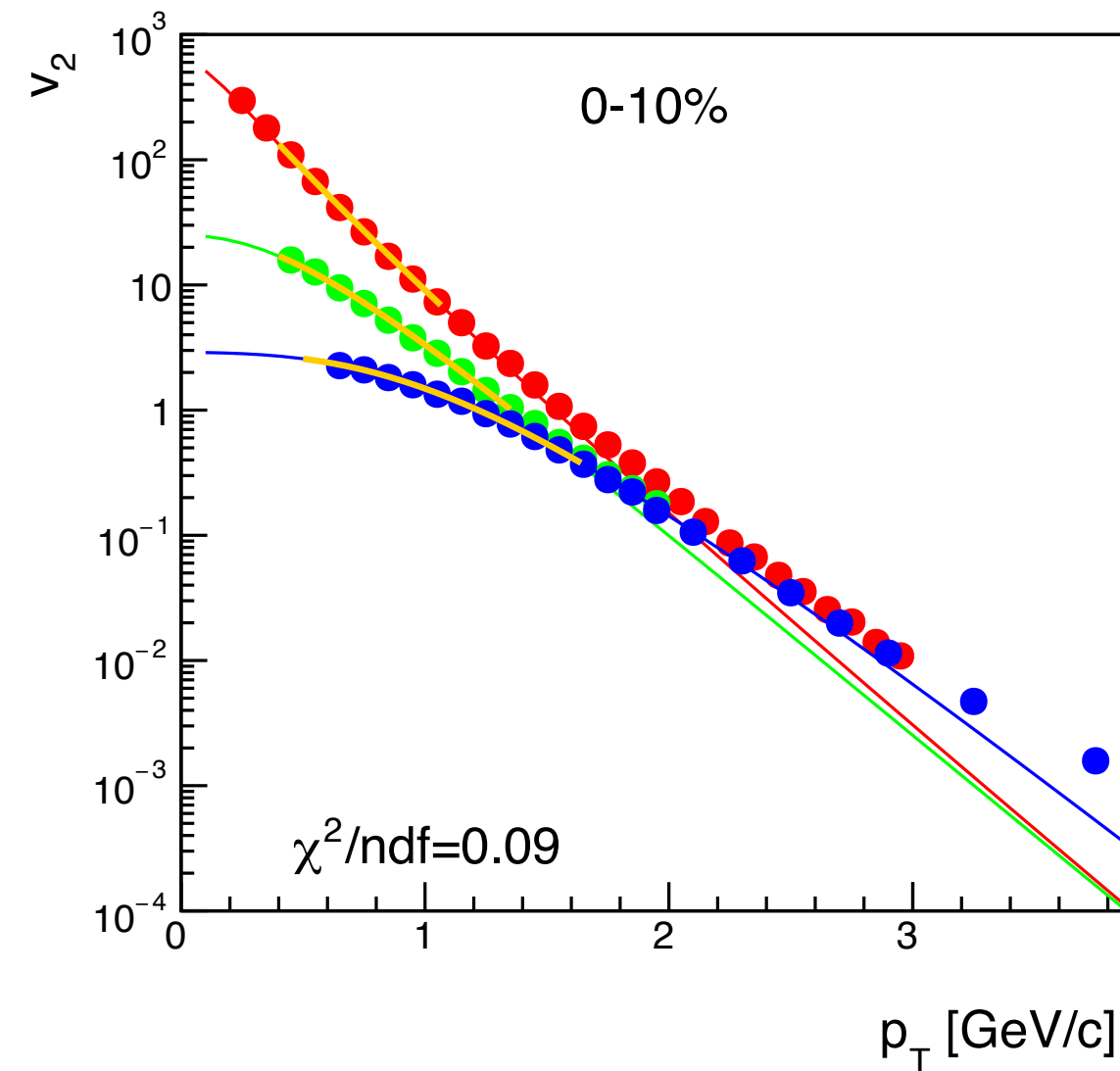


FIG. 2. Schematic illustration of an elliptical subshell of the source. Here, the source is extended out of the reaction plane ( $R_y > R_x$ ). Arrows represent the direction and magnitude of the flow boost. In this example,  $\rho_2 > 0$  [see Eq. (4)].

$\phi_s$ : azimuthal angle of the source element  
 $\phi_b$ : boost angle perpendicular to the elliptical subshell

# $\omega_z$ and $P_z$ from the BW model

e.g. Blast-wave fit to spectra and  $v_2$



Data from:  
PHENIX, PRC69.034909 (2004)  
PHENIX, PRC93.051902(R) (2016)

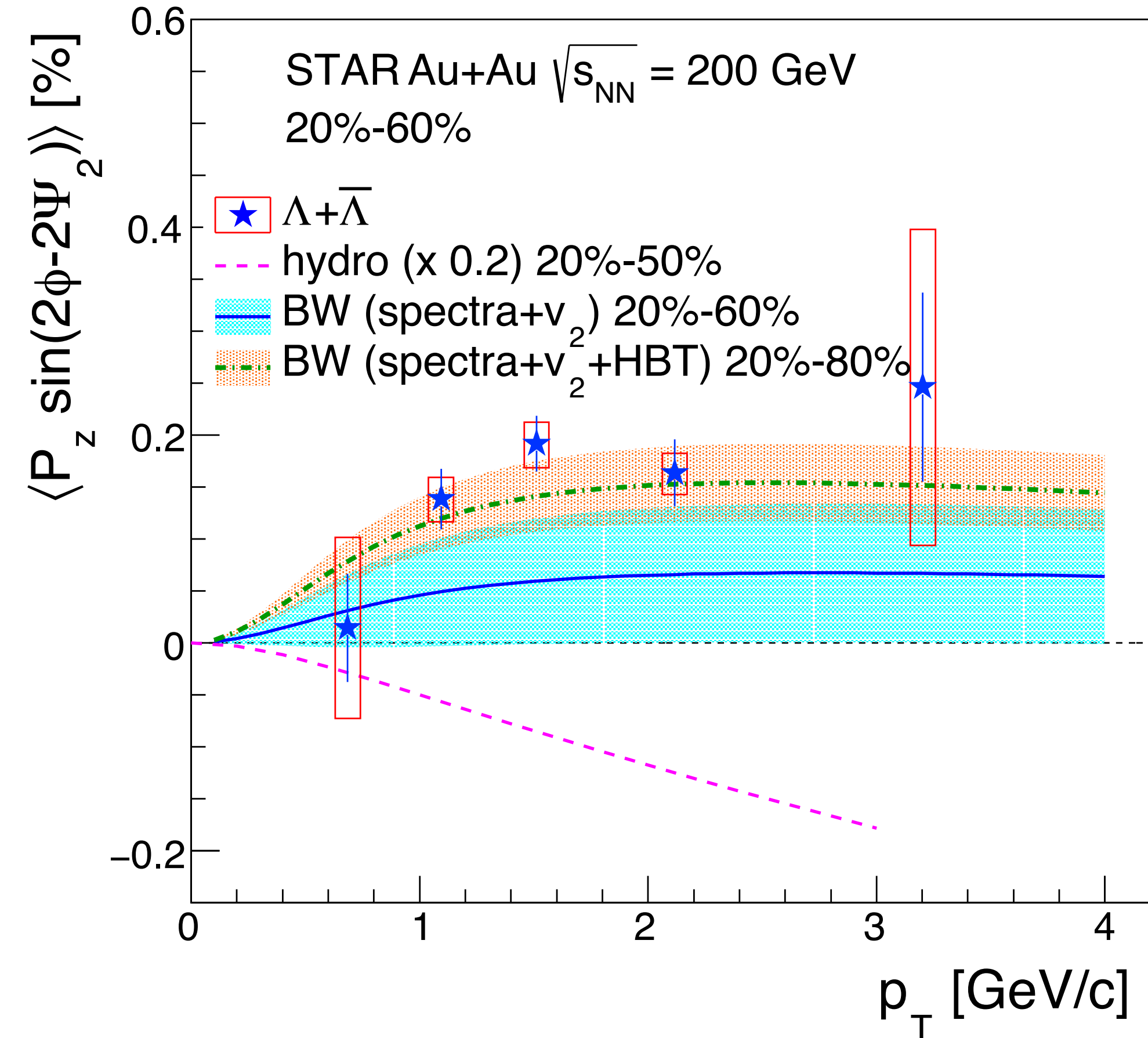
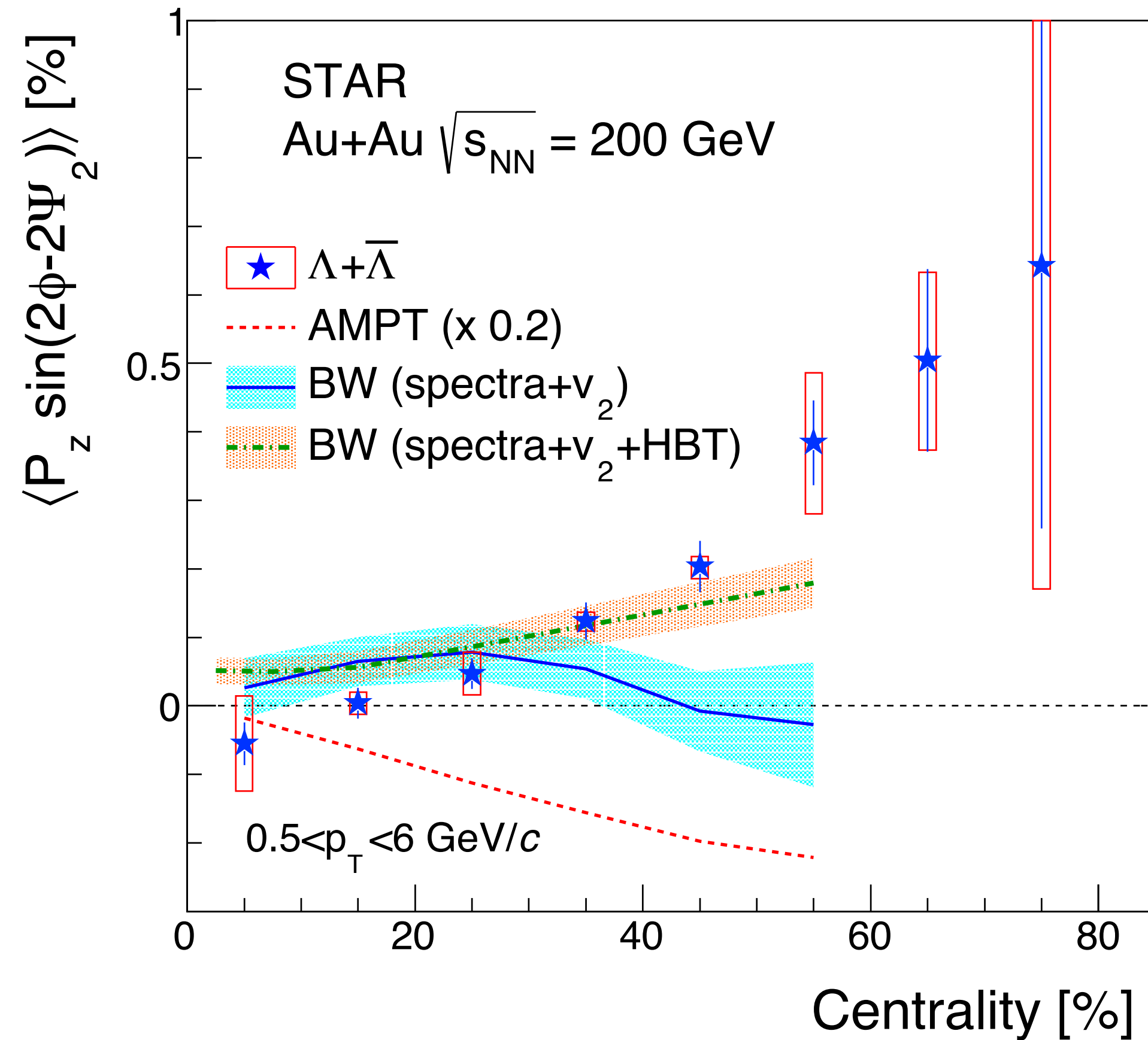
Calculated vorticity  $\omega_z$  shows the sine modulation. Assuming a local thermal equilibrium, z-component of polarization is estimated as follows:

$$P_z \approx \omega_z / (2T)$$

# $P_z$ modulation from the BW model

STAR, PRL123.13201 (2019)

BW parameters obtained with HBT: STAR, PRC71.044906 (2005)



- Simple estimate for kinematic vorticity contribution with BW model

- Similar magnitude to the data

T. Niida and S. Voloshin in preparation

- Inclusion of HBT in the fit affects the sign in peripheral collisions

# Summary

---

- $\Lambda$  global polarization at  $\sqrt{s_{NN}} = 7.7-200$  GeV from STAR
  - Polarization increases in lower energies
    - **Quantitatively consistent with theoretical models**
- $\Lambda$  global polarization at  $\sqrt{s_{NN}} = 2.4$  GeV from HADES and 2.7 TeV from ALICE
  - Preliminary results are consistent with zero but the HADES result indicates the polarization decreases around  $\sqrt{s_{NN}} = 2.4 - 7.7$  GeV
    - STAR-FXT  $\sqrt{s_{NN}} = 3-7.7$  GeV
- First study of  $\Lambda$  polarization along the beam direction at  $\sqrt{s_{NN}} = 200$  GeV
  - Quadrupole structure of the polarization relative to the 2<sup>nd</sup>-order event plane
    - **Qualitatively consistent with a picture of the elliptic flow but agree/disagree among the data and theoretical calculations in the sign**
  - Blast-wave model predicts the same sign and similar magnitude to the data

# Outlook

W.-T. Deng and X.-G. Huang, PRC93.064907 (2016)

D.-X. Wei *et al.*, PRC99.014905 (2019)

X.-G. Deng *et al.*, arXiv:2001.01371

## □ STAR

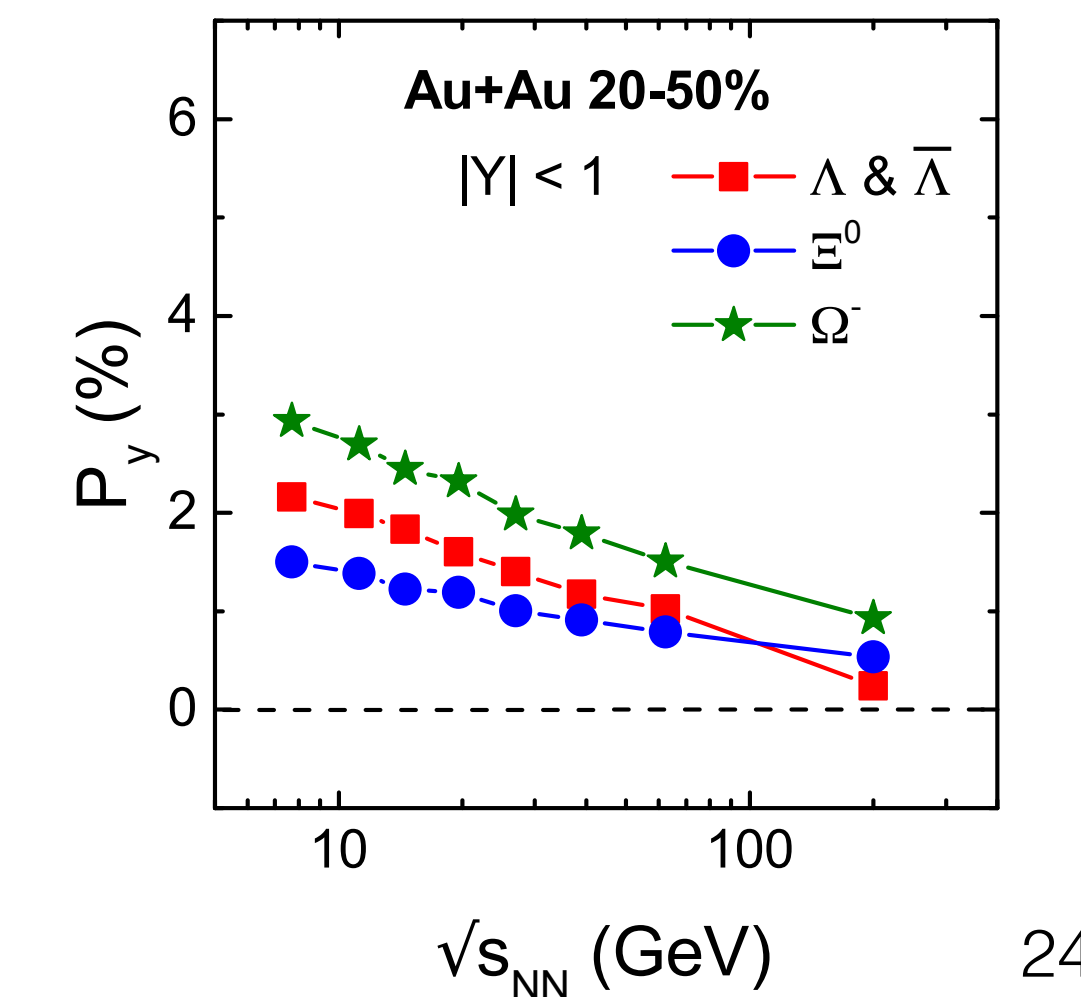
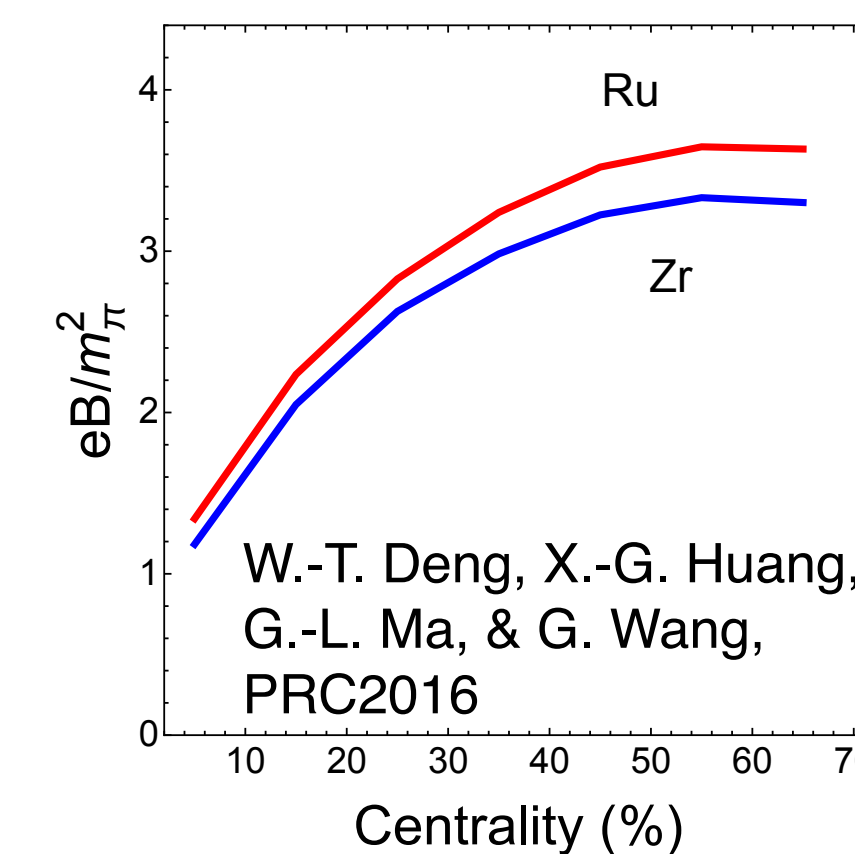
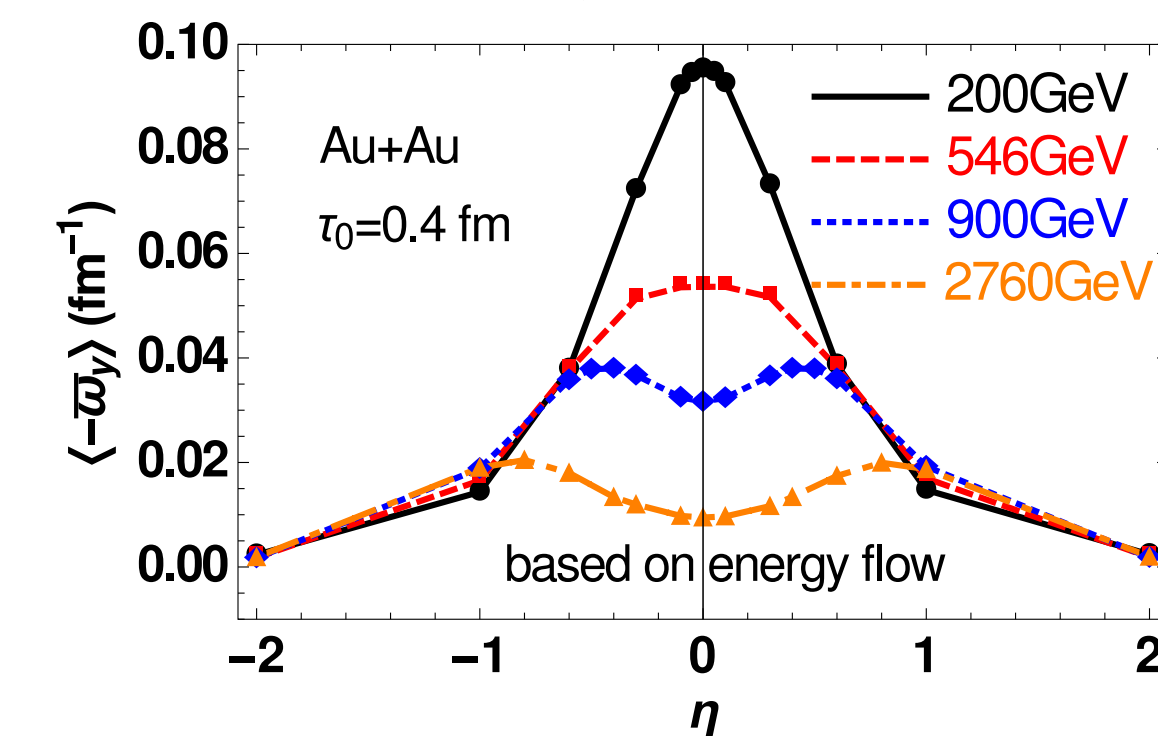
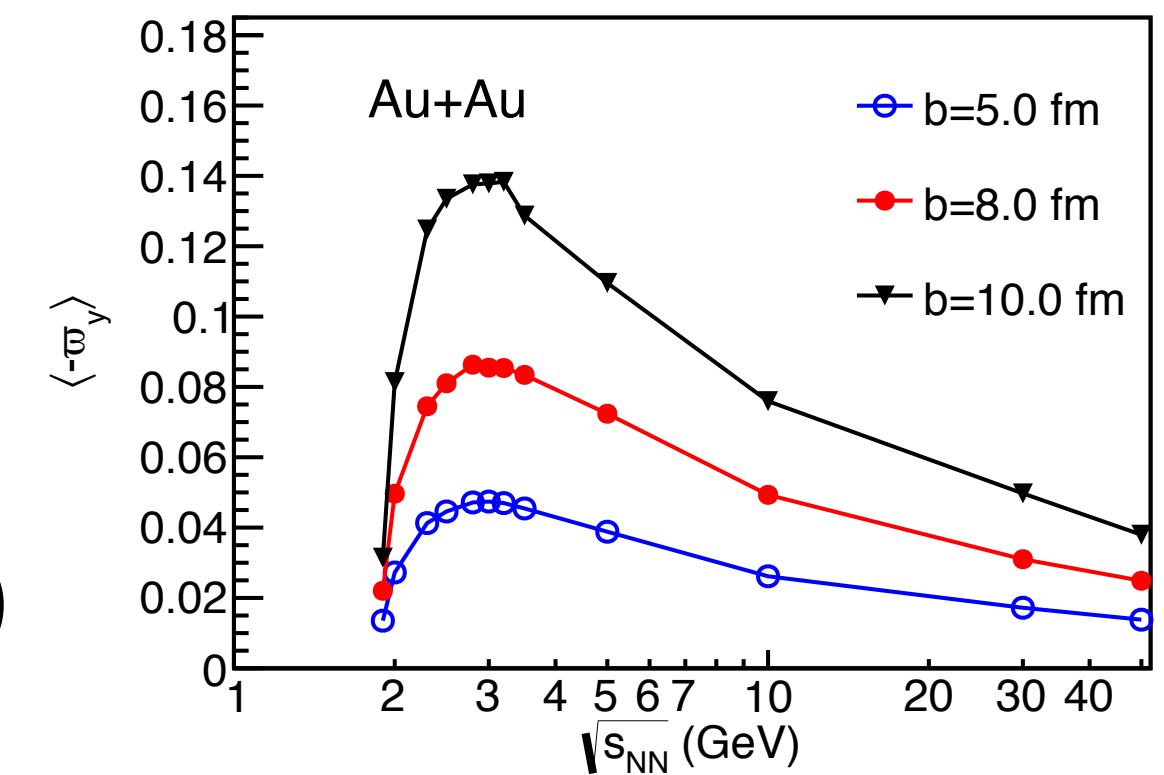
- High statistics data of 27 GeV and BES-II 7.7-19.6 GeV and Fixed-target 3-7.7 GeV with iTPC and EPD (x10 events, better EP,  $|\eta| < 1.5$ )
- Isobaric collision data (Ru+Ru, Zr+Zr), ~10% difference in B-field
- Global polarization of multi-strangeness ( $\Xi$  and  $\Omega$ )
- Forward upgrade

## □ ALICE/CMS/ATLAS(?)

- Global/local polarizations with more data at 5.02 TeV

## □ HADES

- Systematic study with possible improvement is ongoing



# ***Back up***

---



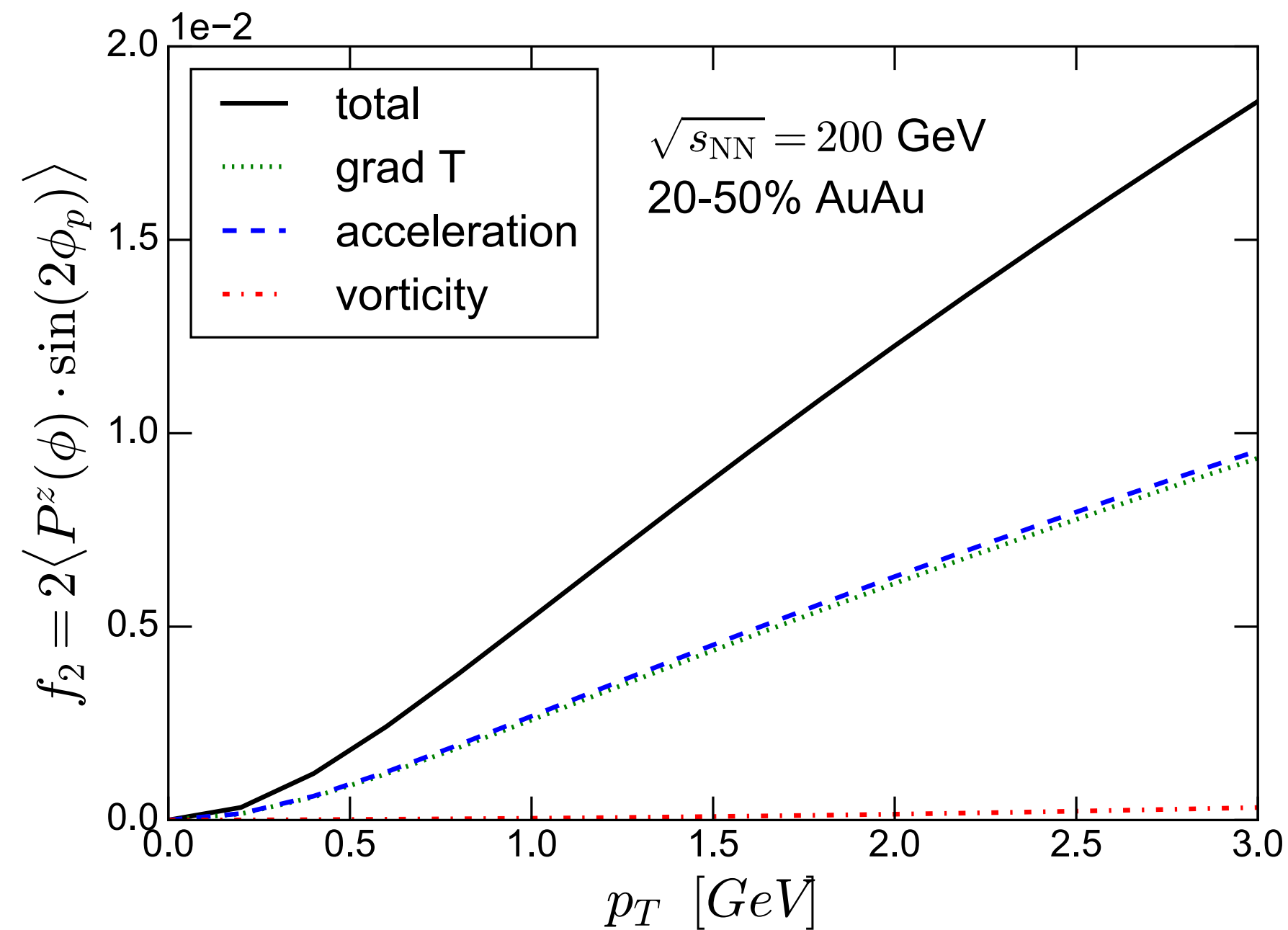
# Contributions to $P_z$ in hydro

I. Karpenko, QM2018

$$S^\mu \propto \varepsilon^{\mu\rho\sigma\tau} \omega_{\rho\sigma} p_\tau = \varepsilon^{\mu\rho\sigma\tau} (\partial_\rho \beta_\sigma) p_\tau = \underbrace{\varepsilon^{\mu\rho\sigma\tau} p_\tau \partial_\rho \left( \frac{1}{T} \right) u_\sigma}_{\text{grad}T} + \underbrace{\frac{1}{T} 2 [\omega^\mu (u \cdot p) - u^\mu (\omega \cdot p)]}_{\text{"NR vorticity"}} + \underbrace{\varepsilon^{\mu\rho\sigma\tau} p_\tau A_\sigma u_\rho}_{\text{acceleration}}$$

**temperature gradient**
**kinematic vorticity**
**relativistic term**

Longitudinal quadrupole  $f_2$ :



$P_z$  dominated by temperature gradient and relativistic term, but not by kinematic vorticity based on the hydro model.

Can we get such a small kinetic vorticity in the blast-wave model?

# Variations of model parameters for $P_H$

I. Karpenko, QM2017

Initial state:

$R_{\perp}$ : transverse granularity

$R_{\eta}$ : longitudinal granularity

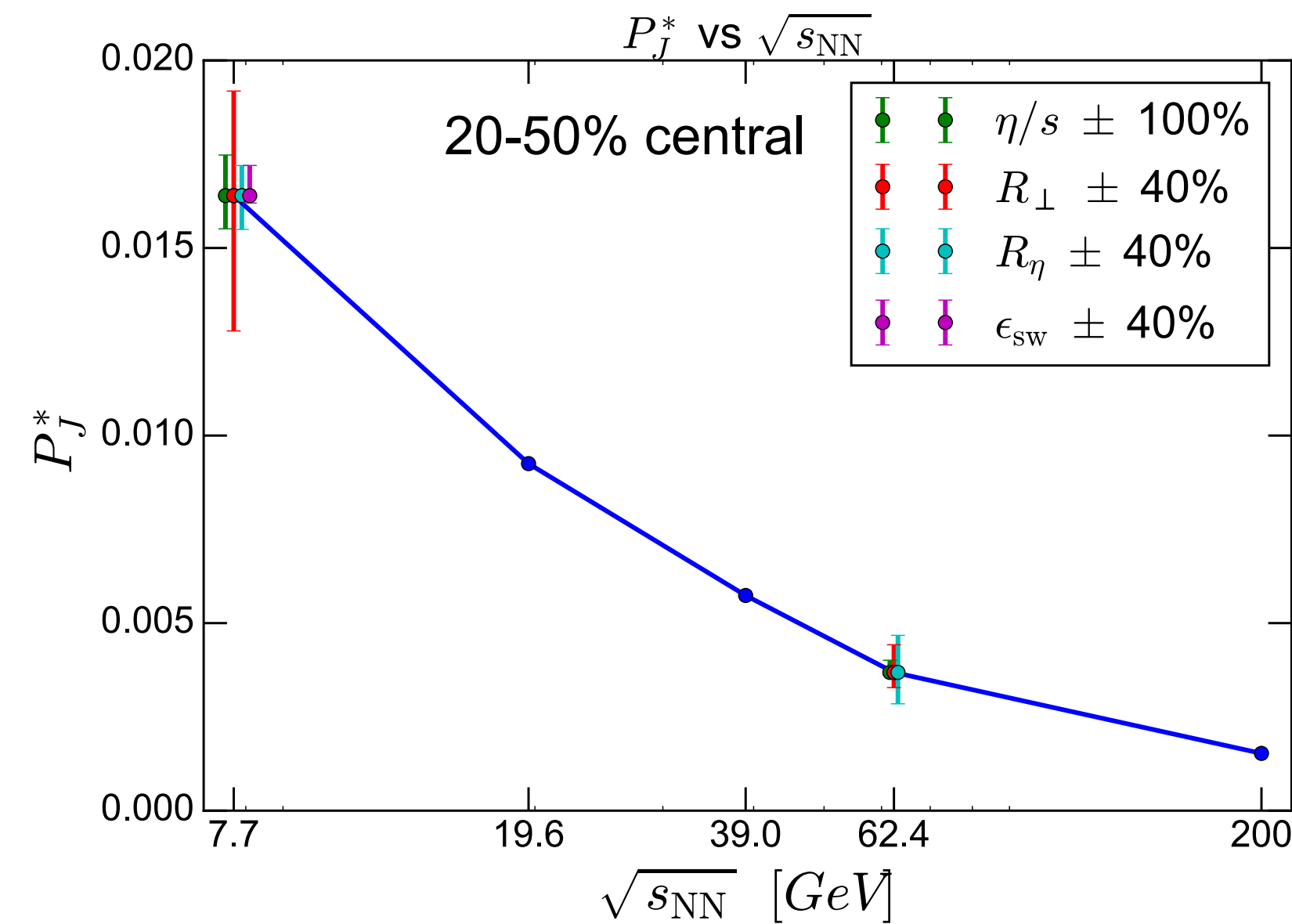
Fluid phase:

$\eta/s$ : shear viscosity of fluid

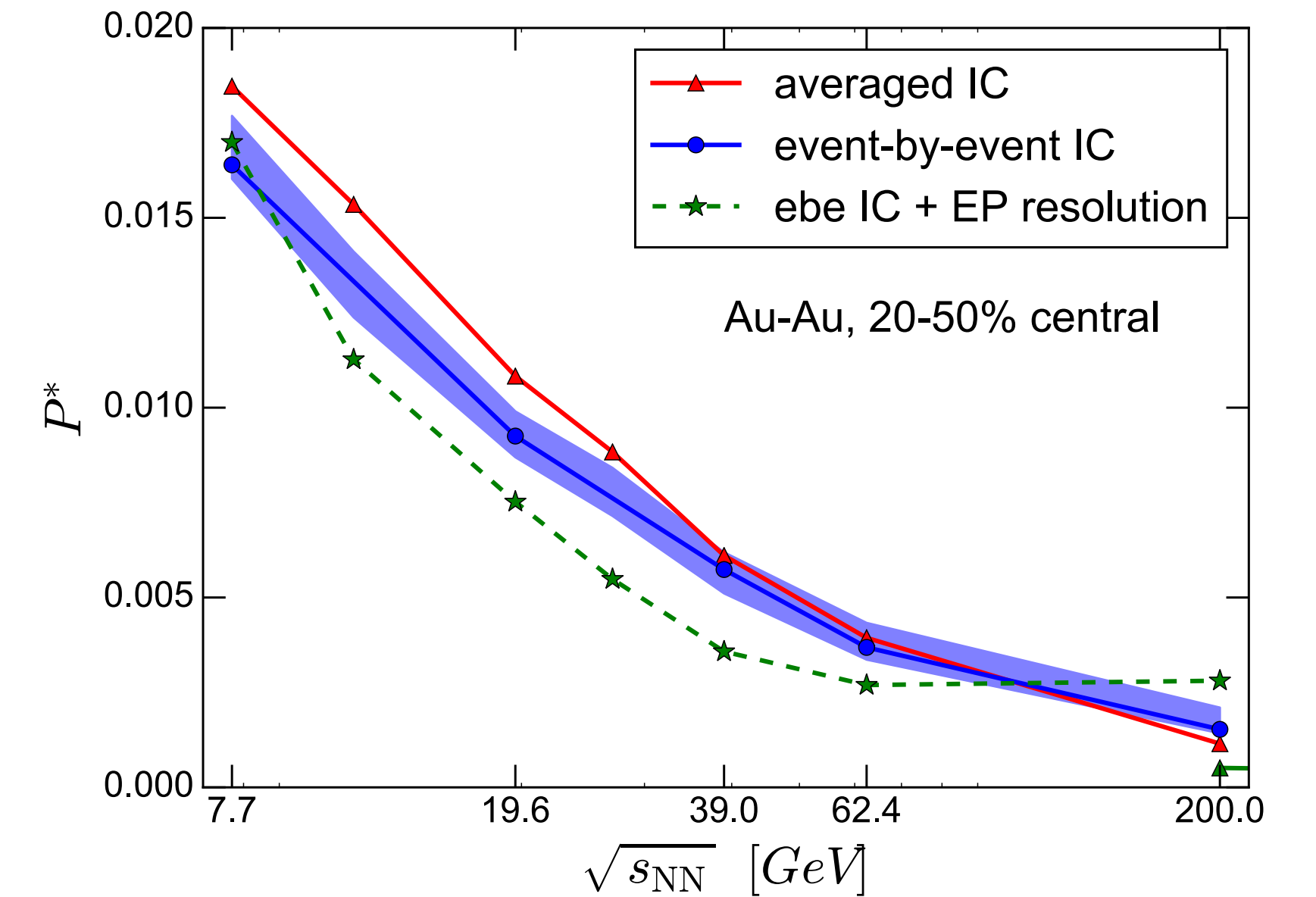
Particlization criterion:

$\epsilon_{\text{sw}} = 0.5 \text{ GeV}/\text{fm}^3$

variation of model parameters

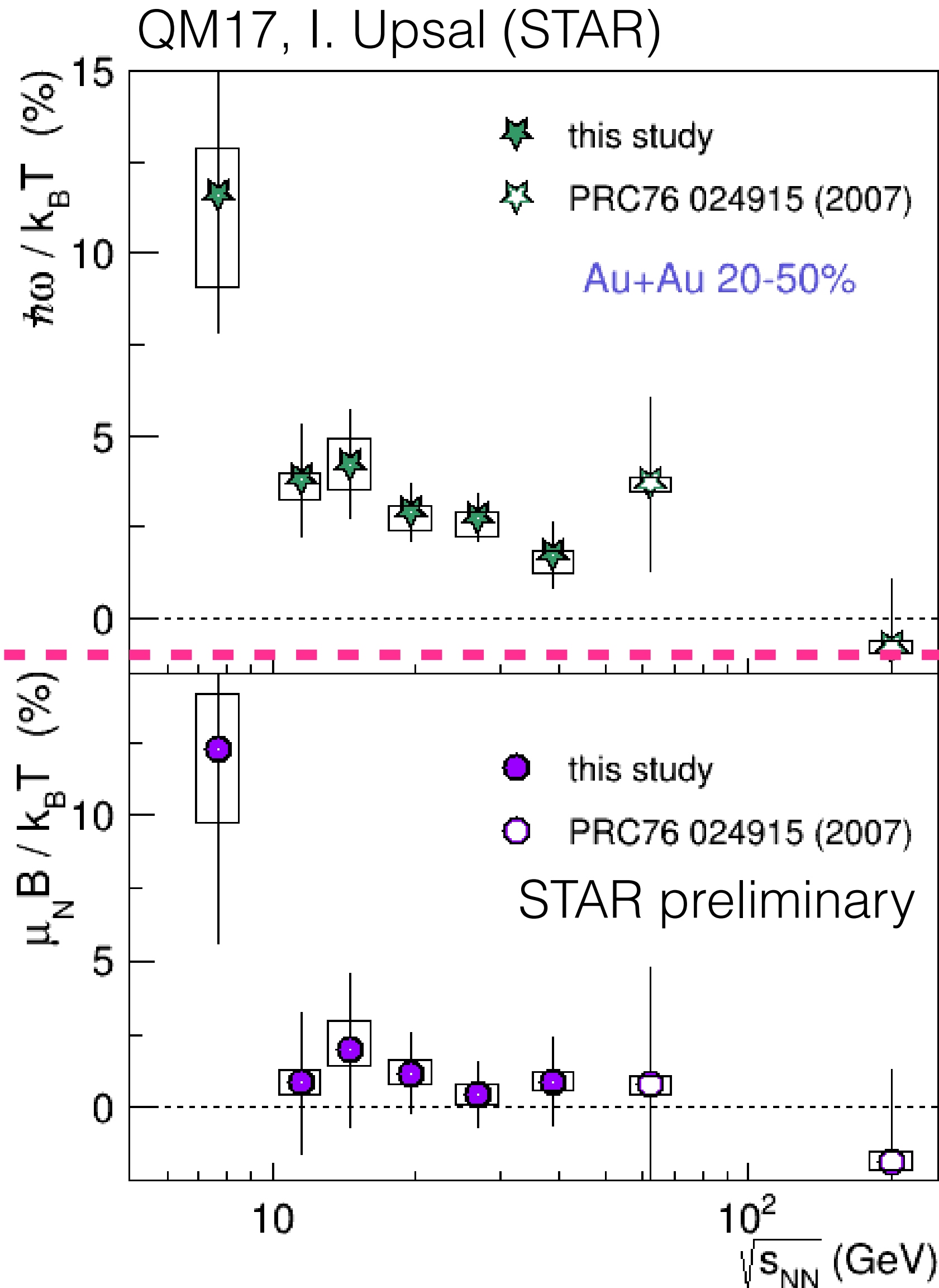


event-by-event vs. averaged



- Collision energy dependence is robust with respect to variation of the parameters of the model.
- There is no big difference between event-by-event and single shot hydrodynamic description.

# Possible probe of magnetic field



Becattini, Karpenko, Lisa, Uppsala, and Voloshin, PRC95.054902 (2017)

$$P_\Lambda \simeq \frac{1}{2} \frac{\omega}{T} + \frac{\mu_\Lambda B}{T}$$

$$P_{\bar{\Lambda}} \simeq \frac{1}{2} \frac{\omega}{T} - \frac{\mu_\Lambda B}{T}$$

$\mu_\Lambda$ :  $\Lambda$  magnetic moment

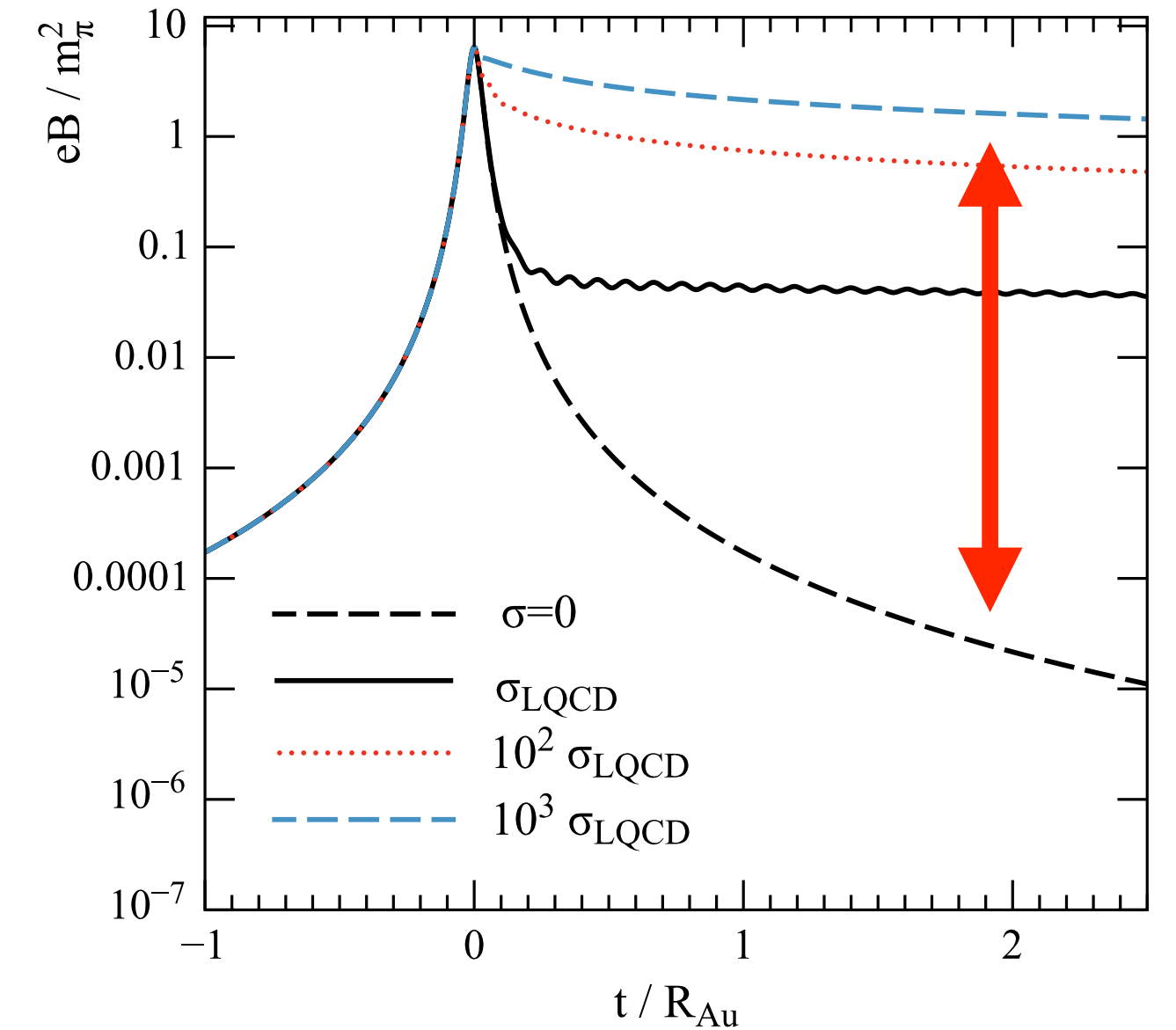
$$B = (P_\Lambda - P_{\bar{\Lambda}}) k_B T / \mu_N$$

$$\sim 5.0 \times 10^{13} \text{ [Tesla]}$$

nuclear magneton  $\mu_N = -0.613\mu_\Lambda$

Extracted B-field is close to our expectation.  
Need more data with better precision  
→ BES-II and Isobaric collisions

McLerran and Skokov, Nucl. Phys. A929, 184 (2014)

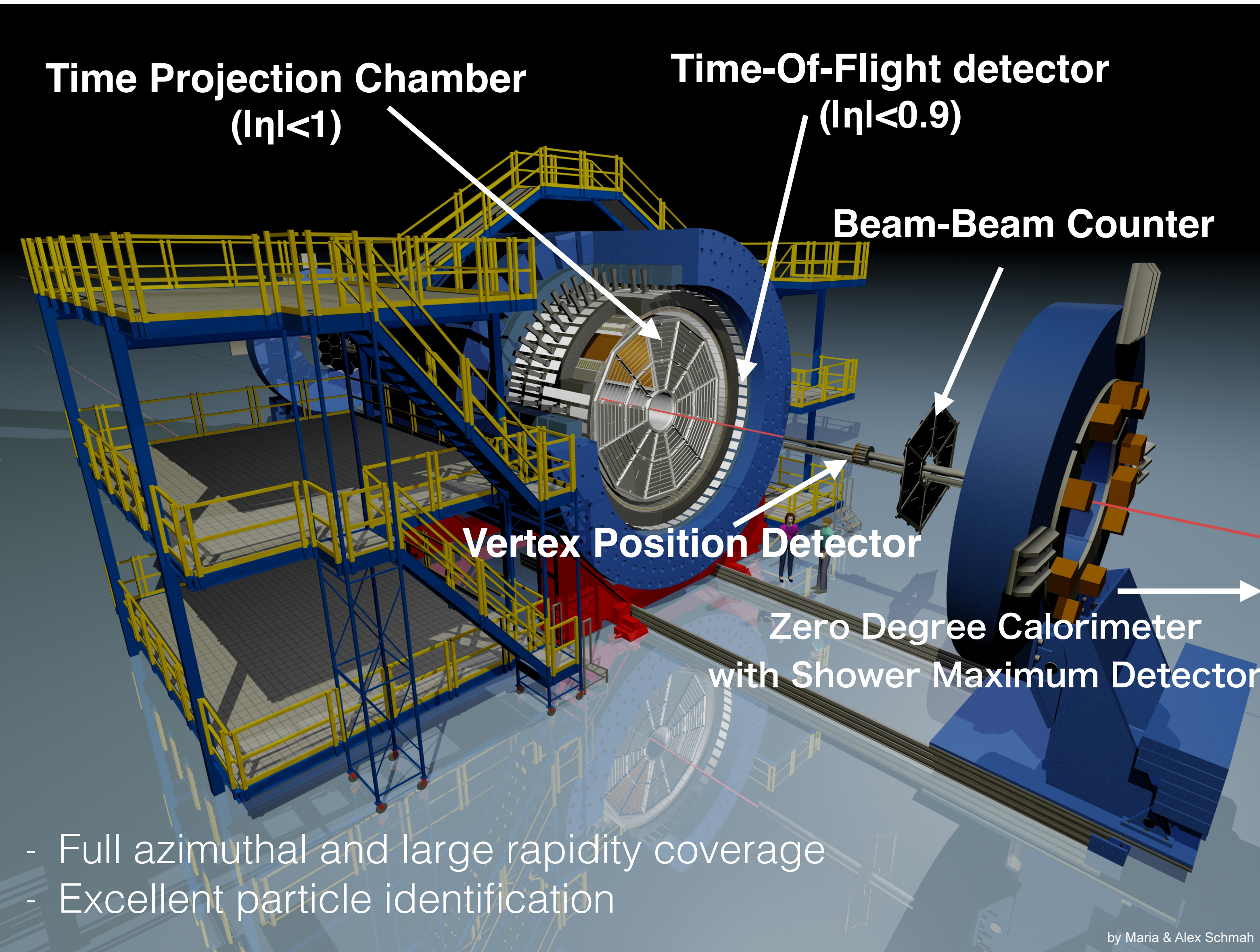


conductivity increases lifetime  
(not magnitude)

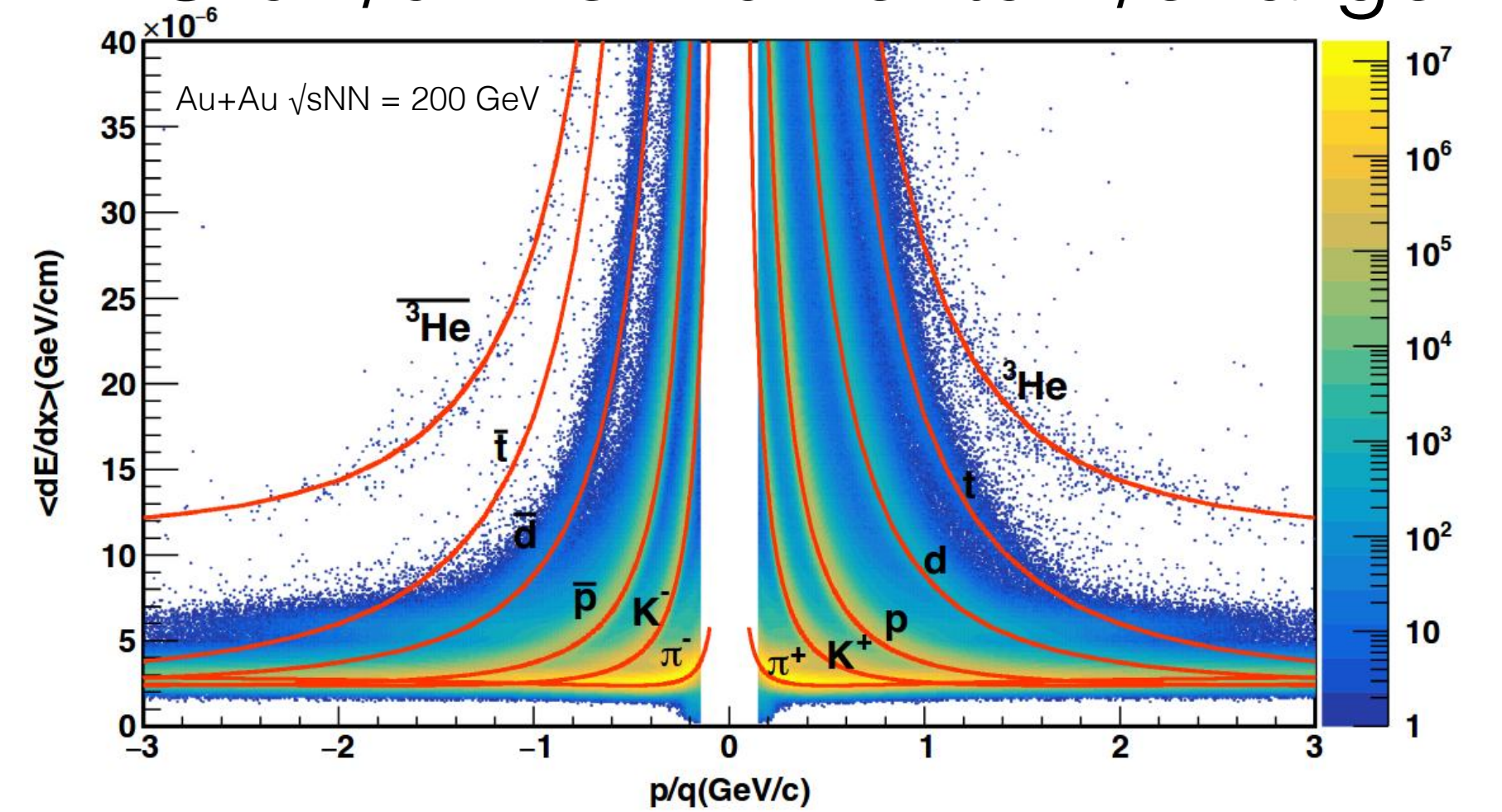
$$B \sim 10^{13} \text{ T}$$

$$(eB \sim \text{MeV}^2 \text{ } (\tau = 0.2 \text{ fm}))$$

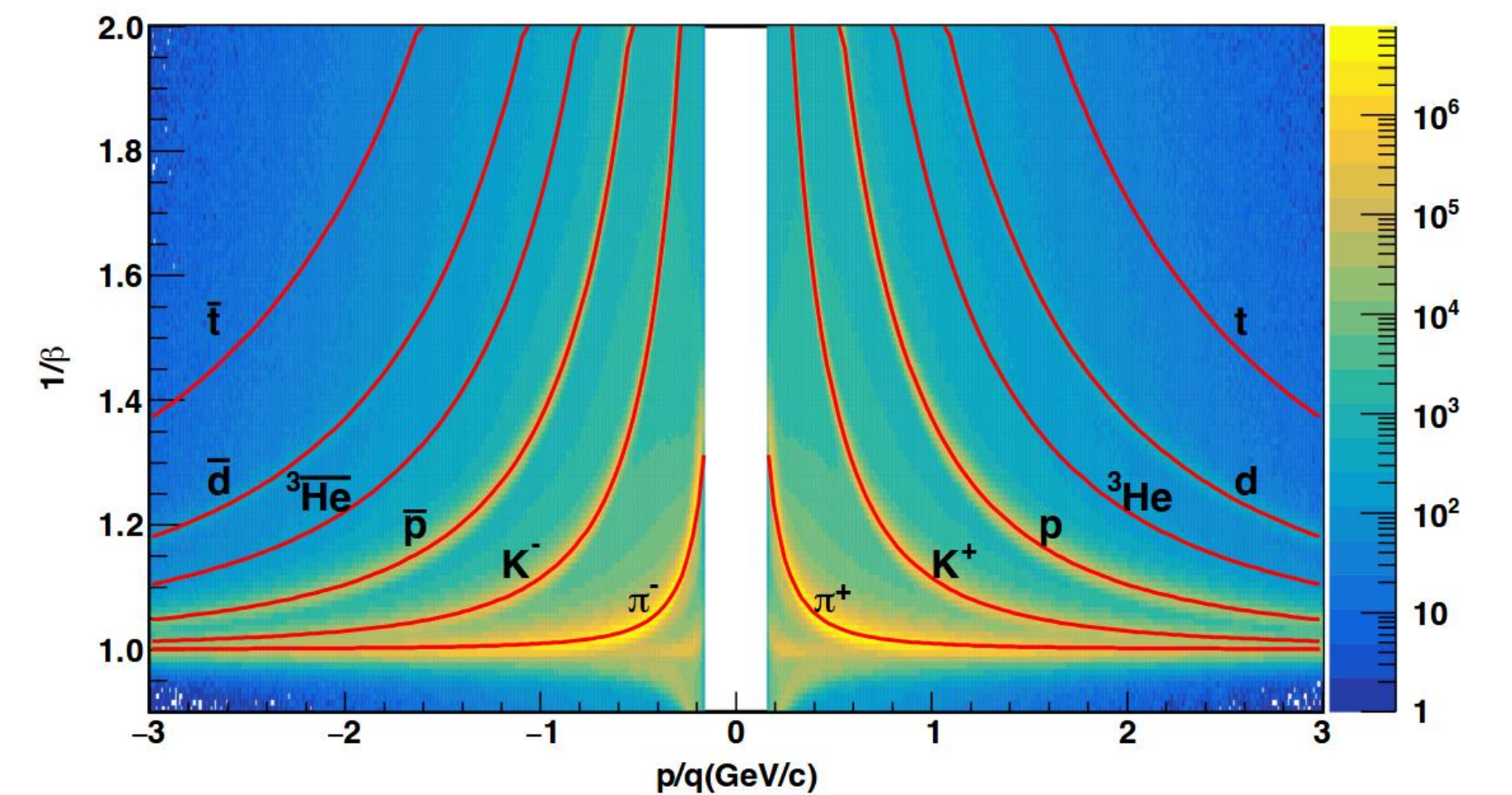
# STAR Detectors



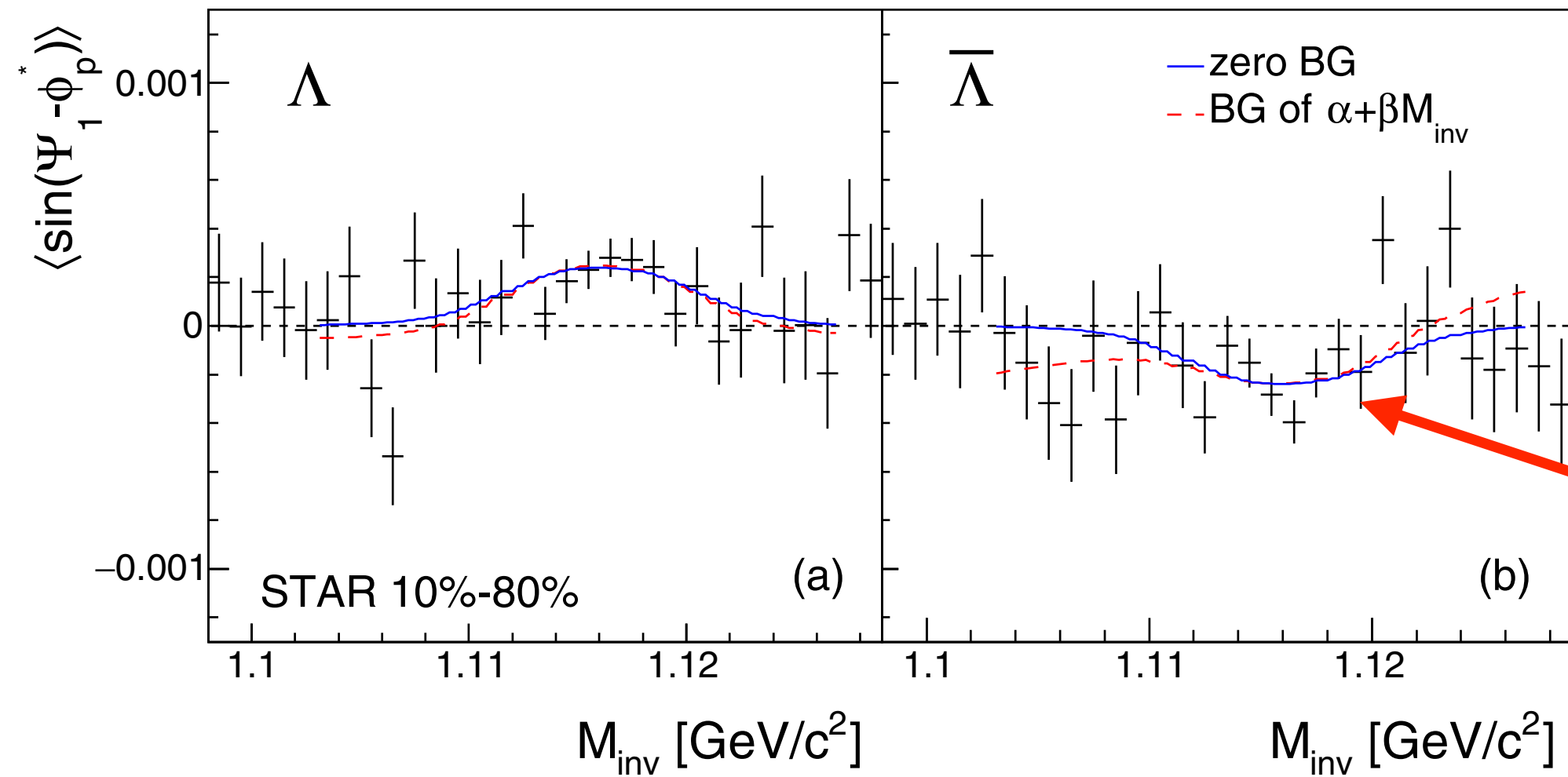
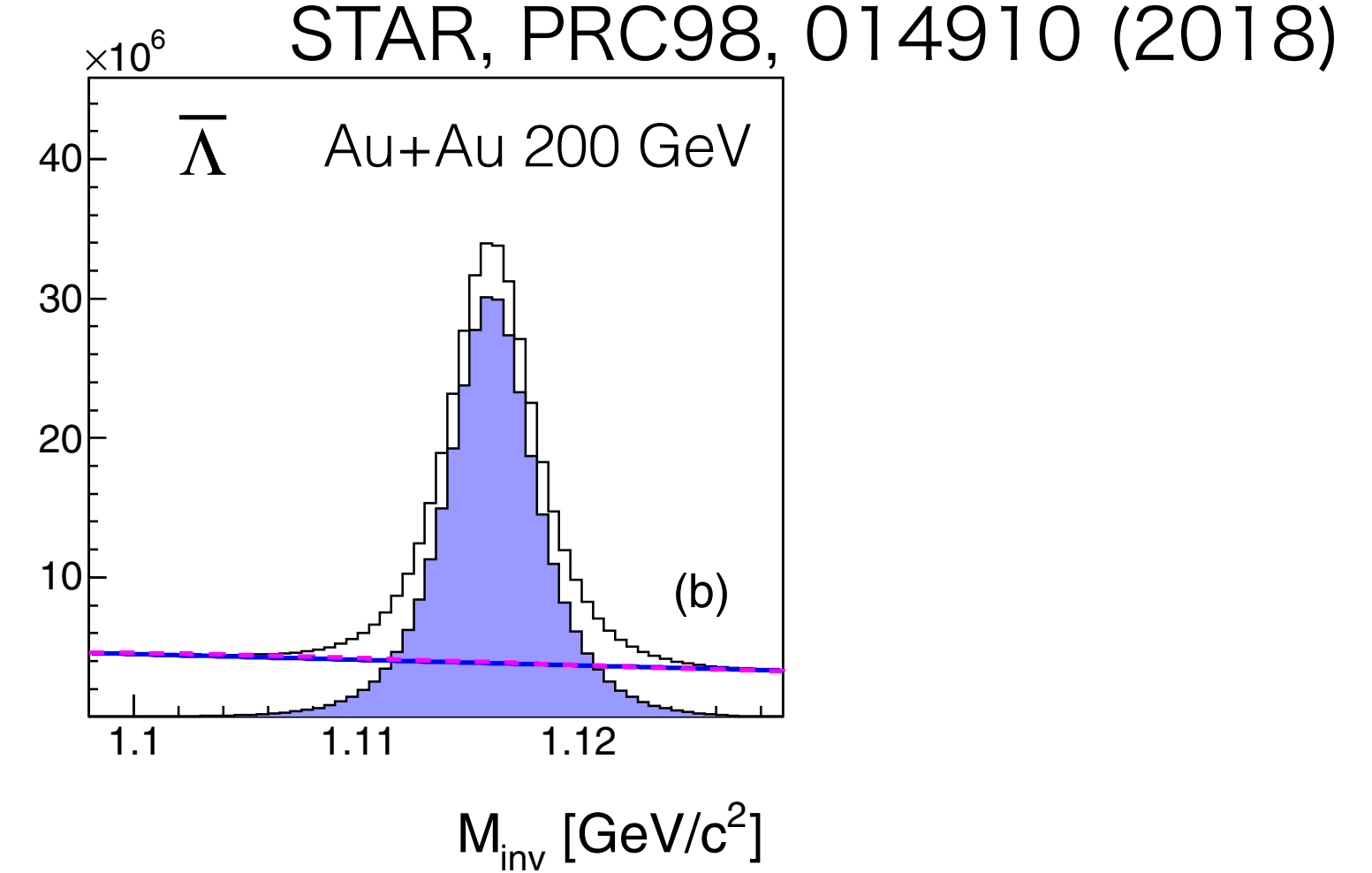
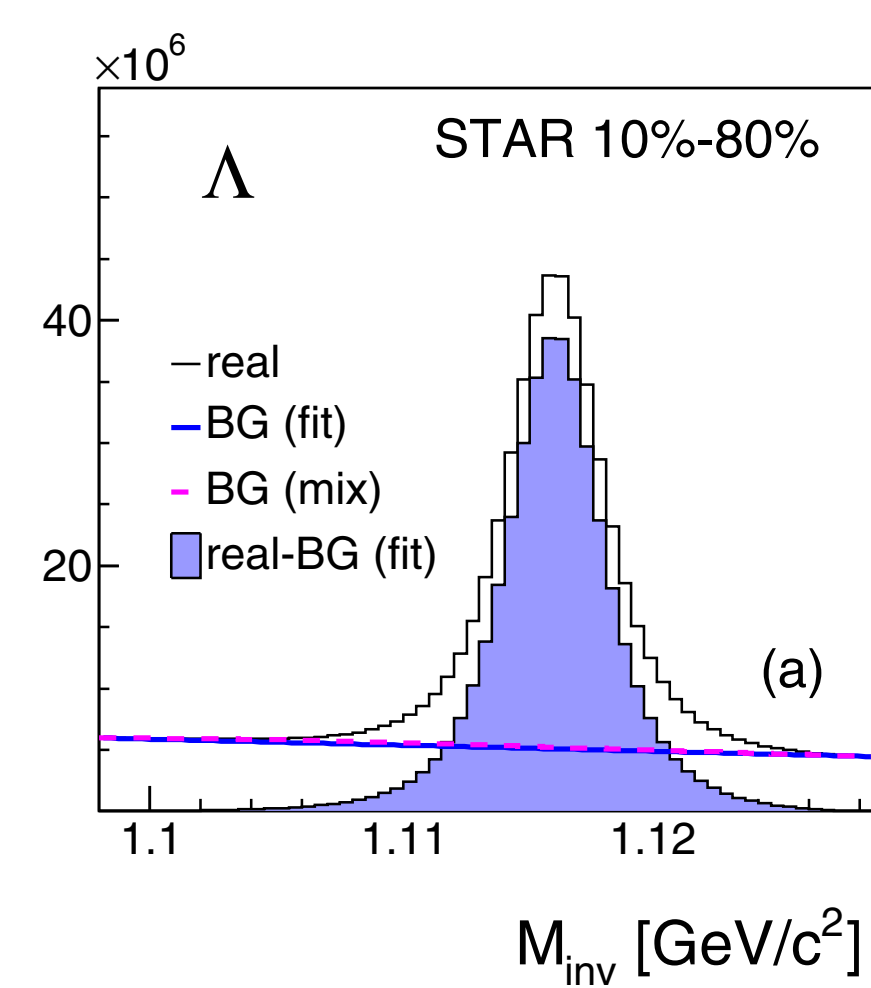
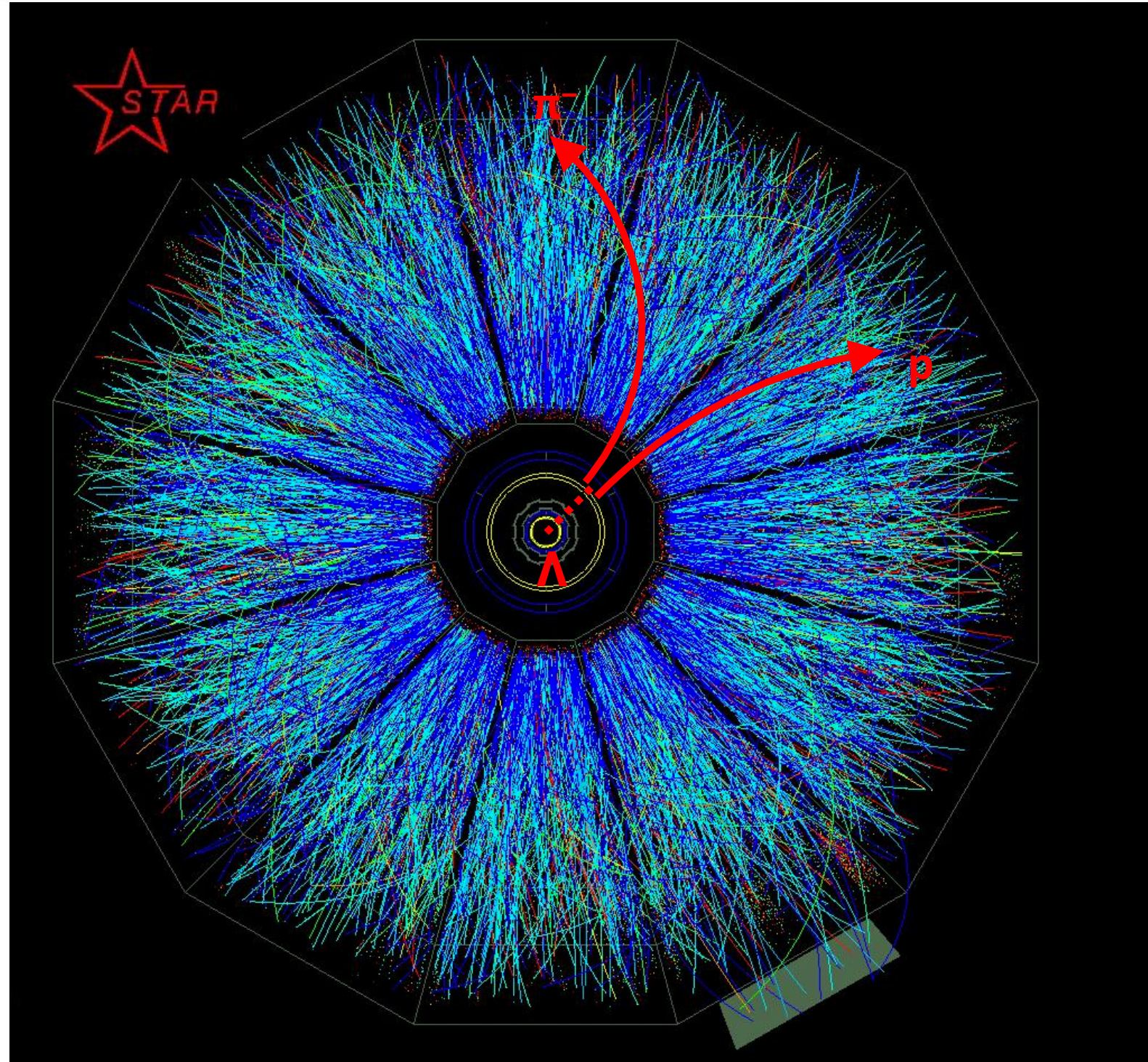
TPC  $dE/dx$  vs momentum/charge



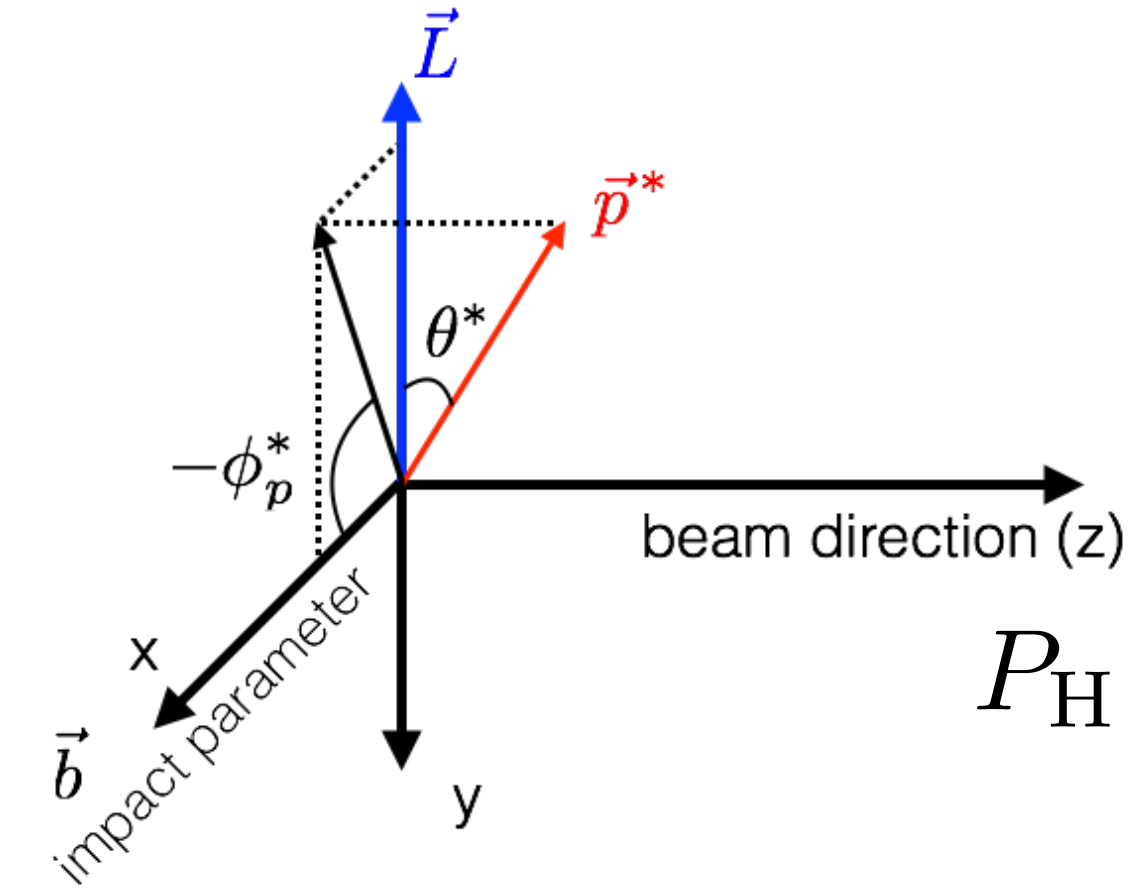
TOF  $1/\beta$  vs momentum/charge



# Signal extraction with $\Lambda$ hyperons



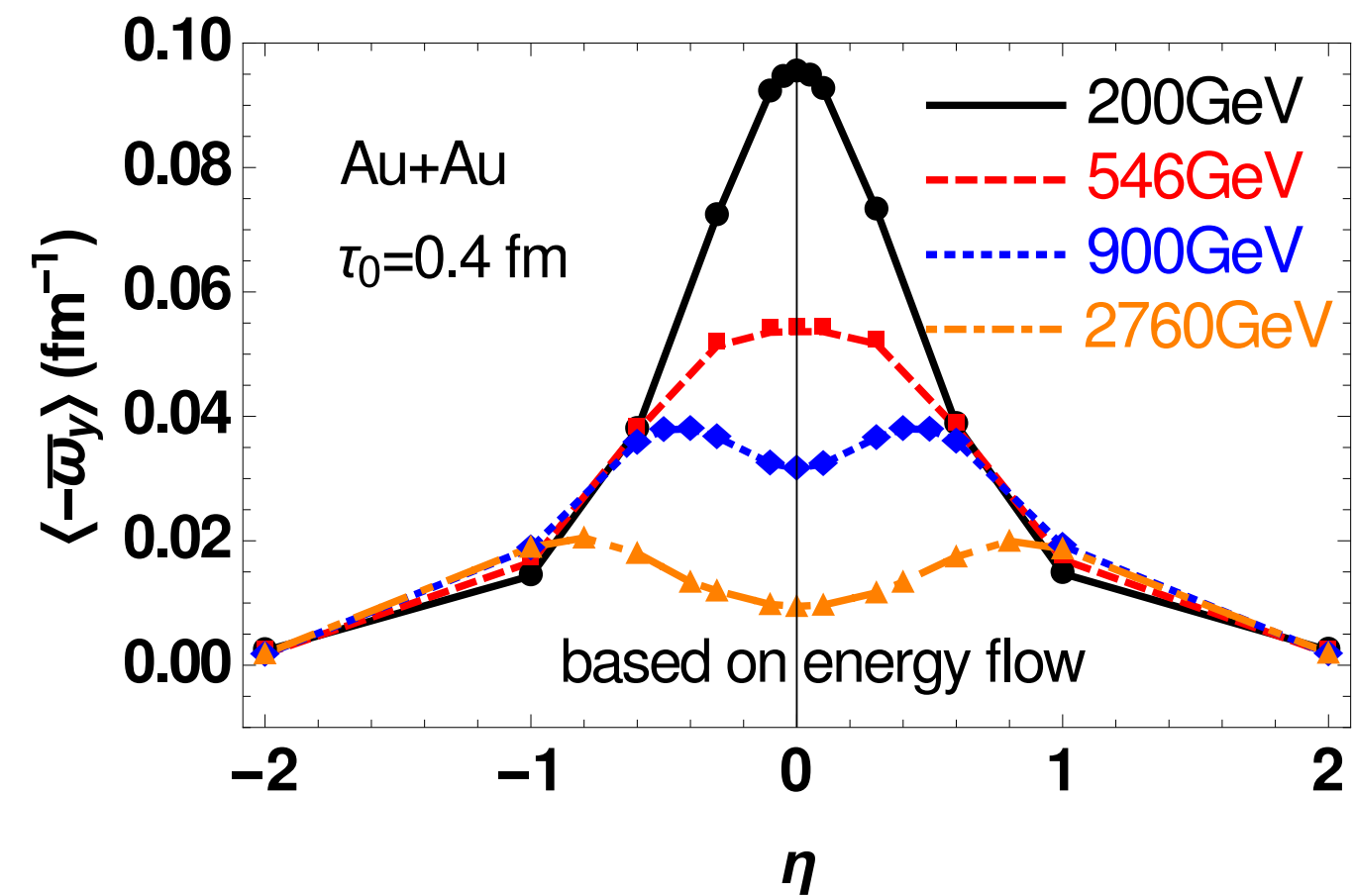
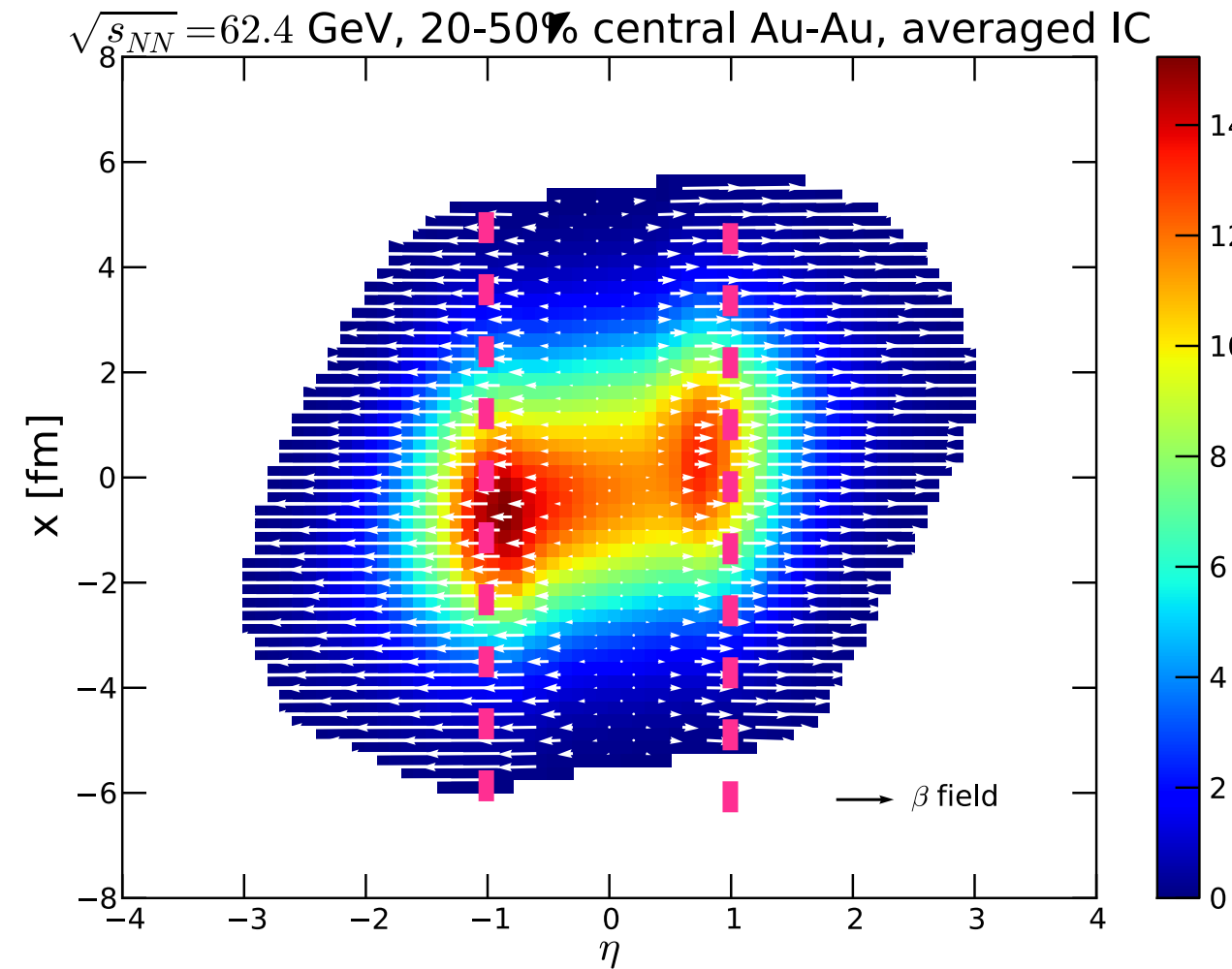
negative for anti- $\Lambda$   
 $\alpha_H = -\alpha_{\bar{H}}$



$$P_H = \frac{8}{\pi \alpha_H} \frac{\langle \sin(\Psi_1 - \phi_p^*) \rangle}{\text{Res}(\Psi_1)}$$

$$\langle \sin(\Psi_1 - \phi_p^*) \rangle^{\text{obs}} = (1 - f^{\text{Bg}}(M_{\text{inv}})) \langle \sin(\Psi_1 - \phi_p^*) \rangle^{\text{Sg}} + f^{\text{Bg}}(M_{\text{inv}}) \langle \sin(\Psi_1 - \phi_p^*) \rangle^{\text{Bg}},$$

# $\eta$ dependence of $P_H$

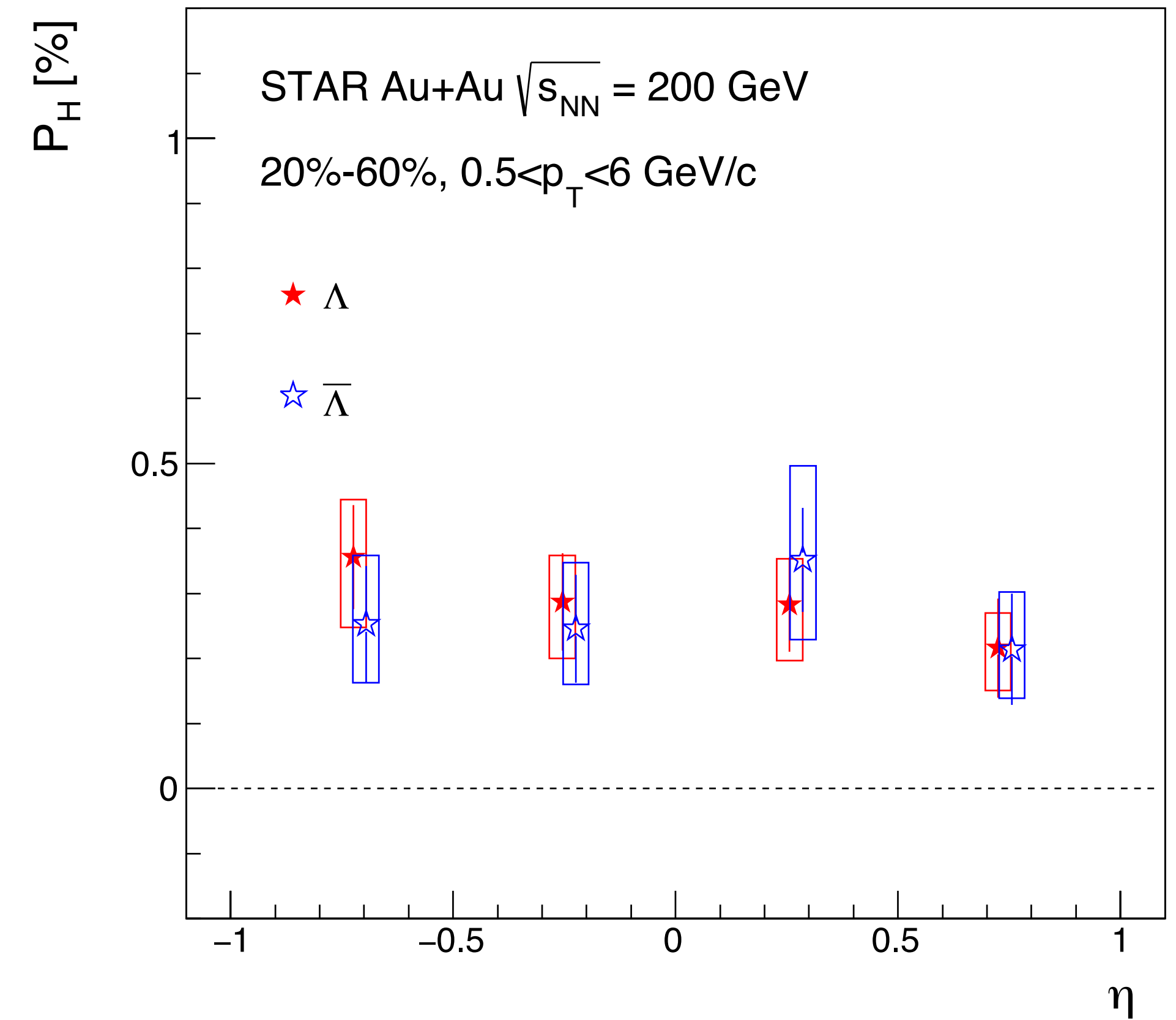


- Shear flow structure/initial flow velocity would be stronger in forward/backward region
- Expect rapidity dependence of the polarization

I. Karpenko and F. Becattini, EPJC(2017)77:213

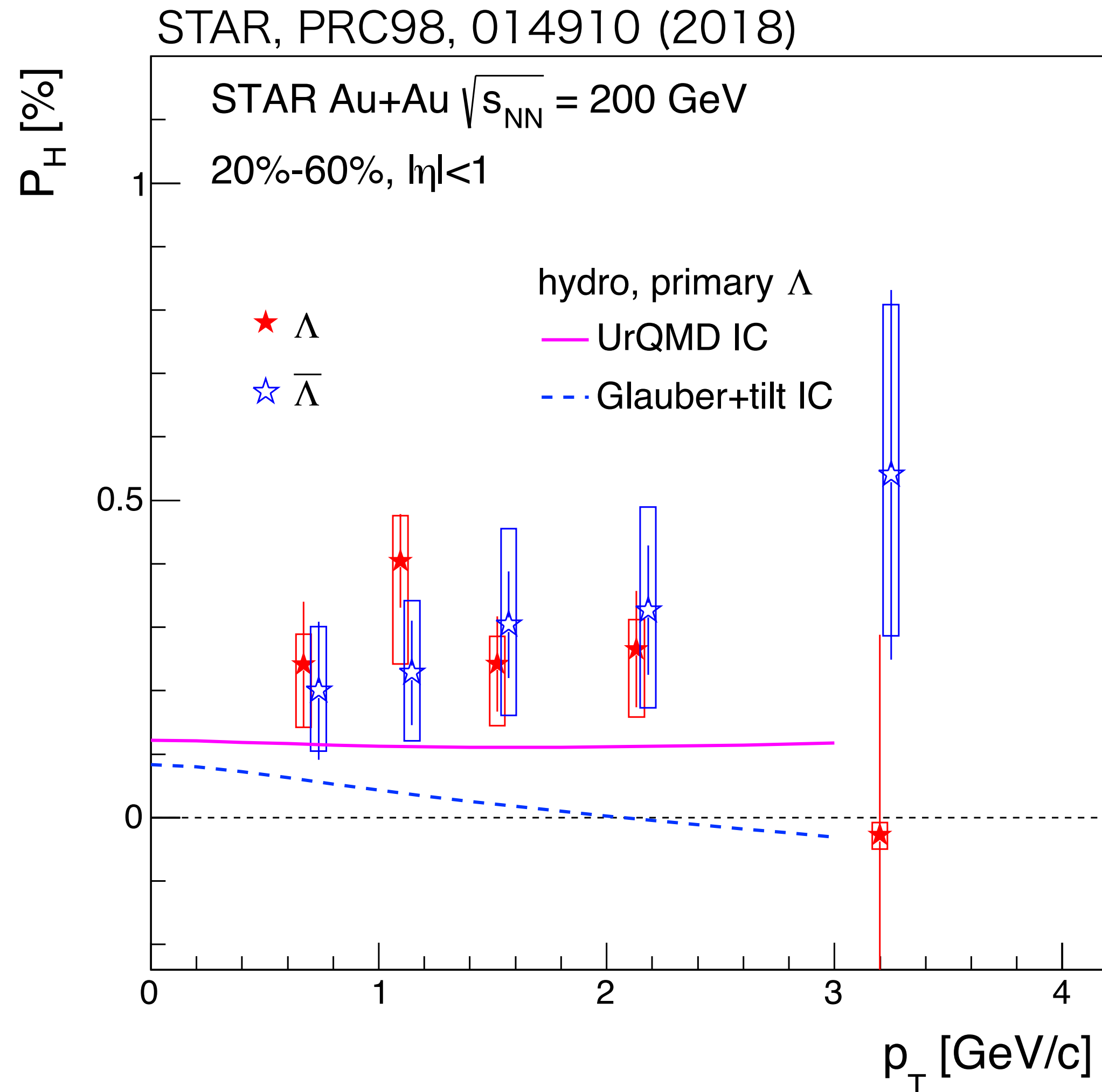
W.-T. Deng and X.-G. Huang, arXiv:1609.01801

STAR, PRC98, 014910 (2018)



- The data do not show significant  $\eta$  dependence
  - Maybe due to baryon transparency at higher energy
  - Also due to event-by-event C.M. fluctuations

# $p_T$ dependence of $P_H$



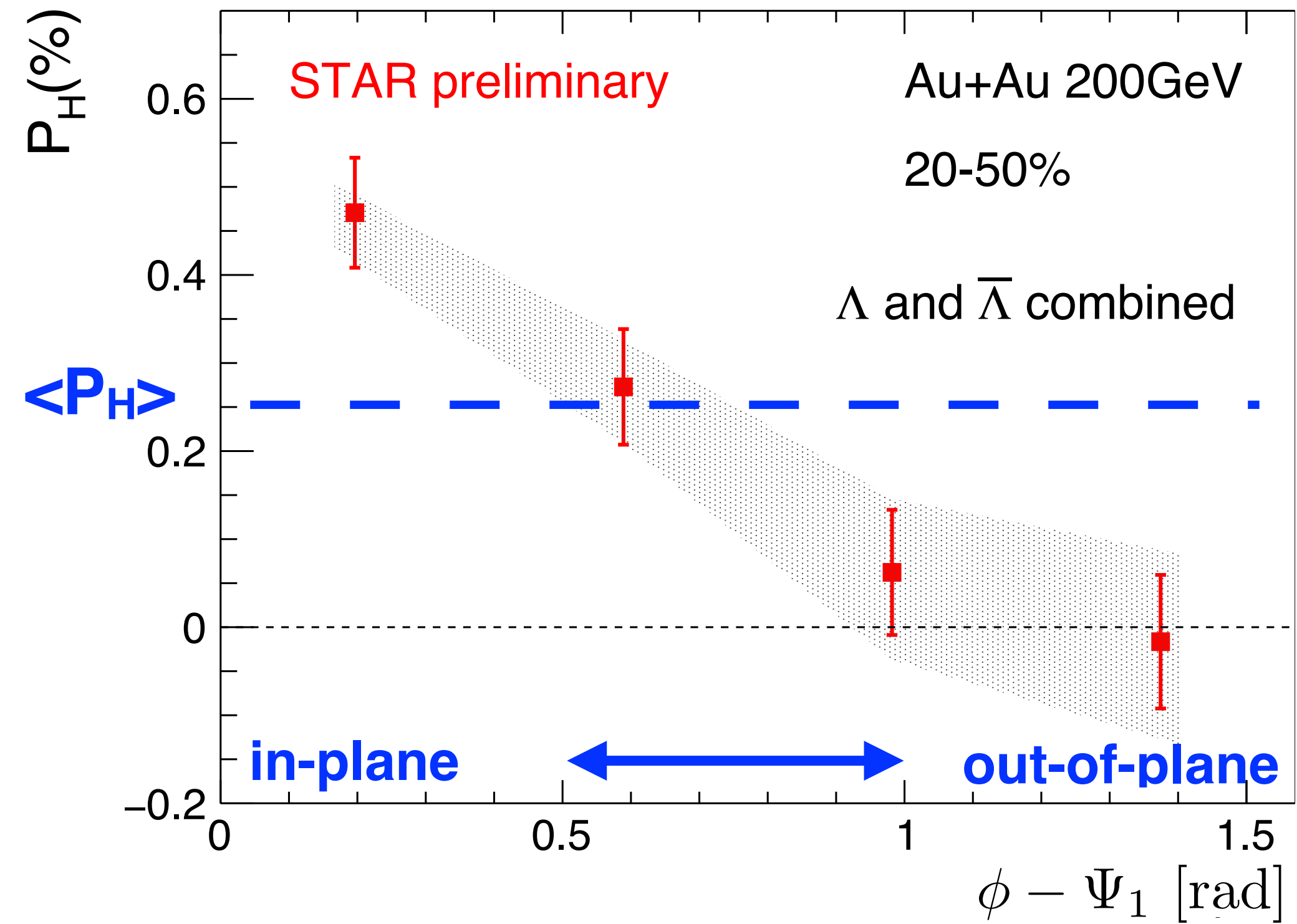
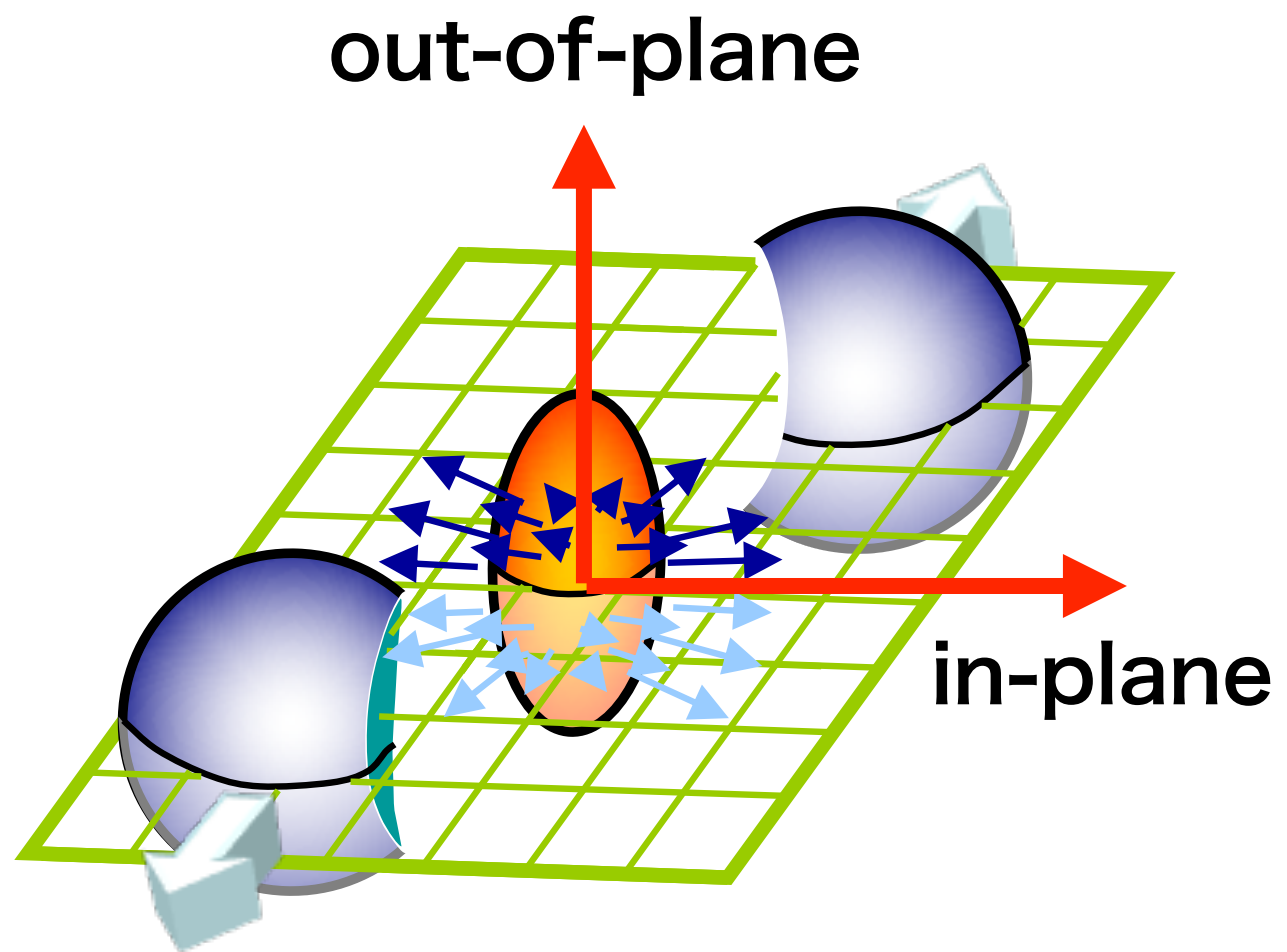
- No significant  $p_T$  dependence, as expected from the initial angular momentum of the system
- Hydrodynamic model underestimates the data. Initial conditions affect the magnitude and dependence on  $p_T$

3D viscous hydrodynamic model with two initial conditions (ICs)

- UrQMD IC
- Glauber with source tilt IC

F. Becattini and I. Karpenko, PRL120.012302, 2018

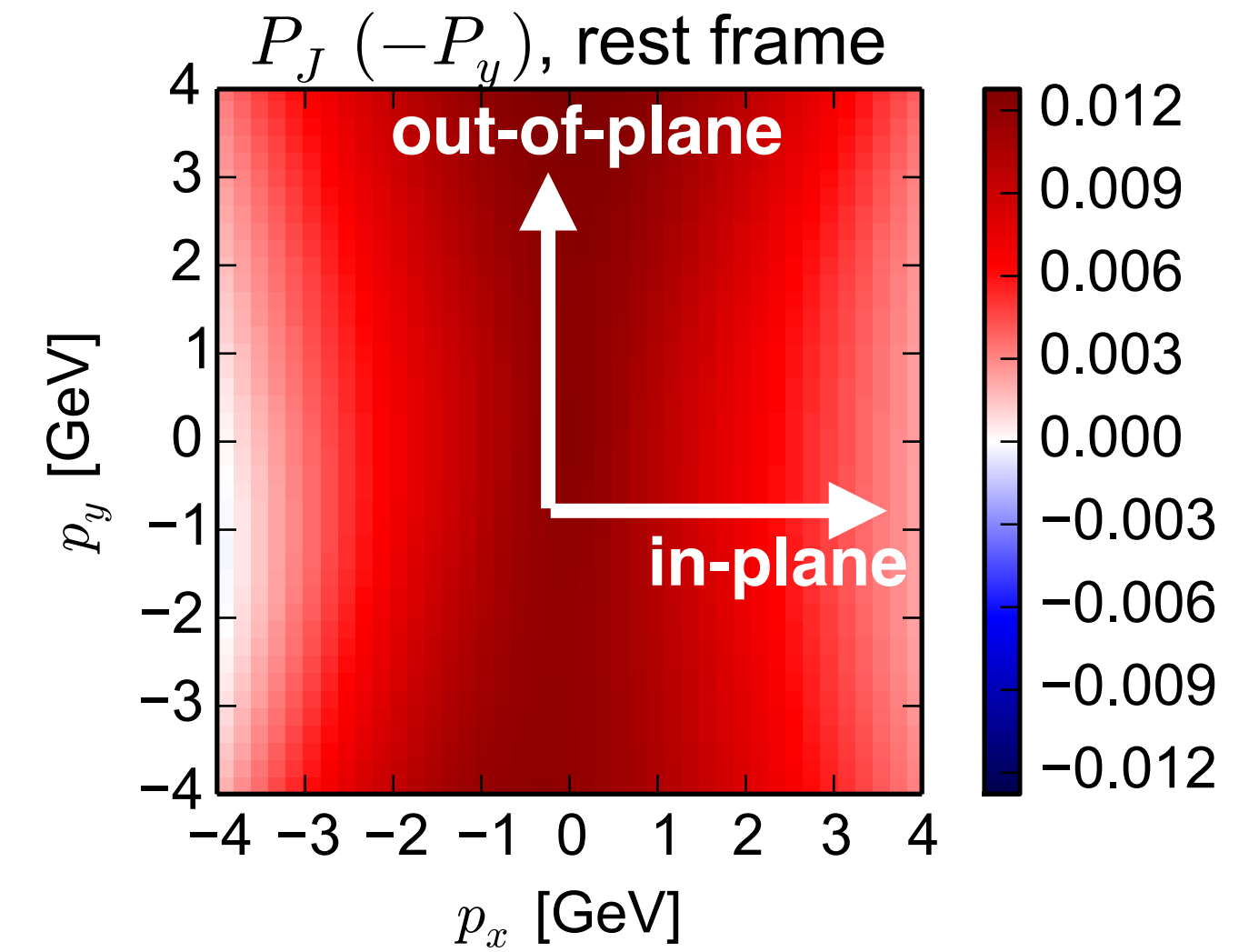
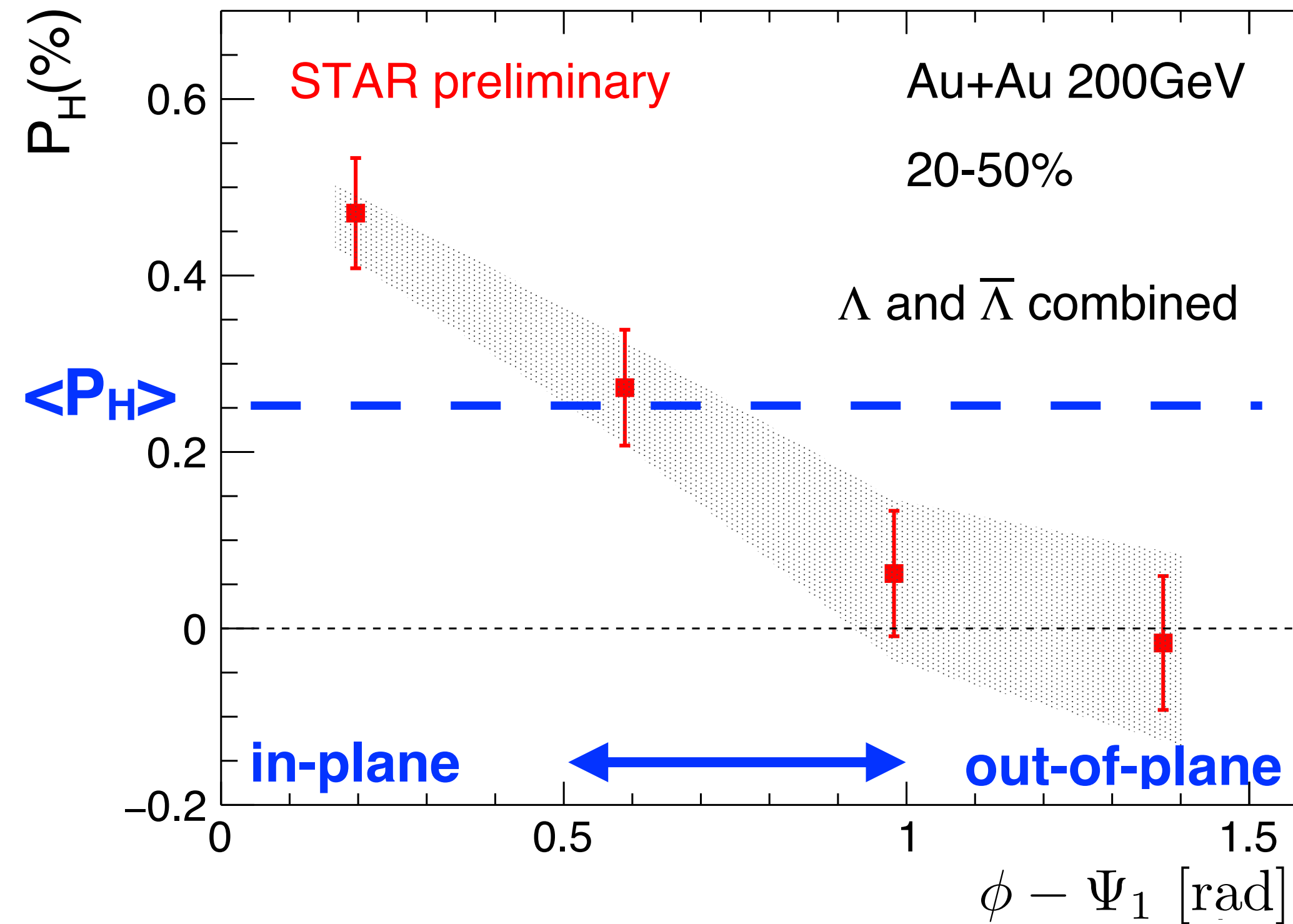
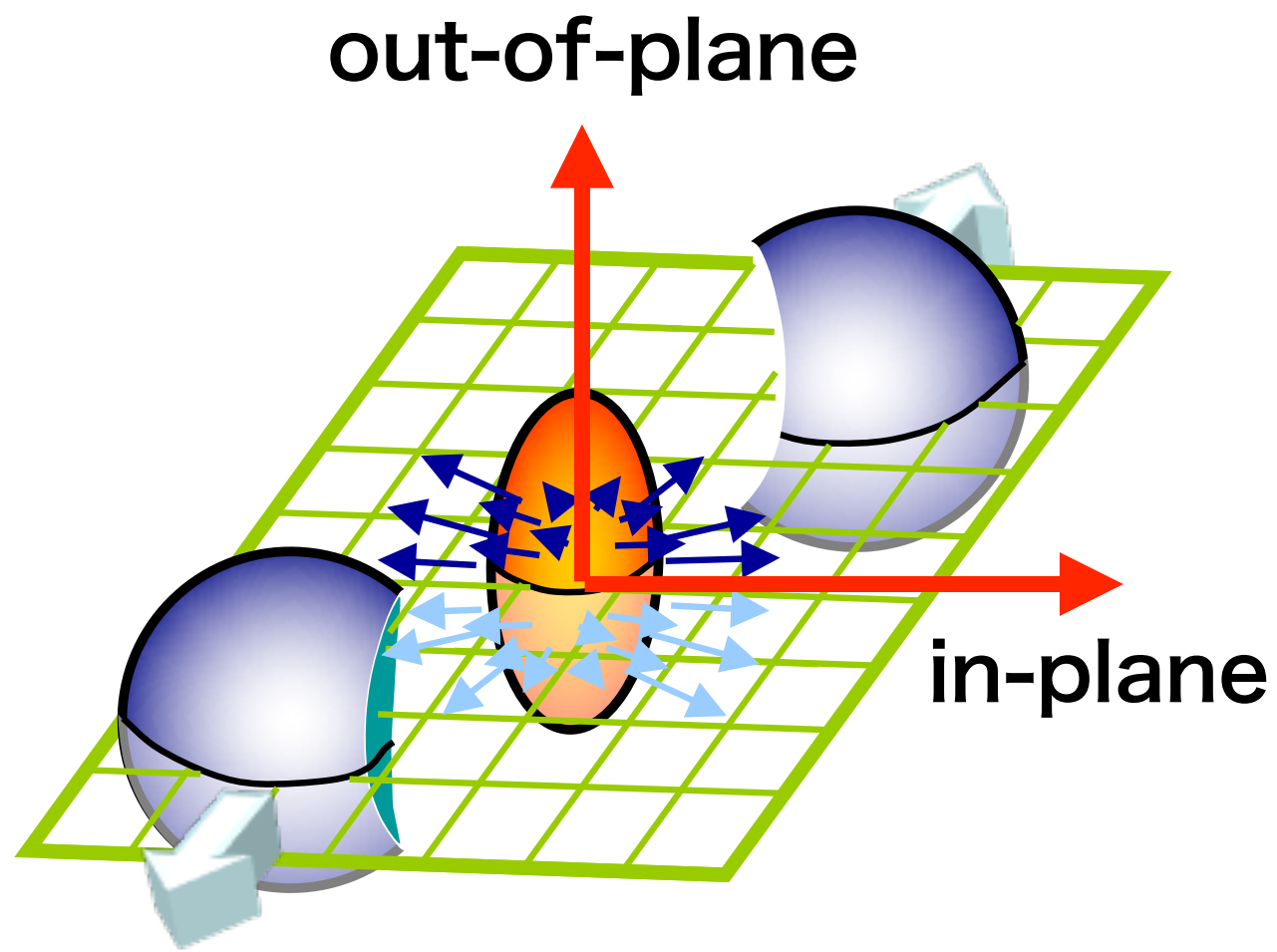
# Azimuthal angle dependence of $P_H$



- ◆ Larger polarization in in-plane than in out-of-plane



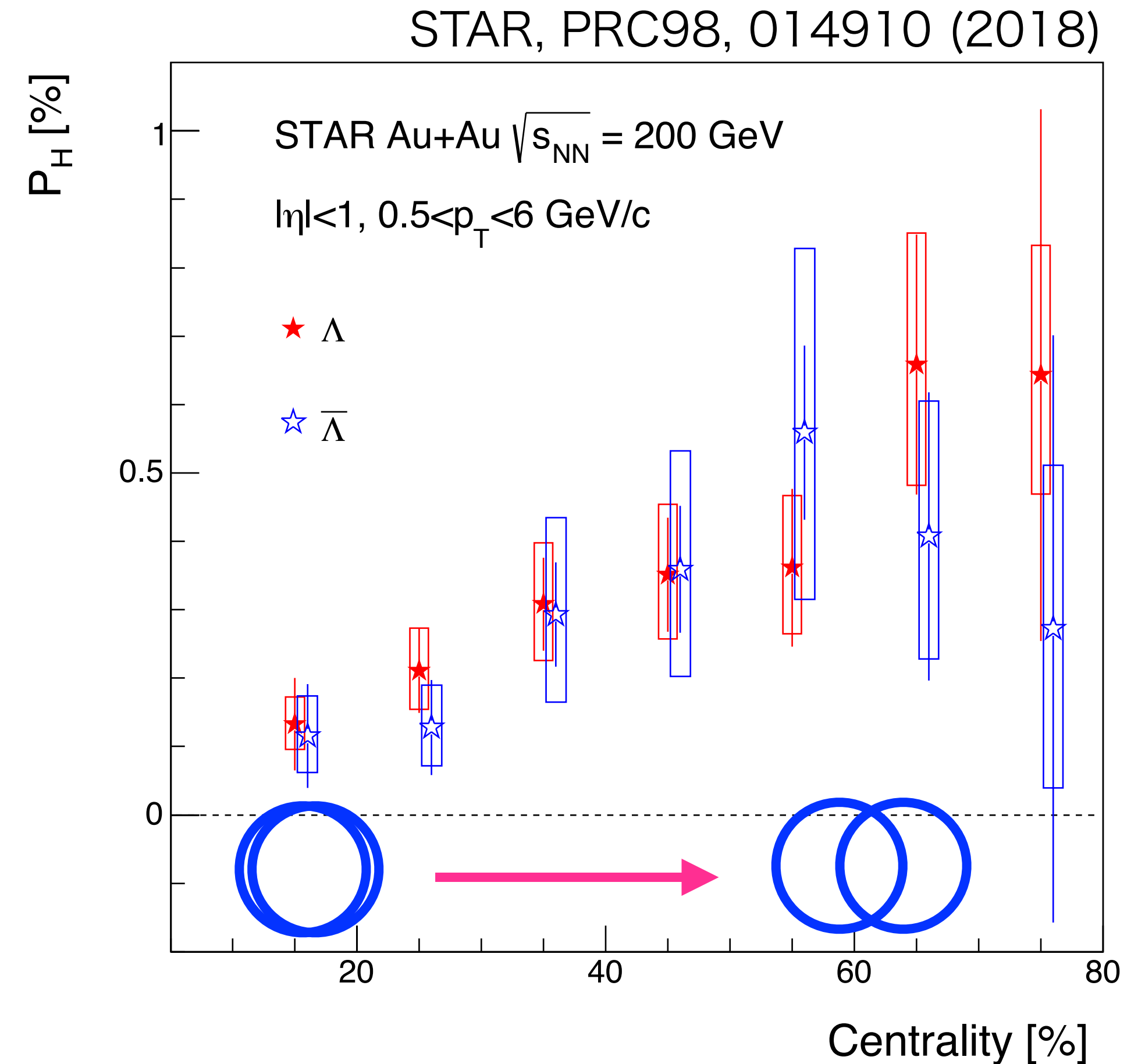
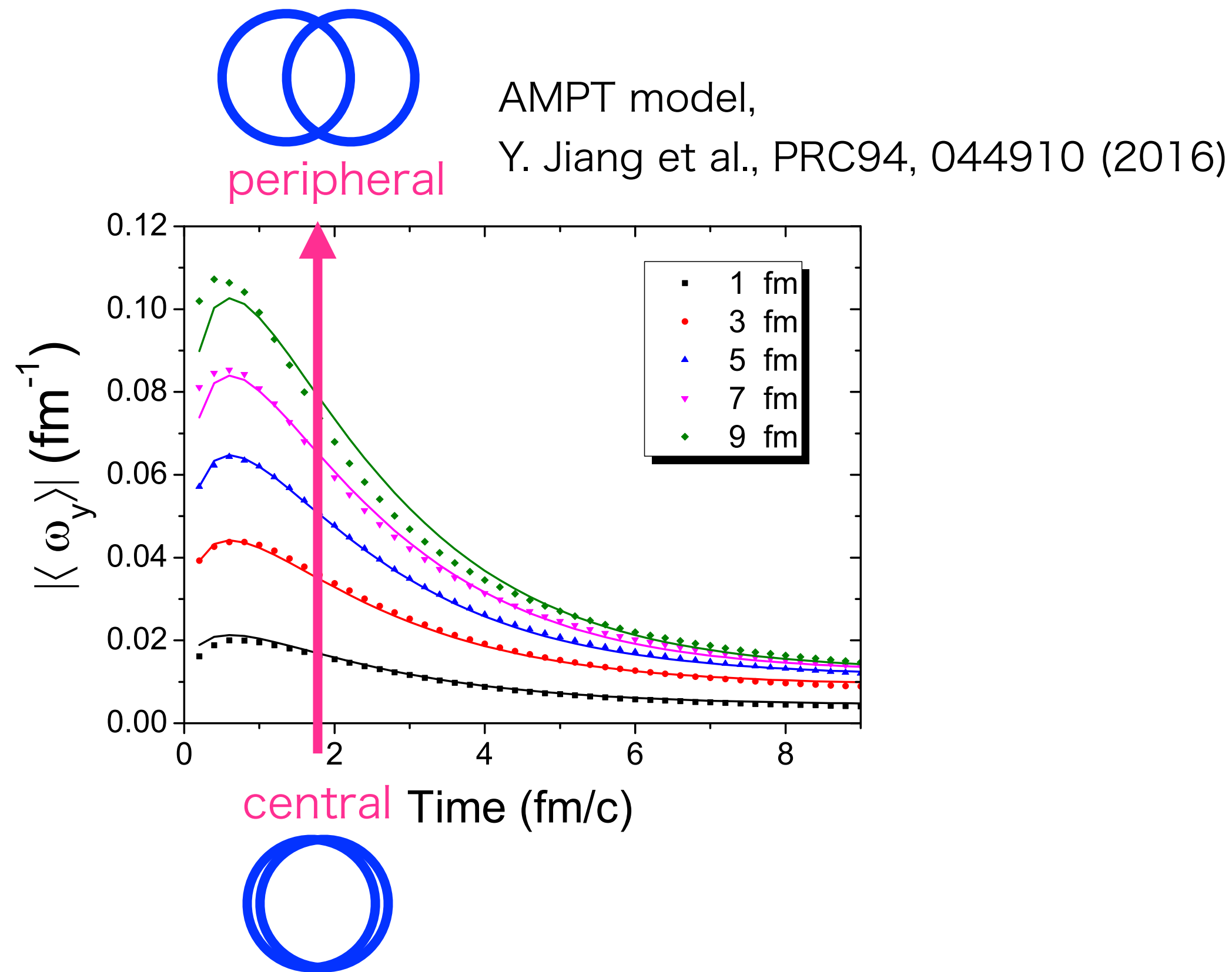
# Azimuthal angle dependence of $P_H$



I. Karpenko and F. Becattini, EPJC(2017)77:213

- ◆ Larger polarization in in-plane than in out-of-plane
- ◆ Opposite to the hydrodynamic expectation (larger in out-of-plane)

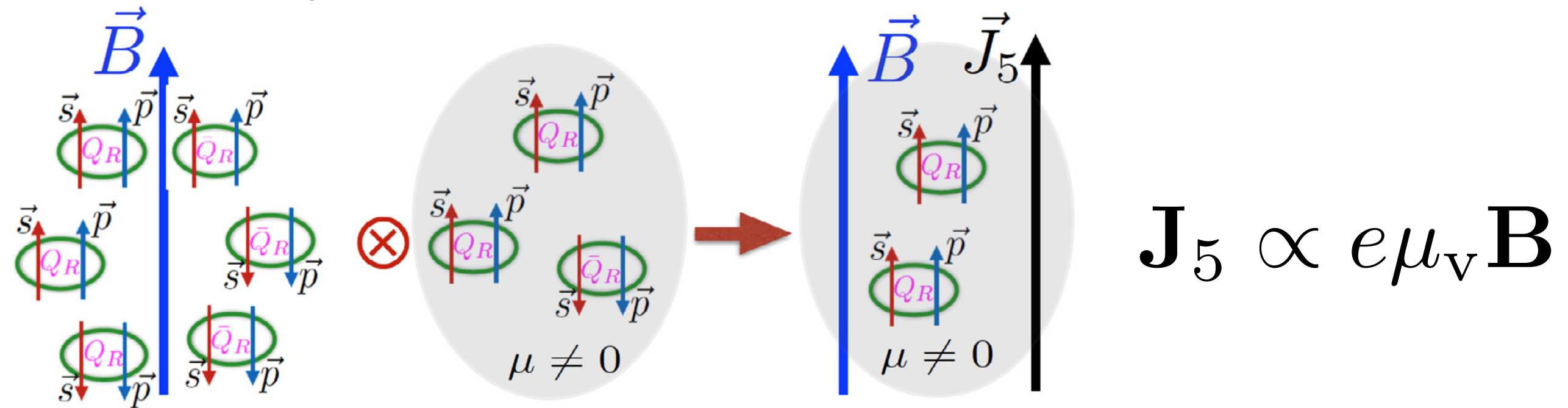
# Centrality dependence of $P_H$



In most central collision  $\rightarrow$  no initial angular momentum  
 As expected, the polarization decreases in more central collisions

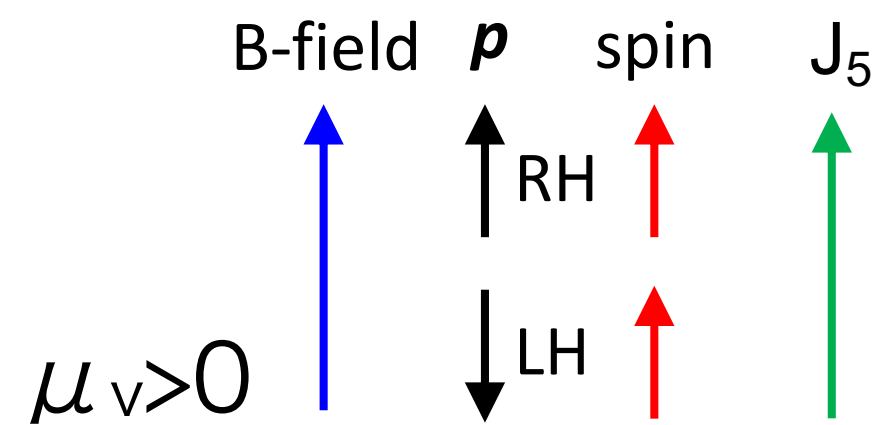
# $\Lambda$ polarization vs. charge asymmetry

Chiral Separation Effect



B-field + massless quarks + non-zero  $\mu_v \rightarrow$  axial current  $J_5$

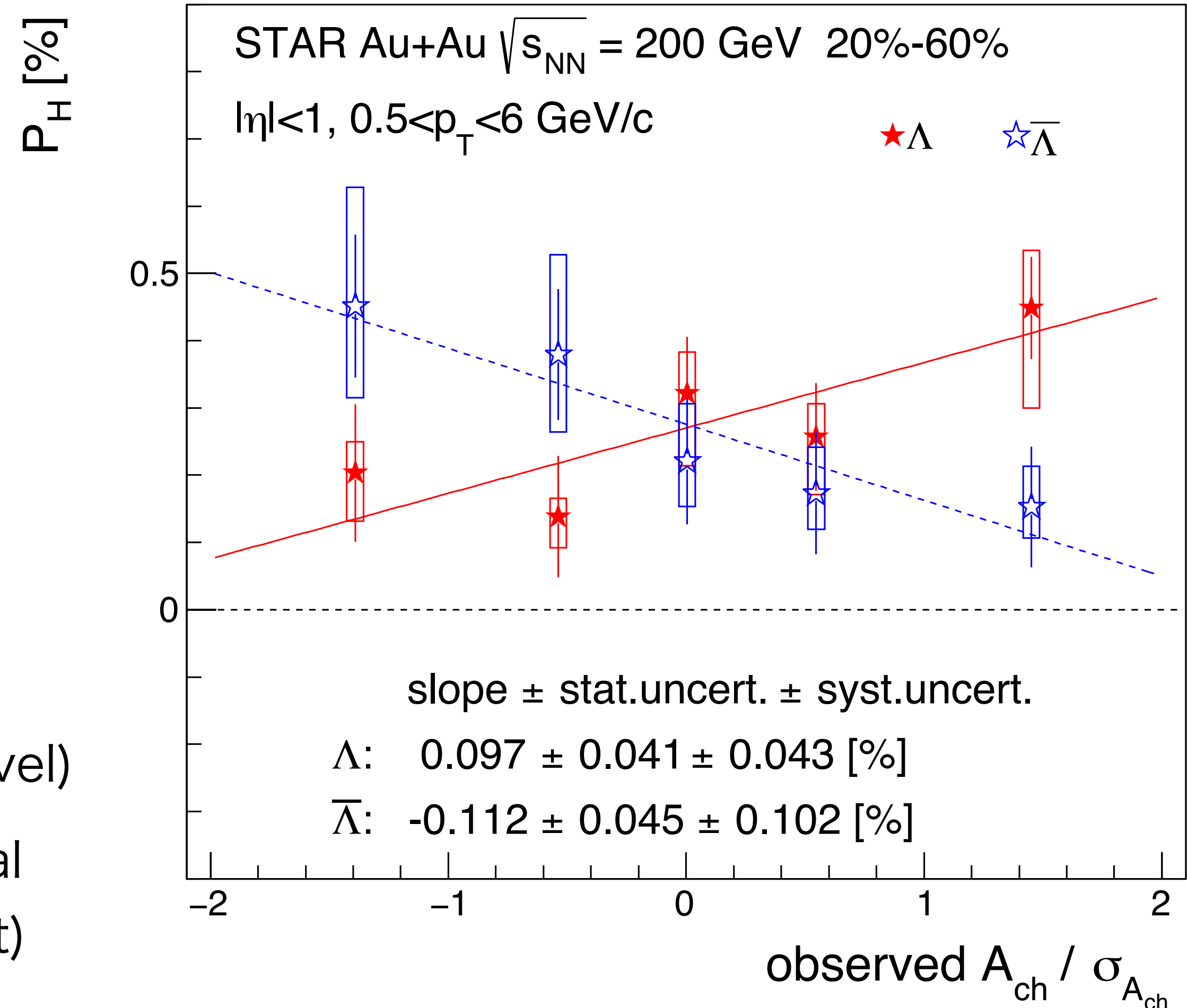
$$\mu_v/T \propto \frac{\langle N_+ - N_- \rangle}{\langle N_+ + N_- \rangle} = A_{\text{ch}}$$



- Slopes of  $\Lambda$  and anti- $\Lambda$  seem to be different ( $\sim 2\sigma$  level)
- Possible contribution to the polarization from the axial current  $J_5$  induced by B-field (Chiral Separation Effect)

S. Shlichting and S. Voloshin

STAR, PRC98, 014910 (2018)



# Rotation vs. Polarization

Barnett effect:  
rotation → polarization

Magnetization of an uncharged body  
when spun on its axis S. Barnett, Phys. Rev. 6, 239 (1915)

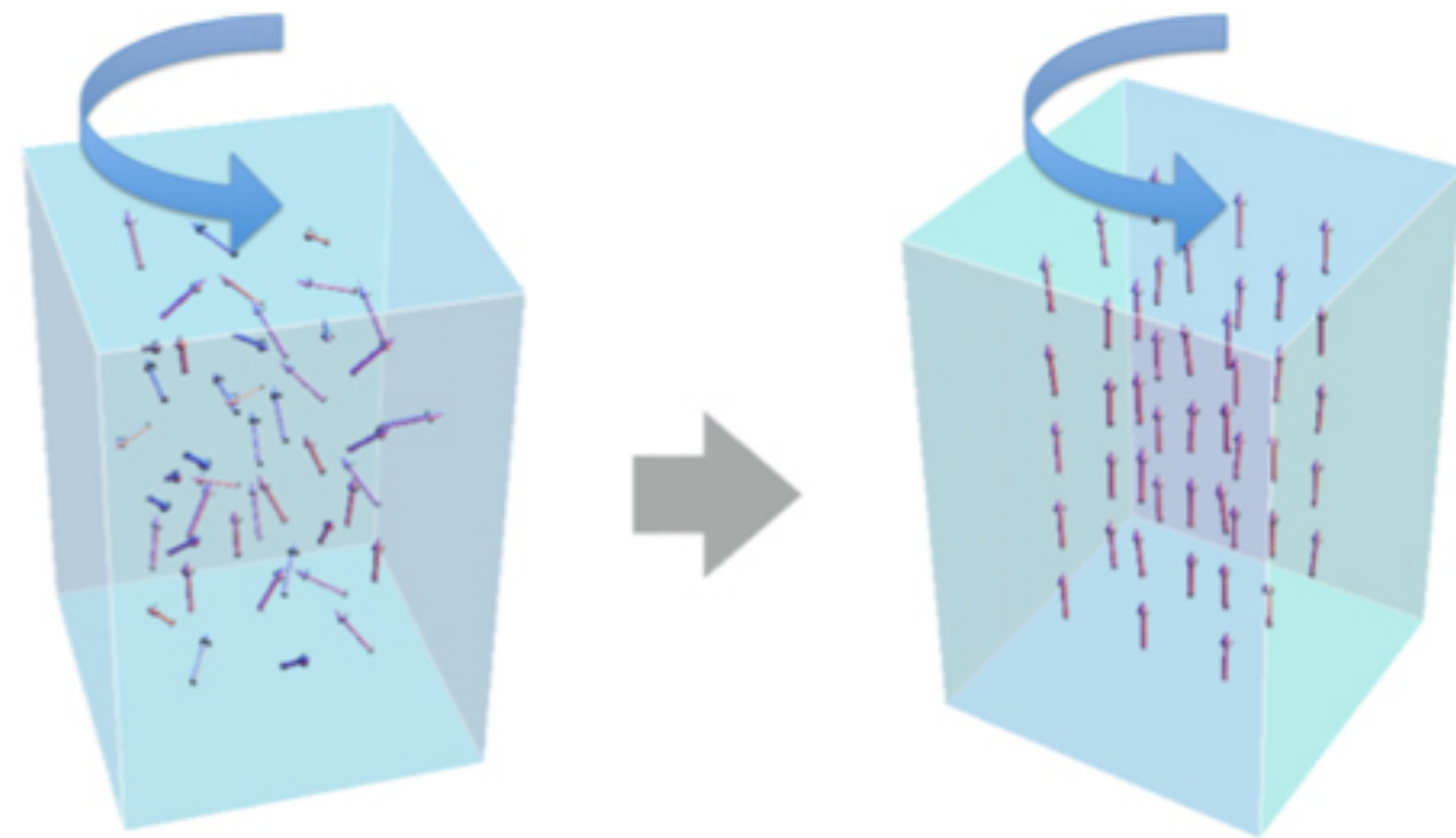


figure: M. Matsuo et al., Front. Phys., 30 (2015)

$$M = \frac{\chi\omega}{\gamma}$$

$\chi$ : magnetic susceptibility  
 $\gamma$ : gyromagnetic ratio

Einstein-de-Haas effect:  
polarization → rotation



“the only experiment by Einstein”

Rotation of a ferromagnet under  
change in the direction/strength  
of magnetic-field to conserve the  
total angular momentum.

$$\vec{J} = \vec{L} + \vec{S}$$

A.Einstein, W. J. de Haas,  
B.Koninklijke Akademie van Wetenschappen te Amsterdam,  
C.Proceedings, 18 I, 696-711 (1915)

# Feed-down effect

- Only ~25% of measured  $\Lambda$  and anti- $\Lambda$  are primary, while ~60% are feed-down from  $\Sigma^* \rightarrow \Lambda \pi$ ,  $\Sigma^0 \rightarrow \Lambda \gamma$ ,  $\Xi \rightarrow \Lambda \pi$
- Polarization of parent particle R is transferred to its daughter  $\Lambda$

$$\mathbf{S}_\Lambda^* = C \mathbf{S}_R^* \quad \langle S_y \rangle \propto \frac{S(S+1)}{3} \left( \omega + \frac{\mu}{S} B \right)$$

$C_{\Lambda R}$  : coefficient of spin transfer from parent R to  $\Lambda$   
 $S_R$  : parent particle's spin  
 $f_{\Lambda R}$  : fraction of  $\Lambda$  originating from parent R  
 $\mu_R$  : magnetic moment of particle R

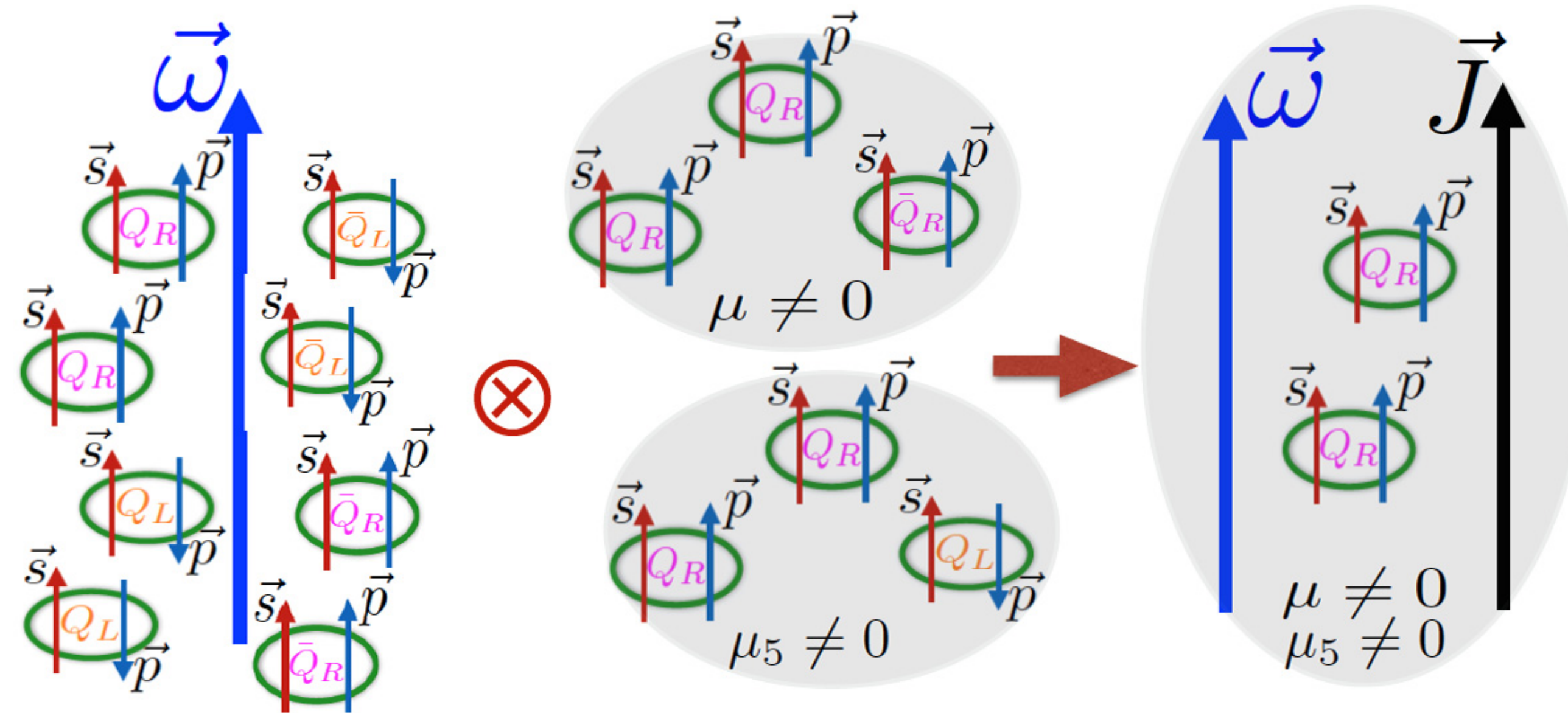
Becattini, Karpenko, Lisa, Upsal, and Voloshin, PRC95.054902 (2017)

$$\begin{pmatrix} \varpi_c \\ B_c/T \end{pmatrix} = \begin{bmatrix} \frac{2}{3} \sum_R (f_{\Lambda R} C_{\Lambda R} - \frac{1}{3} f_{\Sigma^0 R} C_{\Sigma^0 R}) S_R(S_R + 1) & \frac{2}{3} \sum_R (f_{\Lambda R} C_{\Lambda R} - \frac{1}{3} f_{\Sigma^0 R} C_{\Sigma^0 R}) (S_R + 1) \mu_R \\ \frac{2}{3} \sum_{\bar{R}} (f_{\Lambda \bar{R}} C_{\Lambda \bar{R}} - \frac{1}{3} f_{\Sigma^0 \bar{R}} C_{\Sigma^0 \bar{R}}) S_{\bar{R}}(S_{\bar{R}} + 1) & \frac{2}{3} \sum_{\bar{R}} (f_{\Lambda \bar{R}} C_{\Lambda \bar{R}} - \frac{1}{3} f_{\Sigma^0 \bar{R}} C_{\Sigma^0 \bar{R}}) (S_{\bar{R}} + 1) \mu_{\bar{R}} \end{bmatrix}^{-1} \begin{pmatrix} P_\Lambda^{\text{meas}} \\ P_{\bar{\Lambda}}^{\text{meas}} \end{pmatrix}$$

Decay	C
Parity conserving: $1/2^+ \rightarrow 1/2^+ 0^-$	-1/3
Parity conserving: $1/2^- \rightarrow 1/2^+ 0^-$	1
Parity conserving: $3/2^+ \rightarrow 1/2^+ 0^-$	1/3
Parity-conserving: $3/2^- \rightarrow 1/2^+ 0^-$	-1/5
$\Xi^0 \rightarrow \Lambda + \pi^0$	+0.900
$\Xi^- \rightarrow \Lambda + \pi^-$	+0.927
$\Sigma^0 \rightarrow \Lambda + \gamma$	-1/3

15%-20% dilution of primary  $\Lambda$  polarization  
(model-dependent)

# Chiral Vortical Effect

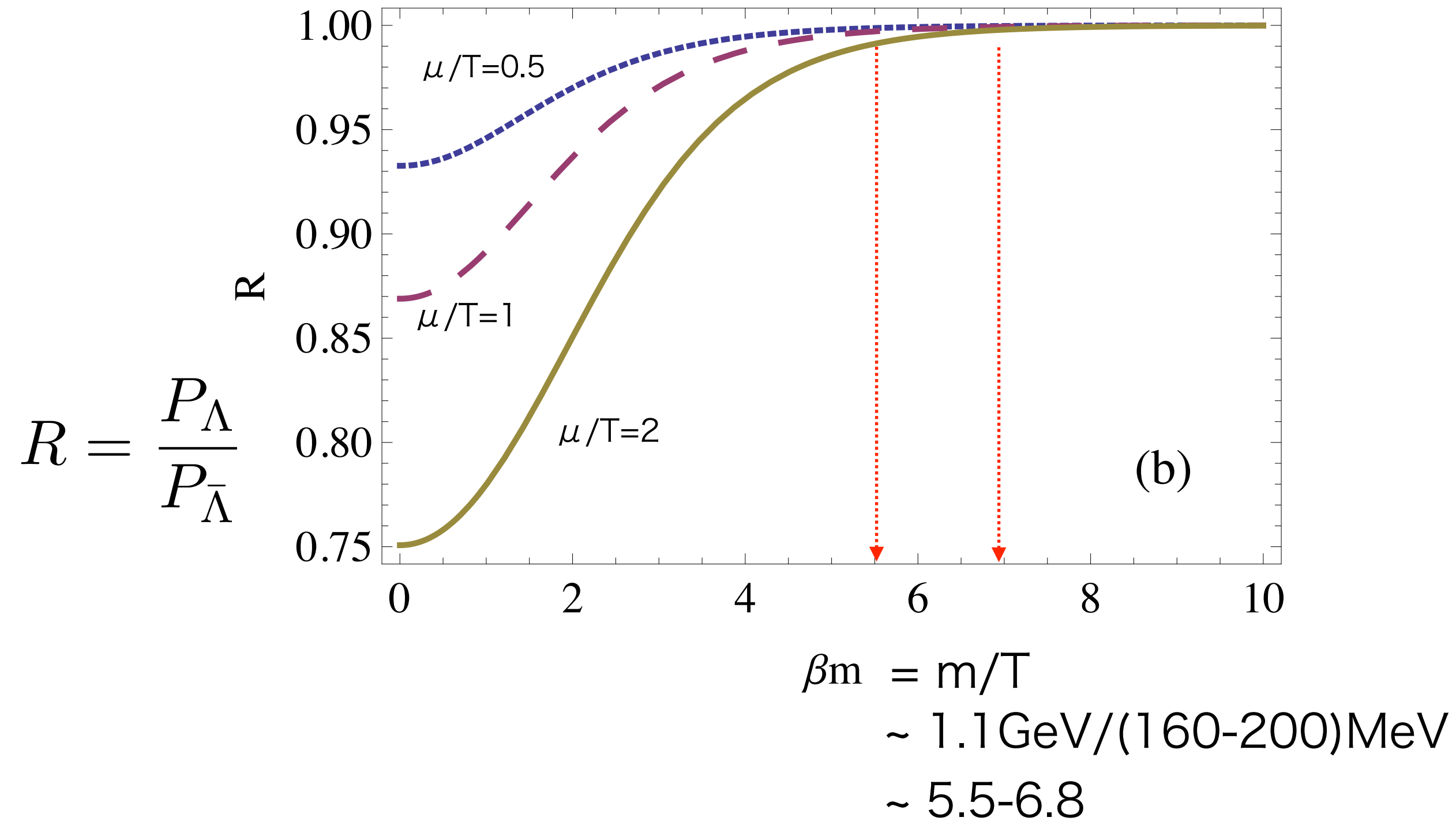


$$\vec{J}_V = \frac{1}{\pi^2} \mu \mu_5 \vec{\omega} \quad \vec{J}_5 = \left[ \frac{1}{2\pi^2} (\mu^2 + \mu_5^2) + \frac{1}{6} T^2 \right] \vec{\omega}$$

Observed polarization may get an offset from CVE

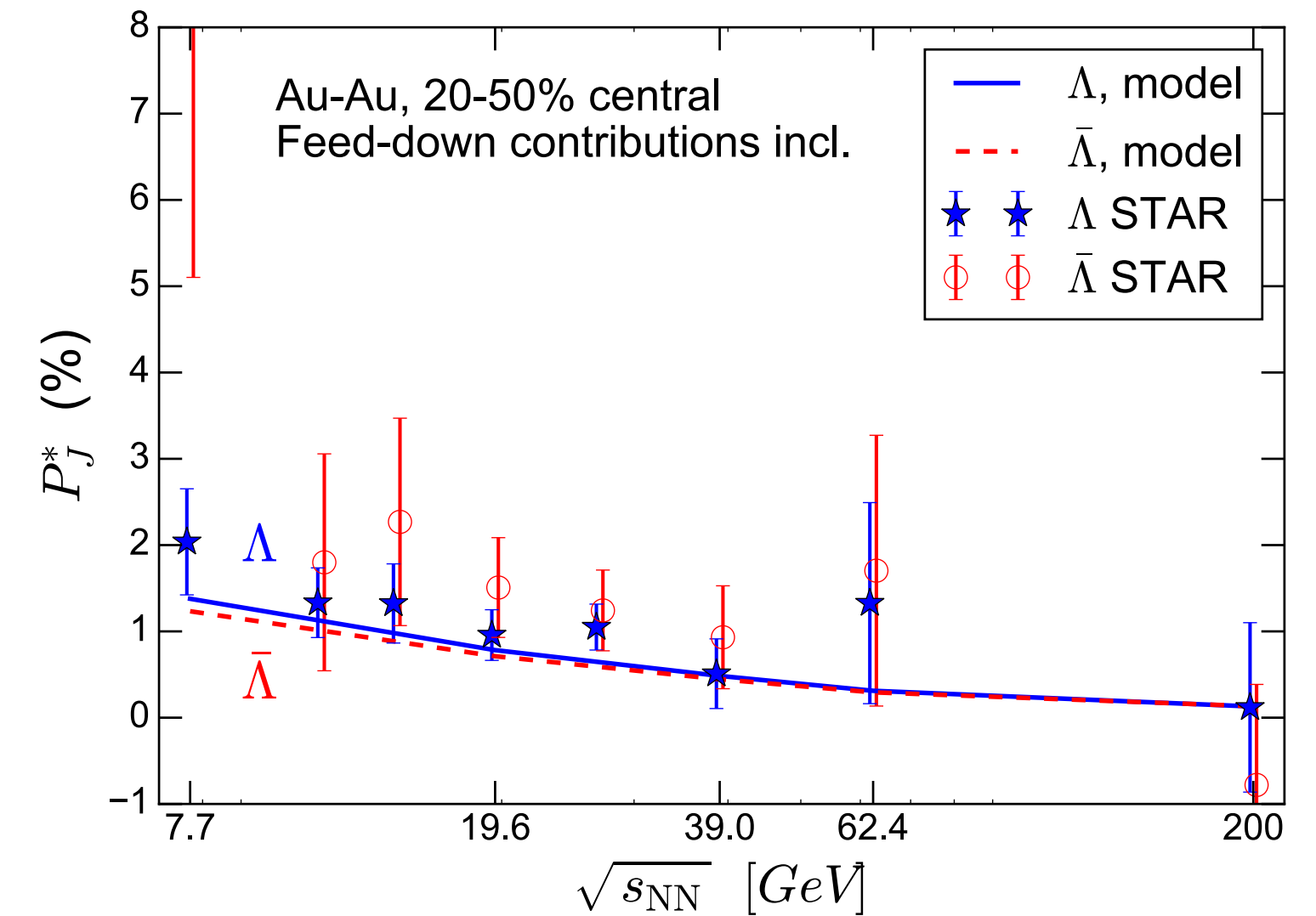
# Effect of non-zero chemical potential

R. Fang, L. Pang, Q. Wang, and X. Wang,  
PRC94, 024904 (2016)



Y. Karpenko, sQM2017

$\Lambda$  and  $\bar{\Lambda}$ : UrQMD+vHLLX vs experiment



only  $\mu_B$  effect in model

Non-zero chemical potential makes polarization splitting between  $\Lambda$  and anti- $\Lambda$ , but the effect seems to be small.